Design, synthesis and characterisation of water-soluble heterobimetallic complexes and their evaluation as aqueous biphasic hydroformylation catalysts

Shepherd Siangwata

University of Cape Town

2015

Design, synthesis and characterisation of water-soluble heterobimetallic complexes and their evaluation as aqueous biphasic hydroformylation catalysts

Shepherd Siangwata

A dissertation submitted in fulfilment of the requirements of the degree

Master of Science in Chemistry

University of Cape Town

Department of Chemistry

Supervisors:

Assoc. Prof G. S. Smith

Dr B. C. E. Makhubela

August 2015

Declaration

I know the meaning of Plagiarism and declare that all of the work in the document "**Design, synthesis and characterisation of water-soluble heterobimetallic complexes and their evaluation as aqueous biphasic hydroformylation catalysts**" is my own, save for that which is properly acknowledged by means of a reference. It is to the best of my knowledge that this work has never been reported or submitted for any degree or examination by any university.

Signed by candidate

……

Shepherd Siangwata

21 / 08 / 2015

Date

Dedication

This dissertation is dedicated to my mum, my dad, and my two sisters with love.

Acknowledgements

Firstly I would like to thank God for everything He has done for me thus far and the blessings with which my future is set.

I also wish to express my gratitude to those who generally helped me colour the mosaic of my work with the tiles of their knowledge, expertise and memories.

My deepest gratitude goes to the stupendous support I received from my supervisors, Assoc. Prof Gregory Smith and Dr Banothile Makhubela throughout the period I carried out this work. I owe them an immeasurable debt of gratitude and appreciation for their expertise, kindness, help and advice. To them I say let your imaginations run along and you will not grasp even a fraction of how much valuable was your support to the successful production of my work.

Specific appreciation extends to my friends/mentors, Ms. Leah Matsinha and Ms. Latisa Maqeda for substantial guidance and the knowledge they offered regarding this work and the critical parameters associated with it.

I would also like to express my special acknowledgement and gratitude to Dr Anwar Jardine for going out of his way to read my thesis, and to the organometallic research group members, in particular Preshendren and Tameryn for their undoubtedly first class academic support and constructive criticism. On the administrative side, I would like to thank Mrs Deirdre Brooks for her remarkable support she offered and the daily dose of good laughter.

Many thanks go to the analytical chemistry staff at the University of Cape Town Mr Pete Roberts and Mr Gianpierro Benincasa for their great job throughout my studies.

For funding, I would like to give thanks to c*change and the National Research Foundation-Department of Science and Technology.

Finally I would like to thank my parents, family and friends for the support, inspiration and encouragement they offered and to so many others whom I cannot mention but trust that they know just how greatly I cherish their help and support.

Table of contents

Publications

Published in the Journal of Organometallic Chemistry,

Shepherd Siangwata, Nadia Baartzes, Banothile C. E. Makhubela and Gregory S. Smith, *Synthesis, Characterisation and Reactivity of Water-Soluble Ferrocenylimine-Rh(I) Complexes as Aqueous biphasic Hydroformylation Catalyst Precursors, J. Organomet. Chem.*, 2015, **796**, 26–32.

Conference/Symposium Contributions

29 March – 1 April 2015: Poster presentation

Conversion of 1-octene to aldehydes using syngas and water-soluble ferrocenylimine-Rh(I) heterobimetallic and dendritic structures. (c*change) SYNGAS CONVENTION, Cape Town.

9 – 12 November 2014: Poster presentation

Aqueous biphasic hydroformylation of 1-octene using water-soluble ferrocenylimine-Rh(I) heterobimetallic complexes. Catalysis Society of South Africa **(**CATSA) Conference, Pretoria.

23 October 2014: Poster presentation

Synthesis, characterisation and application of water-soluble heterobimetallic complexes in the aqueous biphasic hydroformylation of 1-octene. South Africa Chemical Institute (SACI) Young Chemists Symposium, Cape Town.

24 – 26 August 2014: Poster presentation

Evaluation of water-soluble heterobimetallic complexes in the aqueous biphasic hydroformylation of 1-octene. The 2nd International Symposium and Workshop of the Global Green Chemistry Centres, Cape Town.

Awards

3rd runner up for best poster presentation, SACI Young Chemists Symposium, Cape Town (2014).

Abstract

A series of new water-soluble *N,O*-chelating Schiff base ligands were synthesised. These ligands were reacted with ferrocenecarboxaldehyde through Schiff base condensation reactions, leading to new water-soluble ferrocenylimine mononuclear complexes. The mononuclear complexes were reacted with a dimeric rhodium precursor $[RhCl(COD)]_2$ to produce a series of novel ferrocenylimine-Rh(I) heterobimetallic complexes. Both the mononuclear and heterobimetallic complexes were found to have good solubility in water of up to 11 mg/mL. The complexes were characterised fully using various spectroscopic and analytical techniques including ^{1}H NMR, ^{13}C NMR spectroscopy, FT-IR spectroscopy, mass spectrometry and elemental analysis. In addition, mononuclear and heterobimetallic complexes were also synthesised as precursors to dendritic DAB-G1 structures. These were found to be water-soluble and they were also characterised using spectroscopic and analytical techniques. The two monometallic and two heterobimetallic complexes were evaluated as pre-catalysts for the aqueous biphasic hydroformylation of 1-octene.

The mononuclear ferrocenyl complexes were inactive in the aqueous biphasic hydroformylation experiments. Hydroformylation using the heterobimetallic complexes showed that the pre-catalysts are active in 1-octene conversion, yielding aldehydes (linear and branched) as well as isomerisation products (*cis* and *trans* 2- and 3-octene). Linear aldehydes were more favoured with the tertiary-butyl analogue of the heterobimetallic complex.

Although loss of metal from the aqueous layer was detected using ICP-OES, the catalysts exhibited good recyclability and could be reused up to 4 times.

List of Abbreviations

°	degrees
°C	degrees celsius
Å	Angstroms
δ	chemical shift
ν	wavenumber
ν_{max}	maximum wavelength
acac	acetylacetonate
Ar	aromatic
atm	atmospheres
ATR-IR	attenuated total reflectance infrared spectroscopy
br	broad
br s	broad signal
^{13}C NMR	carbon-13 nuclear magnetic resonance
calcd.	calculated
cat	catalyst
$CDCl_3$	deuterated chloroform
cm^{-1}	wavenumber
cm^3	cubic centimetres
COD	1,5-cyclooctadiene
COSY	correlation spectroscopy
d	doublet
DAB-G1	1,4-diaminobutane generation 1
dd	doublet of doublets

DCM	dichloromethane
DMSO	dimethyl sulfoxide
EA	elemental analysis
EI-MS	electron impact mass spectrometry
ESI-MS	electrospray ionisation mass spectrometry
EtOH	ethanol
Fc	ferrocene
FT-IR	Fourier transform infrared spectroscopy
g	gram(s)
GC	gas chromatography
h	hour
^{1}H NMR	proton nuclear magnetic resonance
HSQC	heteronuclear single quantum correlation
Hz	hertz
ICP-OES	inductively coupled optical emission spectrometry
IL	ionic liquid
IR	infrared
J	coupling constant
m	multiplet for nuclear magnetic resonance
MeOH	methanol
mg	milligram(s)
MHz	megahertz
mL	millilitre
mol	mole(s)

mmol	millimole(s)
M.P.	melting point
MS	mass spectrometry
m/z	mass to charge ratio
NMR	nuclear magnetic resonance
PAMAM	polyamidoamine
PGM	platinum group metals
ppm	parts per million
q	quartet
r.t.	room temperature
s	singlet
$S_{25°C}$	solubility in water at room temperature
$scCO_2$	supercritical carbon dioxide
Syngas	synthesis gas
t	triplet
^{t}Bu	tertiary butyl
TOF	turnover frequency
TPP	triphenylphosphine
TPPMS	monosulfonated triphenylphosphine
TPPTS	triphenylphosphine trisulfonate

Chapter 1

Review of the design and synthesis of water-soluble homo- and heterometallic complexes and their application in catalysis: A focus on hydroformylation

1.1 Background

The availability of Platinum Group Metals (PGMs) in Southern Africa necessitates beneficiation of these expensive and less abundant metals for application in catalytic and biological spheres in order to add more value to these resources. A number of transition metal-catalysed reactions are based on the rare, relatively expensive, moisture and air stable second and third–row transition metals.[1] On an economic and elemental supply scale this is not sustainable if catalysts based on these metals are to be the key approach for efficient conversion of raw materials into valuable products.

Incorporation of first row transition metals such as Fe, Co, Ni and Cu in heterobimetallic organometallic complex design and development with the relatively expensive metals (such as Ru, Rh, Pd) may be an economic incentive. This could also lead to enhanced catalytic activity and selectivity of the resultant multimetallic systems.[2,3] When these metals are in close proximity this may result in cooperative interactions leading to reaction pathways with reduced activation energies and a positive economic impact. Moreover, multimetallic systems have been shown to possess enhanced biological activity to their mononuclear counterparts in areas of cancer, malaria and tuberculosis treatment through increased number of active sites.[4–12]

With feedstocks such as alkanes and alkenes readily available from the Fischer-Tropsch Process at Sasol, it is prudent to explore the use of heterometallic organometallic complexes in hydrocarbon conversion. This can be through the design and synthesis of novel catalysts that are more efficient, active and highly selective. The study of heterometallic organometallic complexes in catalysis is still a novel area that warrants further investigation.[13,14]

Catalysis dates back to the 18th century and has developed to become an inter-disciplinary science, making immense contributions in the fields of chemical engineering, organic chemistry and inorganic chemistry.[15,16] Catalytic systems can be divided into two types, heterogeneous and homogeneous catalysis (Table 1.1).[17,18] These are easily distinguished by the different phases present during a reaction. Moreover, of particular interest is the cumbersome separation and recovery of catalyst from the product and solvent that differentiates homogeneous catalysis from heterogeneous catalysis.

Table 1.1 Comparison of homogeneous catalysis against heterogeneous catalysis.[17,18]

Property	Homogeneous catalysis	Heterogeneous catalysis
Phase	Liquid	Solid/liquid ; Solid/gas
Activity	Moderate	High
Selectivity	High	Low
Working temperature / thermal stability	Low (< 250 ºC)	High (250 – 500 ºC)
Catalyst recovery	Difficult and expensive	Easy and cheap
Product separation	Difficult	Easy
Diffusion problems	Facile	May be encountered
Resistance to catalyst poisoning	High	Low
Heat transfer	Easy	Can be problematic

A number of factors are often considered when choosing a catalyst, which include: selectivity; lifetime/ longevity; recyclability, and; loading (amount of catalyst required). A catalyst with good selectivity will yield a high proportion of the desired product with minimum amounts of the side product. Homogeneous catalysts possess good chemoselectivity as well as good regioselectivity characteristics. The high selectivity of homogeneous catalysts makes them ideal for applications in industry and academia. This has contributed to increased interests in homogeneous catalysts and their applications in carbonylation (for example, the Monsanto process)[19–22], hydrogenation (for example, Wilkinson catalyst)[23–25] and hydroformylation reactions.[26–28]

However, due to the drawbacks of homogeneous systems in the recovery of the often expensive organometallic catalysts, research has led to a combination of the two systems to

subdue the disadvantages of a homogeneous system with the advantages of a heterogeneous system. The ultimate goal is to bridge the gap between the two systems through a highly selective system that can operate under mild conditions and offer facile catalyst separation from the product.[18,29]

Several approaches that have been developed are based on catalyst immobilisation onto organic or inorganic supports and immobilisation in biphasic systems (catalysis using two different phases). Employing the former comes with disadvantages of possible leaching of the metal from the catalyst-support matrix into the product, degradation of the support as well as a constrained catalyst which impacts negatively on its mobility for effectiveness.[29–32] In contrast, biphasic catalysis does not only counteract the disadvantage of catalyst separation associated with homogeneous systems but also creates a balance of the advantages of both heterogeneous and homogeneous processes.

1.2 Biphasic Catalysis

Biphasic systems involve the immobilisation of the homogeneous catalyst into another phase, with the catalyst retaining its superior homogeneous catalytic activity and selectivity. The metal catalyst is heterogeneous with respect to the reactants, but the reaction (at an elevated temperature and pressure) occurs in a homogeneous environment. On completion of the reaction, the heterogenised catalyst remains in one phase whereas the product is in the other phase, enabling facile separation of the catalyst for recycling.[30,33]

Various combinations of solvents can be used to create biphasic media, for example, supercritical carbon dioxide – ionic liquids (IL), fluorous – organic and aqueous – organic, all of which have been explored as support media for catalyst immobilisation in biphasic systems (Table 1.2).[30,33,34]

Table 1.2 Common solvents for biphasic systems, their properties and applications.[30,33,34]

Common solvents used in biphasic systems	**Suitability properties to green chemistry principles and immobilisation of metal complexes**	**Applicability of solvent in a biphasic system**
IL	▪ Good stability. ▪ Low volatility. ▪ Ease of modification ▪ Highly polar and suitable for immobilisation of polar complexes.	▪ Hydroformylation. ▪ Hydrogenation. ▪ Oxidation. ▪ Cross coupling. ▪ Metathesis.
$ScCO_2$	▪ Reduced diffusion constraints. ▪ Good catalyst solubility. ▪ Ease of catalyst separation from reaction products.	▪ Hydroformylation. ▪ Hydrogenation. ▪ Cross coupling. ▪ Hydroxylation.
Fluorous solvents	▪ Low polarity and low miscibility with non-polar organic solvents at room temperature. ▪ Inflammable, Low toxicity. ▪ Chemically Inert and resistant to oxidation. ▪ Readily dissolve gases such as oxygen, carbon dioxide and hydrogen.	▪ Hydroformylation. ▪ Epoxidation. ▪ Cross coupling. ▪ Oxidation.
Water	▪ Highly polar and good solvent for many gases. ▪ Abundant and relatively cheap. ▪ Non-flammable and non-toxic. ▪ Immiscible with most organic solvents.	▪ Hydroformylation. ▪ Telomerisation. ▪ Hydrogenation.

The use of eco-friendly support media and the ability of biphasic catalysts to be recyclable reduces the problems associated with the waste generated, in line with green chemistry principles (Figure 1.1).[34–37]

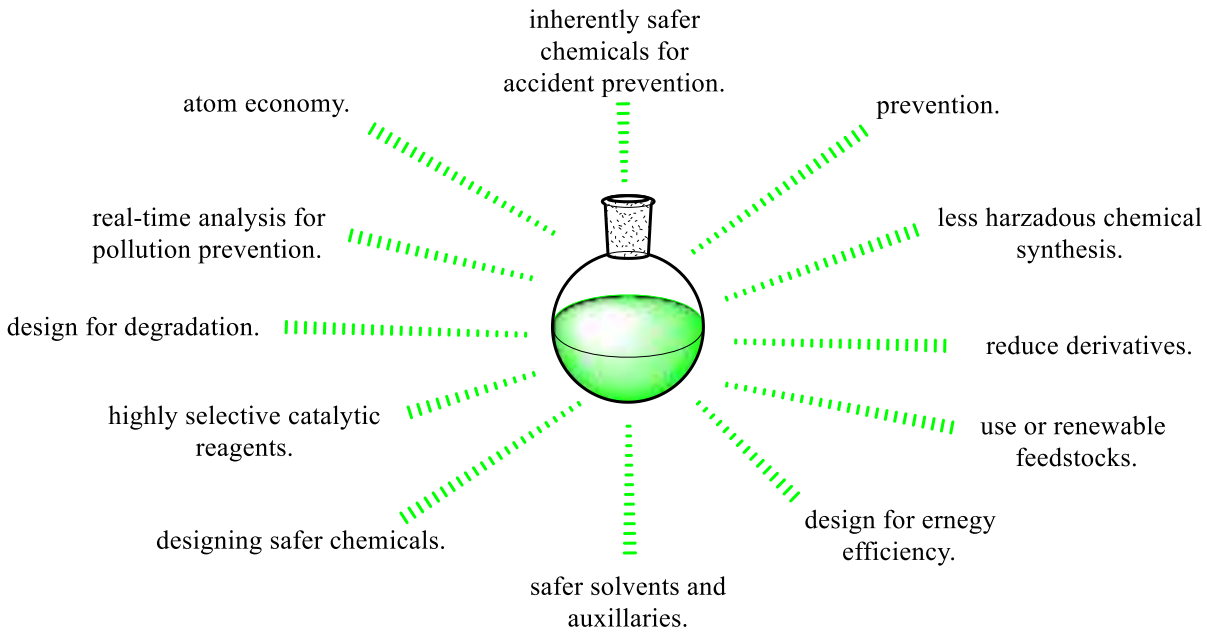

Figure 1.1 Illustration of the 12 Principles of Green Chemistry.[35]

The use of water as a "green" second phase solvent owes to its various properties as an environmentally friendly, relatively inexpensive, abundant, non-flammable and non-toxic solvent. Moreover, water is immiscible with a wide range of organic solvents, a property ideal for separation of a water-soluble catalyst from the hydrophobic reaction products. There is prevention of pollution and waste through the use of eco-friendly solvents (water) and atom-economical processes (hydroformylation).

1.3 Hydroformylation

The hydroformylation process, also known as the "Oxo process", was discovered by Otto Roelen in 1938 on his investigation of the oxygenated products that occurred in Fischer-Tropsch reactions.[38,39] Hydroformylation is an organometallic complex catalysed addition of syngas to olefins leading to aldehydes. The reaction **(**Scheme 1.1**)** has an economical

advantage as the entire reagent atoms are converted to products, a mixture of isomers *n*-aldehydes (linear), and *iso*-aldehydes (branched).[40] Moreover, hydroformylation utilises the easily accessible syngas as its main reagent, making the process more economically favourable as the reagent can be produced from many sources (biomass, coal, natural gas, etc.).

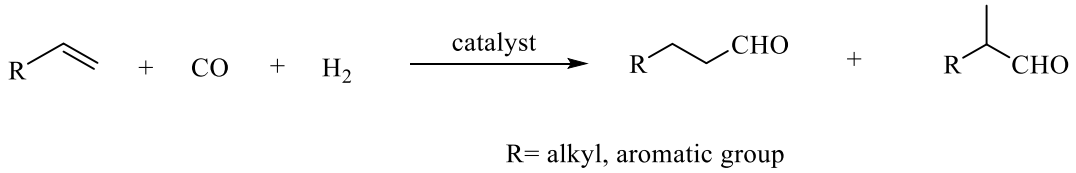

Scheme 1.1 Hydroformylation of olefins.

The first industrial hydroformylation process was based on a cobalt carbonyl complex $H[Co(CO)_4]$. The cobalt-based catalyst had certain drawbacks which included: i) the need for high temperature and pressure to attain average linear selectivity of 80%, ii) formation of unwanted cobalt clusters on industrial reactors, and iii) ease of volatility of the catalytically active species (making catalyst separation and recovery difficult through the conventional distillation process). With growing research interest in hydroformylation, modified cobalt and rhodium-based catalysts were introduced and exhibited improved activity as well as higher selectivity and activity under milder conditions respectively.[26] Use of other transition metal complexes was to follow, though to a lesser extent. These included complexes of iridium, ruthenium, osmium, platinum and palladium. Hydroformylation has become highly important since further conversion of the resultant aldehydes leads to valuable consumer products in the cosmetics, bulk or fine chemicals industries.[39–42]

1.3.1 Mechanism for the rhodium-catalysed hydroformylation

Rhodium is a rare, relatively expensive metal and probably one of the most important transition metals for industrial catalysis applications.[43] Organorhodium is characterised with the ease of oxidative addition to tetra coordinate rhodium(I) and the reductive elimination from octahedral rhodium(III). Such redox reactions bring about the powerful catalytic activity of organorhodium complexes to catalyse a wide range of organic transformations such as hydroformylation, hydrogenation, hydroborations, to mention a few. It is the metal of

preference in transition metal catalysed hydroformylation processes due to its high reactivity and regioselectivity. Unmodified transition metals generally exhibit activities in the order:[44]

$$Rh >> Co > Ir, Ru > Os > Pt > Pd >> Fe > Ni$$

The catalytic cycle for this mechanism **(**Scheme 1.2**)** can be described by the hydroformylation of α-olefin with $[HRh(CO)L_2]$, where L is PPh_3.[45]

The catalytic cycle begins with the 16 electron Rh-H fragment **(1.21)** followed by the coordination of an olefin to a vacant coordination site on Rh to form a 5-coordinate intermediate **(1.22)**. Migratory insertion of olefin into Rh-H gives rise to a 4 coordinate Rh-alkyl compound **(1.23a)** or **(1.23b)** which coordinates a molecule of carbon monoxide in **(1.24a)** or **(1.24b)**. Migratory insertion of CO into the alkyl ligand results in a Rh-acyl complex **(1.25a)** or **(1.25b)**. Anti-Markovnikov addition of hydride onto compound **(1.25b)** gives the linear aldehyde product whereas Markovnikov addition onto compound **(1.25a)** leads to the branched aldehyde product. The hydrogenolysis of the Rh-acyl complex is also accompanied with the regeneration of the Rh-H complex **(1.21)**.[45] The selectivity of the hydride addition is controlled by the hydride acidity and the steric constraints of the ligands. It is therefore expected that sterically demanding ligands such as triarylphosphines will be more inclined to the formation of linear aldehydes through anti-Markovnikov addition.

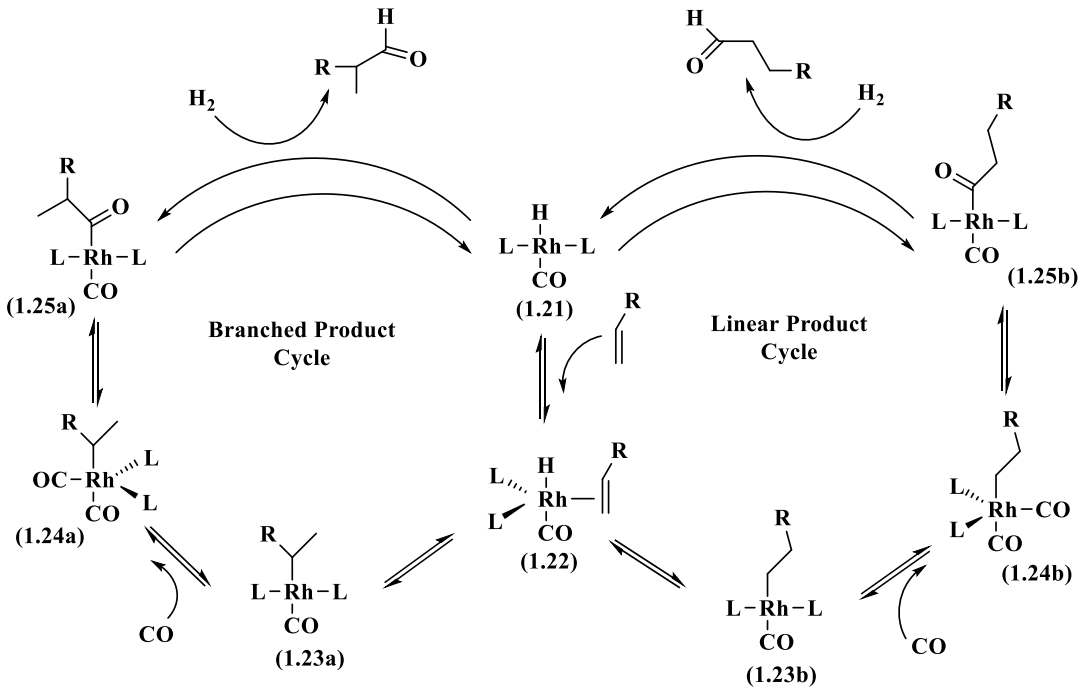

Scheme 1.2 Mechanism of Rh-catalysed hydroformylation.[45]

The bias towards aldehydes (chemoselectivity) as well as the ratio of linear to branched aldehydes (regioselectivity) has a huge bearing on the catalyst evaluation for industrial applications. This can be fine-tuned by varying a number of factors such as pressure, temperature, solvent/ support system as well as ligand modification.[46,47]

The modified Wilkinson-rhodium-based catalyst introduced in the 1970's $[HRh(CO)(PPh_3)_3]$ was only suitable for low boiling/ short chain olefins.[18] The catalyst decomposed at the high temperatures required for distillation of the high boiling/ long chain olefins. Moreover, the poor solubility of the long chain olefins in polar and greener solvents such as water necessitated a new approach to conducting the hydroformylation of the high molecular weight olefins. This led to further ligand modification (discussed in the following section) so as to solubilise the catalyst in the polar solvent for implementation in an aqueous biphasic catalytic system.[48,49] This would immobilise the catalyst in the aqueous phase (good for catalyst recovery and product separation) as well as achieve functionalization of long chain olefins.

1.4 Aqueous biphasic media in hydroformylation

Aqueous biphasic systems represent the more widely studied method of biphasic catalysis.[50,51] The technique was first applied at an experimental level in olefin hydroformylation by E. Kuntz at Rhône-Poulenc, and later commercialised by Ruhrchemie. This two-phase catalysis, formerly known in the industry as the Ruhrchemie/Rhône-Poulenc 'oxo' process, is currently the OXEA Process.[39,40,52,53] The process is based on the water-soluble rhodium metal complex $[Rh(H)(CO)(TPPTS)_3]$, (Figure 1.2).[54]

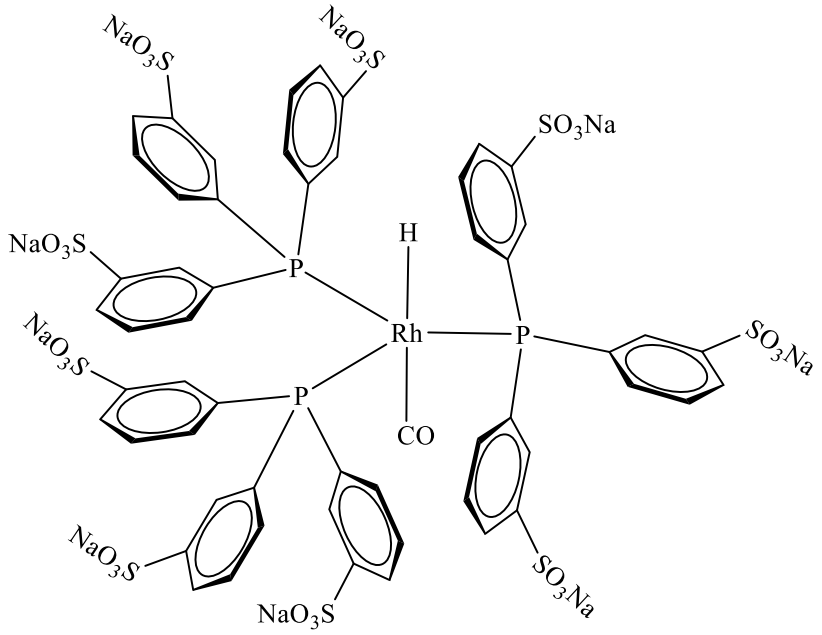

Figure 1.2 Water-soluble catalyst used in the Ruhrchemie/Rhône-Poulenc process.[29]

The catalyst is obtained by ligand modification of the conventional rhodium metal complex [$HRh(CO)(PPh_3)_3$] mentioned in the previous section.[54] The sulfonated triphenylphosphine ligands impart solubility to the metal complex, due to the water-soluble sulfonate group. Various highly polar-substituents (–SO_3H, –OH, –COOH or –NH_2) or their salts can be incorporated into ligands to achieve water-soluble complexes.[55] Varying the nature and number of the substituents as well as the conditions of reaction allows for the manipulation of the two-phase technique to the desired ratio of hydrophilic and hydrophobic properties.[56]

To initiate and effect the catalytic reaction, the two immiscible phases (aqueous and organic) are brought into contact by vigorous stirring and application of heat and pressure (Figure 1.3). On completion of the reaction, the product (in the organic phase) is separated from the water-soluble catalyst by simple decantation, allowing for the recycling of the catalyst-containing aqueous layer.[41,57,58] This separation and recovery technique is appealing in the hydroformylation of long chain alkenes whose aldehydes are of high boiling point and cannot be recovered without decomposition and/ deactivation of the catalyst when conventional thermal techniques such as distillation are employed.[56] Moreover, such value-adding efforts aid in the recovery of the expensive and ever-diminishing transition metal catalysts. [57,59]

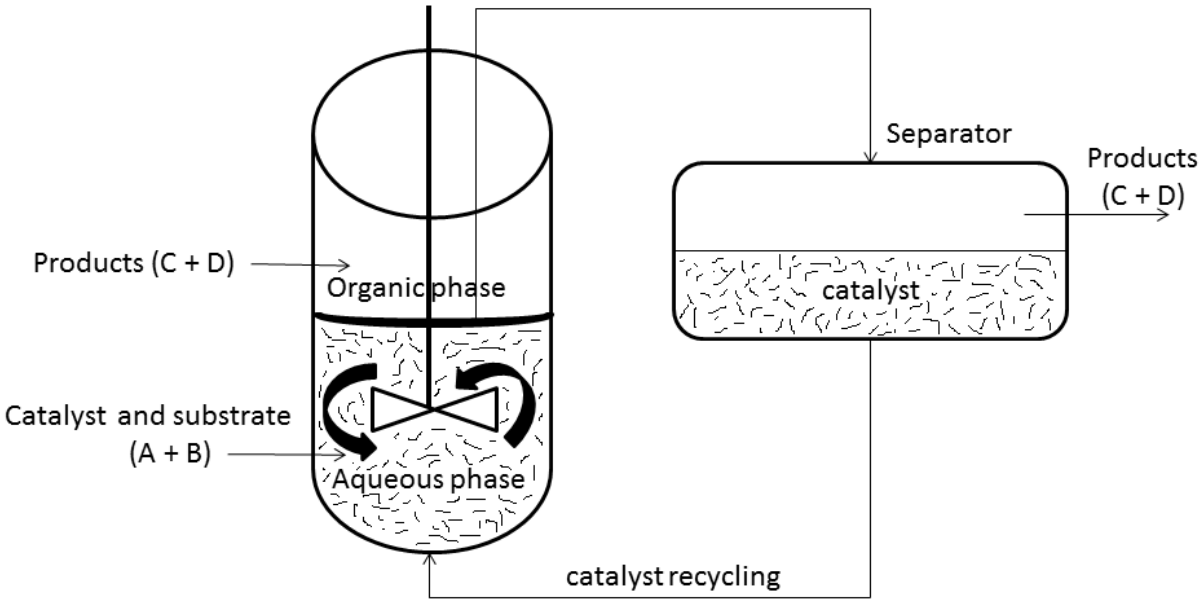

Figure 1.3 Illustration of aqueous biphasic catalysis.[57]

The continued modification of the water-soluble $[Rh(H)(CO)(TPPTS)_3]$ catalyst has given rise to more promising catalytic species with good activity and selectivity towards the hydroformylation of higher olefins.

Chaudhari and co-workers investigated the use of triphenylphosphine as a promoter ligand in the $[Rh(H)(CO)(TPPTS)_3]$ metal complex for hydroformylation of 1-octene.[60] Using their approach, the interaction of the catalyst complex with the poorly water-soluble substrate is improved by the coordination of the hydrophobic promoter ligand to the organometallic catalyst (Figure 1.4) through ligand exchange. The hydrophobic triphenylphosphine ligand has an effect of drawing the resultant mixed-ligand complex $[Rh(H)(CO)(TPPTS)_{3-x}(TPP)_x]$ to the aqueous-organic inter-phase layer. There is an increased catalyst concentration in the aqueous-organic boundary thus enabling the new catalytic species to access the reactants present in the organic phase in significantly higher concentrations with respect to the aqueous phase. An overall reaction rate enhancement by a factor of 10-50 was realised.[60]

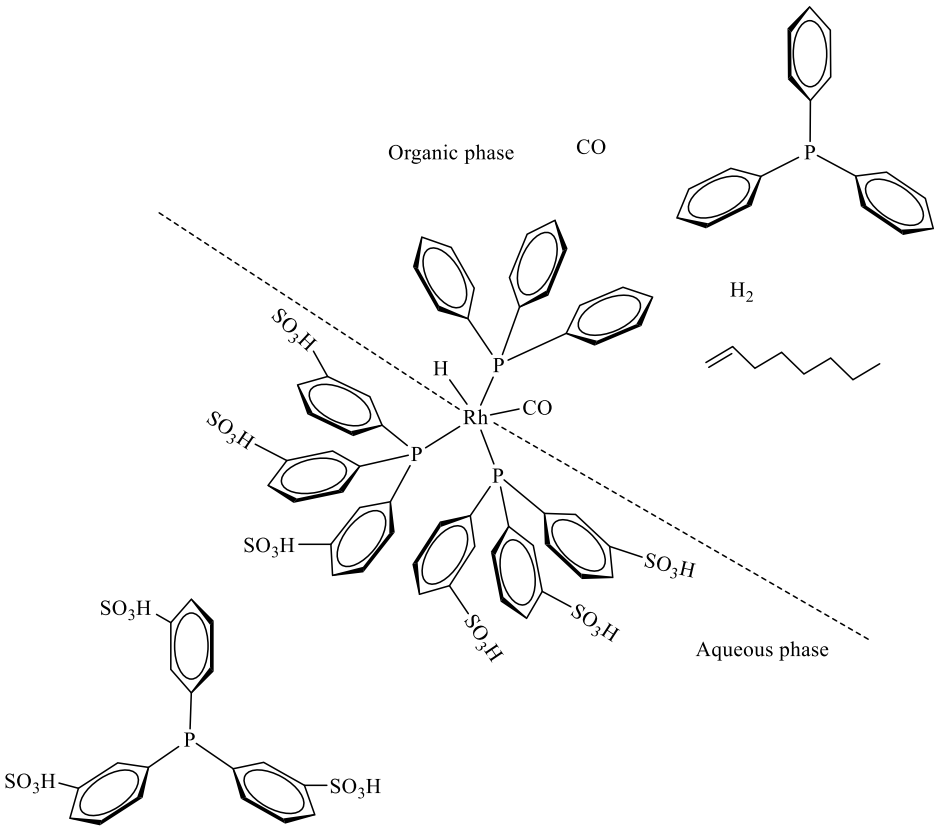

Figure 1.4 Illustration of a promotion in higher olefin hydroformylation.[60]

Barricelli and co-workers carried out a comparative study of rhodium-catalysed hydroformylation of C_6 alkenes and alkene mixtures in homogeneous and aqueous biphasic media using PPh_3, TPPTS and TPPMS ligands.[61] In their study, they determined that the side reactions emanating from isomerisation of the olefins could be suppressed by using higher but reasonable pressures (50 atm), and the aqueous biphasic systems of $[RhH(CO)(TPPTS)_3]$ and $[RhH(CO)(TPPMS)_3]$ can be employed under moderate reaction conditions. These could in the future be used as alternatives for the treatment of naphtha as well as for addressing related fuel upgrading issues.

Water-soluble bidendate ligands have also been shown to possess good catalytic activity. For example, Matsinha and co-workers reported on the water soluble Rh(I) mononuclear complexes in the aqueous biphasic hydroformylation of 1-octene (Figure 1.5).[62] The sulfonated salicylaldimine Rh(I)-based complexes posted good selectivity as well as good catalytic activity and could be recycled up to 5 times. The presence of the chloro- and methyl- groups did not have any significant effect on the chemoselectivity of these catalyst precursors. The bulky tertiary-butyl substituent imparts steric crowding around the metal centre, driving the regioselectivity to the linear aldehyde (nonanal). Hager and co-workers

also observed similar behaviour with the bulkier tertiary-butyl substituent of similar compounds.[63]

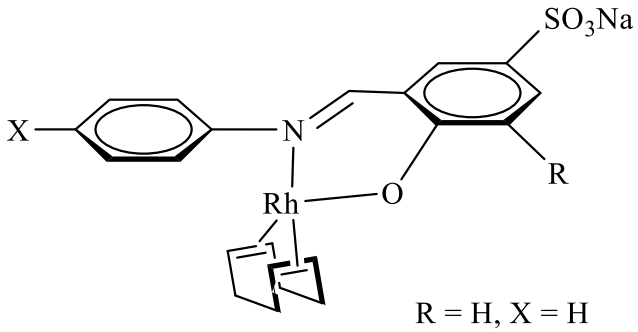

R = H, X = H
R = H, X = CH_3
R = H, X = Cl
R = ^{t}Bu, X = H

Figure 1.5 Water-soluble sulfonated salicyldimine complexes used in the aqueous biphasic hydroformylation of 1-octene.[62]

Aqueous biphasic catalysis is often confounded by phase transfer limitations, catalyst leaching to the organic layer, as well as poor substrate solubility in water. These factors result in low reaction rates and low selectivity of a catalyst. Cyclodextrins have been applied to improve on the reaction rates through their ability to transfer the substrate (often applied for longer chain olefins in hydroformylation) from the organic phase to the aqueous phase during the reaction.[64] Cyclodextrins have extended to a wide range of reactions involving biphasic media, leading to better activity, selectivity and recyclability.[65–78]

1.4.1 Cyclodextrins for aqueous biphasic hydroformylation

Cyclodextrins are a class of cyclic oligosaccharides that are often used to improve mass transfer in aqueous-organic biphasic media (Scheme 1.3). Their classification depends on the number of D-glucopyranose units and these constitute the α-cyclodextrins (six), β-cyclodextrins, (seven) and the γ-cyclodextrins (eight). The β-cyclodextrins are mostly used because they are readily available, lowly priced and possess the optimal size for the cavity compared to the α- and γ-cyclodextrins. The larger aperture (as in γ-cyclodextrins) and the smaller aperture (as in α-cyclodextrins) often results in low conversions.[79,80]

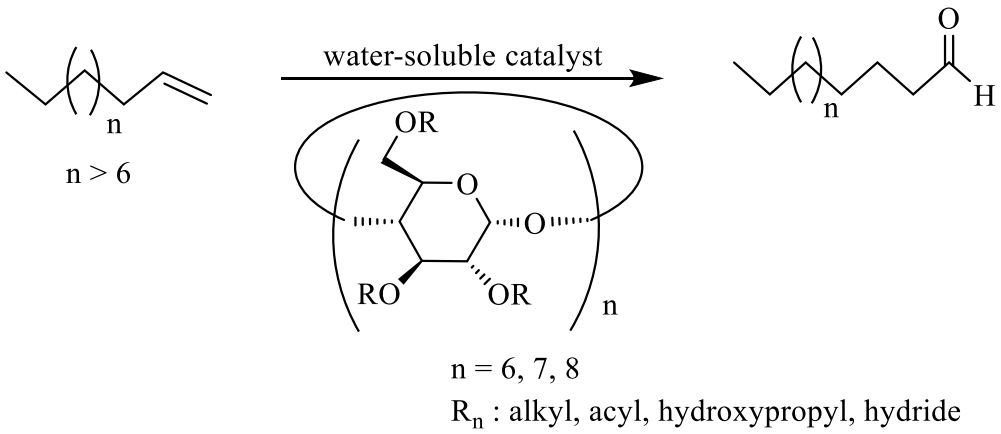

Scheme 1.3 Typical olefin hydroformylation reaction using cyclodextrins.

Their use in aqueous biphasic media stems from the unique structure, that is, the hydrophobic core (inner surface) for inclusion of the organic substrate and the hydrophilic exterior for interaction with water during the reaction. These interesting compounds of supramolecular structure can be chemically modified to: i) improve on the rates and selectivity of reactions in water, ii) stabilise the catalytic species in water, iii) improve on the cyclodextrin inclusion complex properties, iv) afford new water-soluble catalysts, v) reduce the catalyst leaching, and vi) perform substrate-selective catalytic reactions.[81–84] The organometallic catalyst can come into contact with the substrate at the water/organic interface or contact can be in the aqueous phase through inclusion of the substrate in the core of the cyclodextrin or modified cyclodextrin.

Monflier and co-workers reported on the functionalisation of water-insoluble olefins in the rhodium catalysed aqueous biphasic hydroformylation of 1-decene assisted by chemically modified β-cyclodextrins (to improve mass transfer between organic and aqueous phases).[85] Excellent conversion (95%) and high reaction rates were registered with a methylated-β-cyclodextrin, compared to non-modified β-cyclodextrin. Lower reaction rates were registered in the absence of the native β-cyclodextrin. The effectiveness of the chemically modified β-cyclodextrin was ascribed to the solubility in both aqueous and organic phases, allowing inclusion of the organic substrate and facile release of the undecanal product (for the cycle to go on).

Other well documented approaches of achieving water-solubility for high molecular weight substrates and in-turn good reaction rates and selectivity are through thermoregulated

transfer[86–94] as well as use of surfactants.[95–105] These techniques are important for industrially explored reactions such as hydroformylation.

Whereas conventional metal-based catalysts consist of a single metal centre, it has been found that introducing a second metal has the effect of enhancing catalytic activity compared to the mononuclear analogues.[106] This is due to the unique cooperative interactions that may exist between proximate metal centres.

1.5 Bimetallic complexes

Synthetic chemists continue to extend the design of catalysts to mimic naturally occurring metal-containing enzymes (bearing two or more active sites).[107,108] These synthetic catalysts are designed in a way that imitates the characteristics of biocatalysts, having synergistic and cooperative effects between bimetallic active sites contained therein.

Park and Hong reported a detailed structural review on the classification of different kinds of bimetallic catalysts (eight types), (Figure 1.6).[109] The cooperative effects of the metal centres are realised most efficiently when the two metals are in close proximity (optimum separation of 3.5 – 6 Å), with one metal acting as a Lewis acid for activating electrophiles, while the other metal ion serves as the counterion of nucleophiles.[110] At the optimum separation, even without direct interactions between the metal centres, their close proximity will allow interaction of the substrate with both metal centres or close binding of two reactants to the adjoining metal centres.

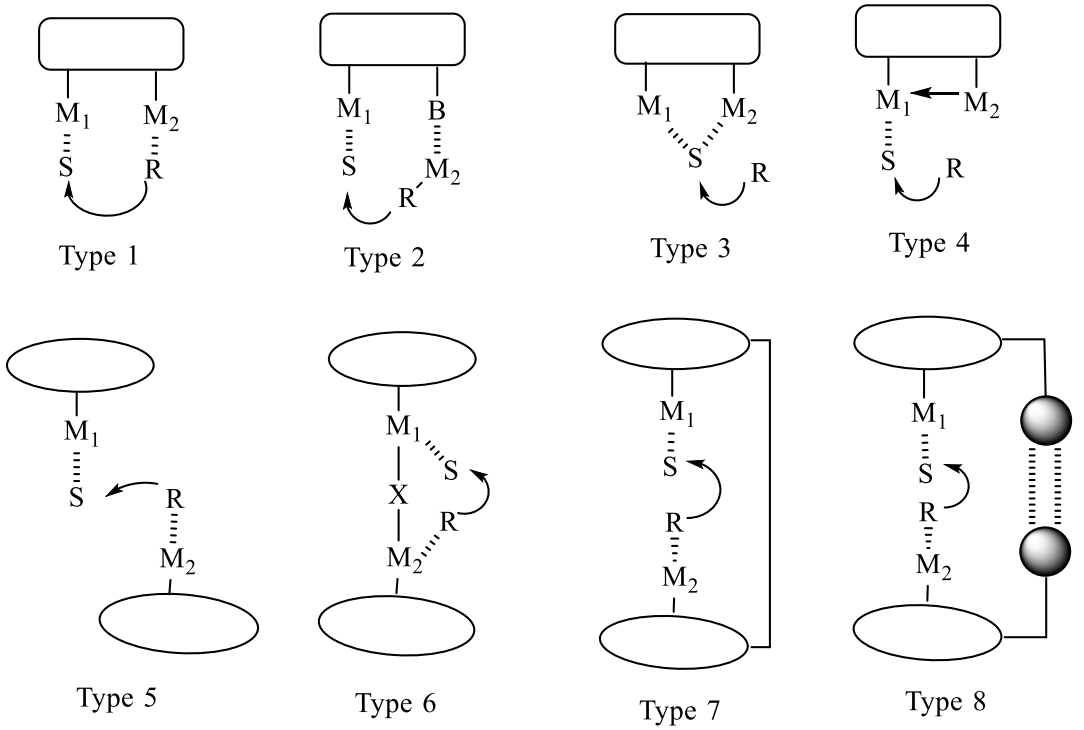

Figure 1.6 Illustration of bimetallic catalysts, where S: substrate, M: metal, and R: reactant.[109]

Combining multiple catalytic sites into a single ligand structure can improve the reactivity of a catalytic system through induced cooperative activation, selective substrate binding, and improved catalytic efficiency (activity and/or selectivity). The metals can either be the same (homobimetallic compounds), or different (heterobimetallic compounds).[110–113]

Stanley and co-workers have used a *racemic* bimetallic rhodium complex *rac*-$[Rh_2(nbd)_2(et,ph\text{-}P_4)](BF_4)_2$ (nbd = norbonadiene, et = ethyl, ph = phenyl) for the hydroformylation of 1-hexene, giving both a higher rate of reaction and higher regioselectivity for linear aldehydes compared to the same reaction with the Rh/PPh_3 which is considerably slower and less selective.[112] They proposed a catalytic cycle that entails an intramolecular transfer of a hydride from one rhodium centre to the other centre which contains the acyl chain, resulting in the aldehyde. The close proximity of the metal centres permits such a transfer.

Where different metals have been used (as in heterobimetallics), the two metals are often expected to perform different functions. This allows for selective functionalisation of the substrate.

1.6 Heterobimetallic complexes

Unlike homometallic systems, cooperation between two different metals in heterobimetallic organometallic complexes offers a more diverse application of multimetallic systems, since the two metals can perform different tasks.[114–117] One metal can act as the catalytic centre whereas the second metal can serve as a reservoir for electrons, stabilising the electron density around the catalytic centre. [111,112,118,119] Such cooperative interactions between the metals depend on the proper arrangement of the different metals in close proximity.

The redox active, chemically robust and synthetically versatile ferrocene has been studied in heterobimetallic complexes with other active metal centres bound by various ligand structures. Phosphorus donor sites have been dominantly used to provide the required modification of the ferrocene moiety.[120] Moreover, ferrocene is an ideal structural motif for application in heterobimetallic complexes owing to its good thermal stability as well as its high tolerance to moisture, air, and in a number of reagents.[121]

Trzeciak and co-workers reported the hydroformylation of 1-hexene using mono- and bidentate complexes of Rh(I) with 1′-(diphenylphosphino)ferrocenecarboxylic acid.[122] The catalysts showed good chemoselectivity for aldehydes (approximately 80%) under mild reaction conditions (80 °C, 10 bar). The ferrocene moiety served as a support for varying the stereoelectronic properties of the substituents through phosphine and phosphite modifying ligands. The ferrocene-based strong σ-donor phosphines revealed reduced chemoselectivities for aldehydes, in contrast to the π-acceptor phosphites. The activity and selectivity can be tailored by the substituents on the ferrocenyl moiety of the complexes and this has been observed in similar ferrocenyl-Rh(I) catalytic systems.[123–126]

The versatility of ferrocene as a result of its rich chemistry, stability and redox properties has seen growing interests for its use as a backbone for phosphines in hydroformylation.[121,127] Since the development of the phosphorous containing Wilkinson catalyst [$RhCl(PPh_3)_3$], the development of new phosphines has been a focus for synthetic chemists.[128] Hey-Hawkins and co-workers prepared heterobimetallic complexes of Rh(I) with a series of ferrocenyl-substituted phosphaheterocycles bearing sulphur and oxygen atoms (to influence electronic properties).[129] The premise of their study was on the versatility of ferrocene as well as the bulky phosphorus ligands which might offer improved selectivity. The oxygen containing ferrocenyl-substituted phosphaheterocycle (Figure 1.7) was evaluated as a ligand for *in situ*

monophasic (in toluene) hydroformylation of various substrates (styrene, 1-hexene, ethyl methacrylate and dimethyl itaconate) catalysed by $[Rh(acac)(CO)_2]$. The heterobimetallic catalytic species showed an increased reactivity and regioselectivity for branched aldehydes with respect to ethyl methacrylate, a significant improvement over when $[Rh(acac)(CO)_2]$ was used without the ferrocenyl ligand.

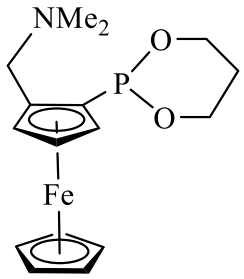

Figure 1.7 The ferrocenyl-phosphaheterocycle ligand used for *in situ* hydroformylation reactions.

The flexibility of a ligand has also been proven to influence selectivity in the hydroformylation experiments conducted with 1-octene substrate. Bourissou and co-workers reported the hydroformylation of 1-octene using *in situ* generated heterobimetallic pre-catalyst formed from $[Rh(acac)(CO)_2]$ with the flexible ferrocenyl-based ambiphilic ligand as well as a rigid phosphine-borane system (**1** and **2** respectively, Figure 1.8).[130] Good selectivity for nonanal (72%) was obtained with the ferrocenyl based ligand. In the same study, similar results were obtained with a related borane-free ligand (diphenylphosphinoferrocene). This suggests that the observed linear product selectivity was not sterically influenced by the $BMes_2$ substituent group. Moreover, further hydroformylation experiments with the rigid phosphine-borane ligand (that is, in the absence of ferrocene) gave reduced activity and selectivity (54% linear product), revealing the influence of ferrocene to the selectivity for linear aldehydes in the heterobimetallic system. Hughes and Unruh also reported increased linear selectivity with similar flexible and rigid ligands in the hydroformylation of 1-hexene.[131]

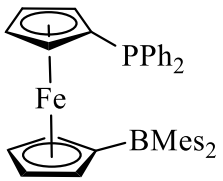

1

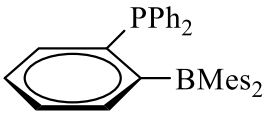

2

Figure 1.8 Flexible (**1**) and rigid (**2**) ligands used for the hydroformylation of 1-octene.

Increasing the nuclearity of a catalyst is another avenue that is at its infancy; the research is slowly gathering momentum (discussed in the section to follow). Having multiple active centres has the effect of improving on reaction rates. Moreover, steric effects due to the bulkiness of a multinuclear structure can be fine-tuned to manipulate the selectivity of a catalyst. This is being explored through metallodendritic structures.

1.7 Metallodendrimers

Metallodendrimers are large highly branched macromolecular structures that incorporate metals into dendritic arms propagating from the core of the dendrimer.[132] The metals anchored onto the dendrimer surface act as multiple catalytically active sites, allowing for enhanced catalytic activity over monometallic catalysts. These structures of unique conformation have been largely explored for biological and catalytic applications.[132–138]

Fonseca and co-workers investigated the hydroformylation of 1-hexene and naphtha using a water-soluble [RhCl(CO)($PySO_3Na)_2$] complex. The complex exhibited good catalytic activity for both substrates as well as good regioselectivity to the linear aldehyde for 1-hexene.[139]

Water-soluble rhodium based metallodendrimers have also been developed for catalytic applications.[138] Hager and co-workers investigated the aqueous biphasic hydroformylation of 1-octene using complexes of $[RhCl(COD)]_2$ with dendritic ligands based on tris-2-(5-sulfonato salicylaldimine ethyl)amine and DAB(5-sulfonato salicylaldimine).[63] Thermal and pressure regulated selectivity was observed through varying the conditions of pressure and temperature. Also reported is the good recyclability of the catalyst precursors over at least five cycles and consistent chemoselectivities as well as regioselectivities throughout the

cycles. However, the dendritic complexes did not show any improved catalytic activity over their mononuclear counterparts, an observation they attributed to poor stability of the macromolecular structures in water.

Gong and co-workers prepared water-soluble dendritic ligands of phosphine on PAMAM molecular surface complexed with Rh(I).[140] These were evaluated as aqueous biphasic catalysts for the hydroformylation of styrene and 1-octene. The phosphonated PAMAM dendrimers revealed good regioselectivity towards *iso*-aldehydes (i/n, 15:1) when used in the hydroformylation of styrene. The branched *iso*-aromatic aldehydes are of significance as intermediates in the pharmaceutical industry. Hydroformylation of 1-octene was however characterised with poor *iso*-aldehyde selectivity of 1:2. The water-soluble Rh(I) metallodendrimers showed high *iso*-aldehyde selectivity in the hydroformylation reactions of both substrates (styrene and 1-octene) compared to the mononuclear TPPTS-based Rh(I) complexes reported by Cornils and Kuntz[48], and Hanson et al[141] respectively. Similar behaviour has been reported with the organic mono-phase hydroformylation using dendritic complexes and their monomeric analogues. [133,142–144]

While the use of metallodendrimers in hydroformylation is yet to make profound breakthrough over their monomeric analogues, efforts to fine-tune dendritic catalytic properties through a tailor-made systematic adjustment of their structure, solubility, shape and size remain of interest.

1.8 Motivation for this study

Combining rhodium complexes with the chemically robust and redox-active ferrocene to form new water-soluble heterometallic complexes is of interest. This is in view of the continued pursuit towards the design of new organometallic complexes that possess intriguing properties. It is hypothesised that the heterometallic complexes would fuse together the well-known high catalytic activity and selectivity properties of rhodium complexes with the versatile properties of ferrocene. Application of such complexes in the aqueous-organic biphasic hydroformylation reaction of higher olefins from an efficient catalyst design and green chemistry perspective is also intriguing. Moreover, despite the known improved reactivity of catalyst systems containing two or more metals as compared to their monometallic counterparts, application of heterobimetallic systems in catalysis is still at its

infancy. There is minimal documentation about heterometallic systems in hydroformylation, prompting our interest to investigate the application of heterometallic systems as hydroformylation catalyst precursors.

1.9 Summary/ Concluding remarks

Hydroformylation is an industrially significant catalytic reaction that supplies aldehydes for a wide range of downstream applications, such as in the polymer industry (plastics), pharmaceuticals, soaps and detergents industry, to mention a few. Industrial application of the reaction for long chain olefins is limited by the poor solubility of the olefins as well as the associated recovery challenges of the products and the catalyst (for recycling). The use of biphasic media serves as a support for the catalyst and the substrate. Moreover, the products and catalyst are easily recovered by simple phase separation techniques. New ligand design and synthesis continue to be explored as a means to improve reaction rates and selectivity of catalysts. Natural metalloenzymes (bearing two or more metals) display improved rates for catalysis, and this has served as a platform to design catalysts bearing two or more metals for application in aqueous biphasic hydroformylation. Different metals anchored on an organic framework can perform different tasks in a heterobimetallic catalytic species, allowing manipulation of the rate and selectivity. In light of the minimal available research findings on enhancement of catalytic activity through heterometallic catalyst systems, research pertaining to these systems is slowly gathering momentum.

1.10 Research Aims and Objectives

1.10.1 General Aims

The aim of this project is to design, synthesise and characterise water-soluble ferrocenyl-rhodium heterometallic organometallic complexes, and to evaluate their effectiveness as aqueous biphasic hydroformylation catalysts.

1.10.2 Specific Objectives

- Syntheses and characterisation of water-soluble sulfonate ligands.[63]

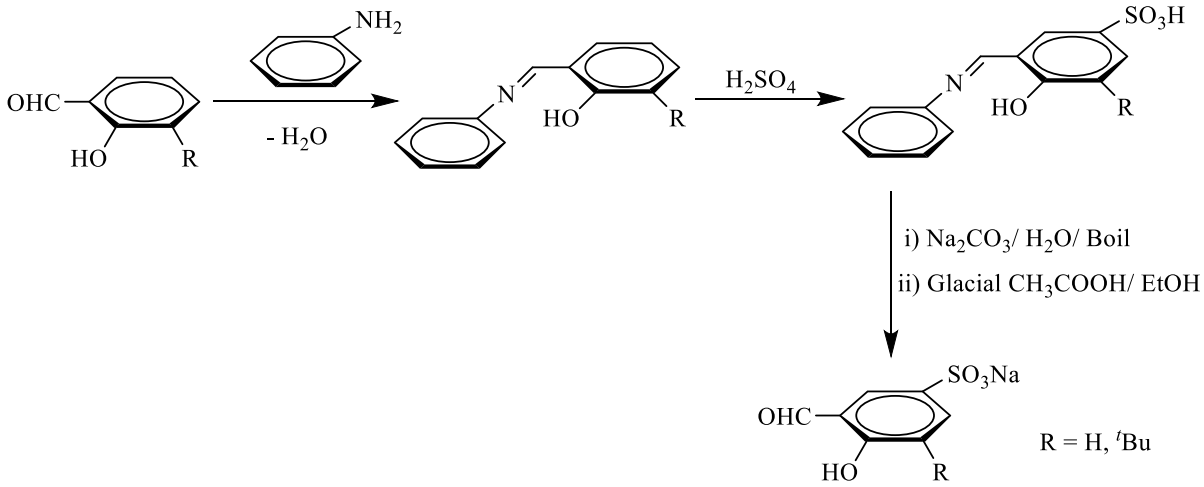

Scheme 1.4 Syntheses of water-soluble monosulfonate ligands.

- Syntheses and characterisation of 5-sulfonatosalicylaldimine ligands.

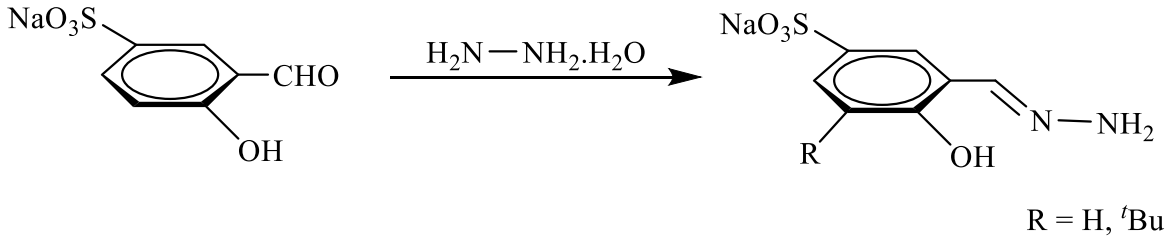

Scheme 1.5 Syntheses of water-soluble hydrazone-based ligands.

- Syntheses and characterisation of sulfonatosalicylaldimine-ferrocenylimine mononuclear complexes.

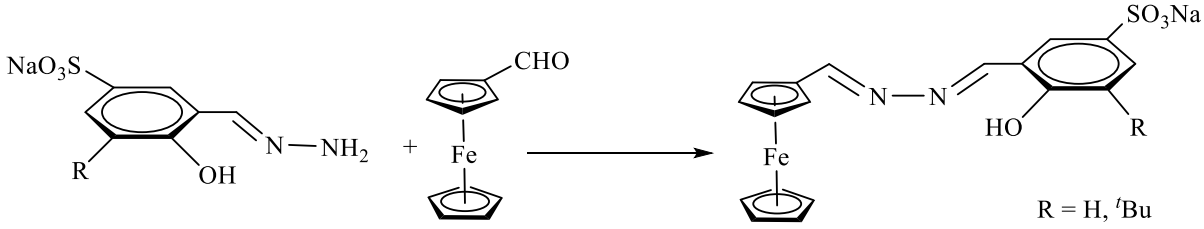

Scheme 1.6 Syntheses of water-soluble ferrocenylimine mononuclear complexes.

- Syntheses and characterisation of heterobimetallic sulfonatosalicylaldimine-ferrocenylimine-Rh(I) complexes.

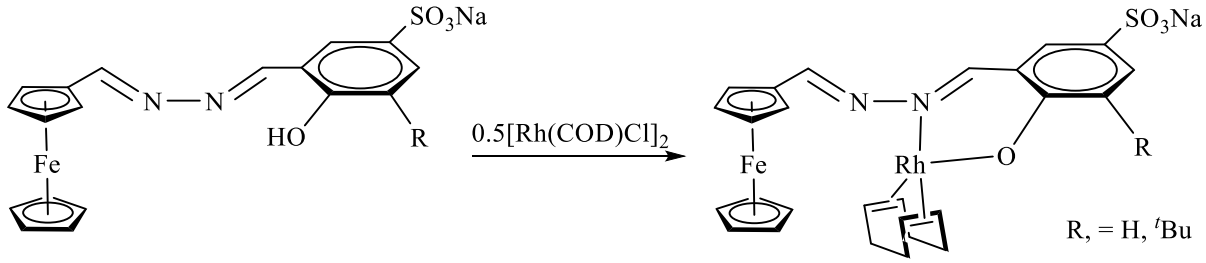

Scheme 1.7 Syntheses of water-soluble ferrocenylimine-Rh(I) heterobimetallic complexes.

- Syntheses and characterisation of formylated ferrocenylimine mononuclear complexes.

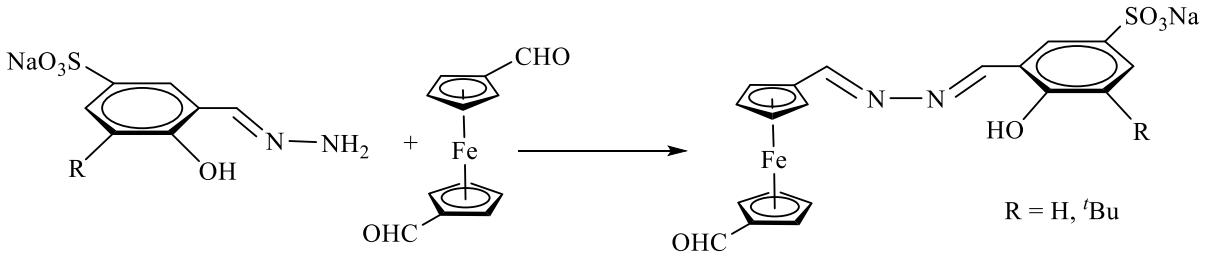

Scheme 1.8 Syntheses of water-soluble formylated mononuclear complexes.

- Syntheses and characterisation of formylated ferrocenylimine-Rh(I) heterobimetallic complexes.

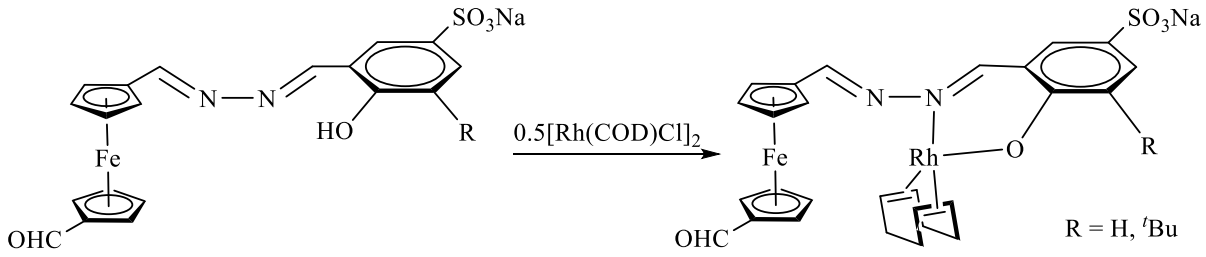

Scheme 1.9 Syntheses of water-soluble formylated heterobimetallic complexes.

- Syntheses of low generation water-soluble heterometallic dendrimers based on DAB.

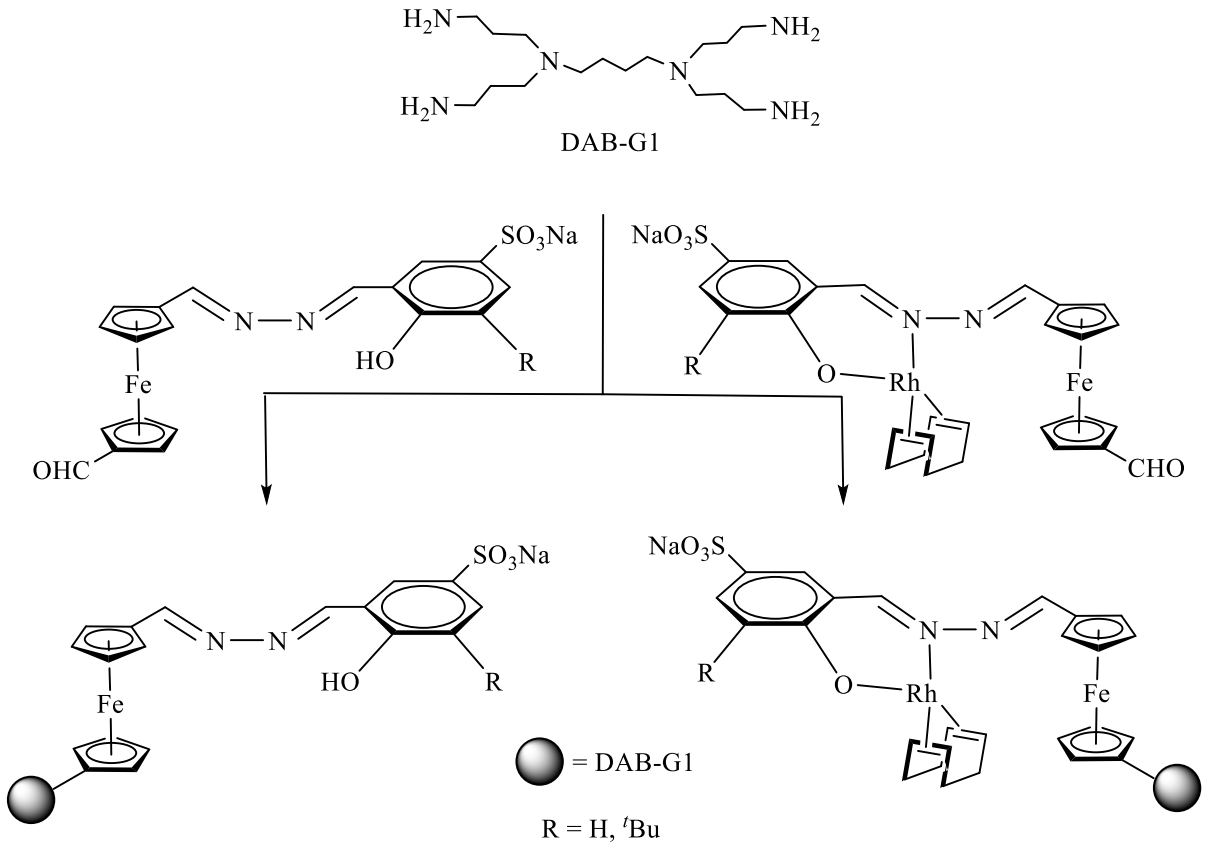

Scheme 1.10 Syntheses of water-soluble DAB-G1 metallodendrimers.

- Evaluation of the water-soluble complexes as potential catalysts for the aqueous biphasic hydroformylation of 1-octene.

1.11 References

1. J. I. van der Vlugt, *Eur. J. Inorg. Chem.*, 2012, **2012**, 363–375.

2. P. Buchwalter, J. Rosé, and P. Braunstein, *Chem. Rev.*, 2015, **115**, 28–126.

3. H. Pellissier, *Tetrahedron*, 2013, **69**, 7171–7210.

4. M. Adams, C. De Kock, P. J. Smith, P. Malatji, A. T. Hutton, K. Chibale, and G. S. Smith, *J. Organomet. Chem.*, 2013, **739**, 15–20.

5. N. Lease, V. Vasilevski, M. Carreira, A. De Almeida, M. Sanau, P. Hirva, and A. Casini, *J. Med. Chem.*, 2013, **56**, 5806–5818.

6. P. Govender, A. K. Renfrew, C. M. Clavel, P. J. Dyson, B. Therrien, and G. S. Smith, *Dalton Trans.*, 2011, **40**, 1158–1167.

7. C. Ornelas, *New J. Chem.*, 2011, **35**, 1973.

8. S. H. van Rijt and P. J. Sadler, *Drug Discov. Today*, 2009, **14**, 1089–1097.

9. W. Nkoana, D. Nyoni, P. Chellan, T. Stringer, D. Taylor, P. J. Smith, A. T. Hutton, and G. S. Smith, *J. Organomet. Chem.*, 2014, **752**, 67–75.

10. P. Chellan, K. M. Land, A. Shokar, A. Au, S. H. An, D. Taylor, P. J. Smith, K. Chibale, and G. S. Smith, *Organometallics*, 2013, **32**, 4793–4804.

11. M. Berardini, T. J. Emge, and J. G. Brennan, *Inorg. Chem.*, 1993, **32**, 2724–2728.

12. M. Serrano-Ruiz, L. M. Aguilera-Sáez, P. Lorenzo-Luis, J. M. Padrón, and A. Romerosa, *Dalton Trans.*, 2013, **42**, 11212–9.

13. S. K. Goforth, R. C. Walroth, and L. McElwee-White, *Inorg. Chem.*, 2013, **52**, 5692–701.

14. K. Nakao, G. Choi, Y. Konishi, H. Tsurugi, and K. Mashima, *Eur. J. Inorg. Chem.*, 2012, **17**, 1469–1476.

15. B. Lindström and L. J. Pettersson, *CatTech*, 2003, **7**, 130–138.

16. J. Wisniak, *Educ. quim.*, 2010, **21**, 60–69.

17. E. Farnetti, R. Di Monte, and J. Kašpar, *Inorg. Bio-inorganic Chem.*, 1999, 2, 1–15.

18. C. E. Housecroft and A. G. Sharpe, in *Inorganic Chemistry*, Pearson Education Limited, Edinburgh, 2nd edn., 2002, vol. 63, pp. 786–807.

19. T. L. Church, Y. D. Y. L. Getzler, C. M. Byrne, and G. W. Coates, *Chem. Commun.*, 2007, 657–74.

20. N. Yoneda, S. Kusano, M. Yasui, P. Pujado, and S. Wilcher, *Appl. Catal. A Gen.*, 2001, **221**, 253–265.

21. G. J. Sunley and D. J. Watson, *Catal. Today*, 2000, **58**, 293–307.

22. P. W. N. M. Leuman, in *Homogeneous Catalysis: Understanding the Art*, Kluwer Academic Publishers, Netherlands, 1st edn., 2004, pp. 75–81.

23. C. O'Connor, G. Yagupsky, D. Evans, and G. Wilkinson, *Chem. Commun.*, 1968, **38**, 420–421.

24. I. P. Theor, B. J. A. Osborn, F. H. Jardine, J. F. Young, and G. Wilkinson, *J. Chem. Soc.*, 1966, 1711 – 1731.

25. R. E. Harmon, S. K. Gupta, and J. Brown, *Chem. Rev.*, 1973, **73**, 21–52.

26. M. Beller, B. Cornils, C. D. Frohning, and C. W. Kohlpaintner, *J. Mol. Catal. A Chem.*, 1995, **104**, 17–85.

27. R. L. Pruett, *J. Chem. Educ.*, 1986, **63**, 196–198.

28. S. M. Mercer, T. Robert, D. V. Dixon, and P. G. Jessop, *Catal. Sci. Technol.*, 2012, **2**, 1315–1318.

29. A. E. C. Collis and I. T. Horváth, *Catal. Sci. Technol.*, 2011, **1**, 912–919.

30. B. Cornils, W. A. Herrmann, I. T. Horvath, W. Leitner, S. Mecking, H. Olivier-Bourbigou, and D. Vogt, in *Multiphase Homogeneous Catalysis*, Wiley-VCH Verlag GmbH & Co. KGaA, Weinheim, 2nd edn., 2005, pp. 3–21.

31. Â. C. B. Neves, M. J. F. Calvete, M. V. D. Pinho, and M. M. Pereira, *Eur. J. Org. Chem.*, 2012, 6309–6320.

32. D. J. Cole-Hamilton, *Catalysis*, 2003, **299**, 1702–1707.

33. E. A. Karakhanov and A. L. Maksimov, *Russ. J. Gen. Chem.*, 2009, **79**, 1370–1383.

34. M. Lombardo and C. Trombini, in *RSC Green Chemistry Series: Eco-Friendly Synthesis of Fine Chemicals*, Royal Society of Chemistry, 1st edn., 2009, pp. 1–79.

35. P. T. Anastas and J. C. Warner, *The 12 Principles of Green Chemistry*, Oxford University Press, New York, 1998.

36. P. T. Anastas and J. B. Zimmerman, *Environ. Sci. Technol.*, 2003, **37**, 95–101.

37. R. A. Sheldon, I. Arends, and U. Hanefeld, in *Green Chemistry and Catalysis*, Wiley-VCH Verlag GmbH & Co. KGaA, Weinheim, 1st edn., 2007, pp. 1–2.

38. R. Franke, D. Selent, and A. Börner, *Chem. Rev.*, 2012, **112**, 5675–732.

39. B. Cornils, W. A. Herrmann, and M. Rasch, *Angew. Chem. Int. Ed.*, 1994, **33**, 2144–2163.

40. G. D. Frey, *J. Organomet. Chem.*, 2013, **754**, 5–7.

41. B. Cornils, *J. Mol. Catal. A Chem.*, 1999, **143**, 1–10.

42. G. T. Whiteker and C. J. Colbey, *Top. Organomet. Chem.*, 2012, **42**, 35–46.

43. L. A. Oro and D. Carmona, in *The Handbook of Homogeneous Hydrogenation*, Weinheim, 1st edn., 2007, pp. 3–30.

44. B. R. James, P. W. N. M. Van Leeuwen, S. D. Ittel, A. Nakamura, R. L. Richards, and A. Yamamoto, in *Rhodium Catalyzed Hydroformylation*, Kluwer Academic Publishers, New York, 1st edn., 2002, pp. 6–277.

45. S. Gladiali, J. Carles Bayón, and C. Claver, *Tetrahedron: Asymmetry*, 1995, **6**, 1453–1474.

46. C. P. Casey, E. Lin Paulsen, E. W. Beuttenmueller, B. R. Proft, L. M. Petrovich, B. A. Matter, and D. R. Powell, *J. Am. Chem. Soc.*, 1997, **119**, 11817–11825.

47. Y.-Q. Li, P. Wang, H. Zhang, X.-L. Zhao, Y. Lu, Z. Popović, and Y. Liu, *J. Mol. Catal. A Chem.*, 2015, **402**, 37–45.

48. B. Cornils and E. G. Kuntz, *J. Organomet. Chem.*, 1995, **502**, 177–186.

49. C. De Rumpa, S. Sumanta, A. Ghosh, K. Mukherjee, S. Bhattacharyya, Sekhar, and B. Saha, *Res. Chem. Intermed.*, 2013, **39**, 3463–3474.

50. D. Adams, P. Dyson, and S. Taverner, in *Chemistry in Alternative Reaction Media*, John Wiley & Sons Ltd, Chichester, 2nd edn., 2004, pp. 37–39.

51. S. K. Sharma and R. V. Jasra, *Catal. Today*, 2015, **247**, 70–81.

52. B. Cornils, W. A. Herrmann, and R. W. Eckl, *J. Mol. Catal. A Chem.*, 1997, **116**, 27–33.

53. C. W. Kohlpaintner, R. W. Fischer, and B. Cornils, *Appl. Catal. A Gen.*, 2001, **221**, 219–225.

54. B. Cornils, *Org. Process Res. Dev.*, 1998, **1**, 121–127.

55. K. H. Shaughnessy, *Chem. Rev.*, 2009, **109**, 643–710.

56. B. Cornils and W. A. Herrmann, in *Applied Homogeneous Catalysis with Organometallic Compounds*, Wiley-VCH Verlag GmbH & Co. KGaA, Weinheim, 2nd edn., 2002, pp. 601–625.

57. W. Keim, *Green Chem.*, 2003, **5**, 105–111.

58. B. Cornils and W. A. Herrmann, in *Aqueous-Phase Organometallic Catalysis*, Wiley-VCH Verlag GmbH & Co. KGaA, 2nd edn., 2004, pp. 7–8.

59. B. Cornils, *Top. Curr. Chem.*, 1999, **206**, 133–149.

60. N. Pinault and D. W. Bruce, *Coord. Chem. Rev.*, 2003, **241**, 1–25.

61. P. J. Baricelli, E. Lujano, M. Modroño, A. C. Marrero, Y. M. García, A. Fuentes, and R. A. Sánchez-Delgado, *J. Organomet. Chem.*, 2004, **689**, 3782–3792.

62. L. C. Matsinha, S. F. Mapolie, and G. S. Smith, *Dalton Trans.*, 2015, **44**, 1240–1248.

63. E. B. Hager, B. C. E. Makhubela, and G. S. Smith, *Dalton Trans.*, 2012, **41**, 13927–35.

64. S. Menuel, E. Bertaut, E. Monflier, and F. Hapiot, *Dalton Trans.*, 2015, **44**, 13504–13512.

65. J. Cabou, H. Bricout, F. Hapiot, and E. Monflier, *Catal. Commun.*, 2004, **5**, 265–270.

66. M. Elard, J. Denis, M. Ferreira, H. Bricout, D. Landy, S. Tilloy, and E. Monflier, *Catal. Today*, 2014, **247**, 47–54.

67. M. Ferreira, F. Jérôme, H. Bricout, S. Menuel, D. Landy, S. Fourmentin, S. Tilloy, and E. Monflier, *Catal. Commun.*, 2015, **63**, 62–65.

68. M. Ferreira, F.-X. Legrand, C. Machut, H. Bricout, S. Tilloy, and E. Monflier, *Dalton Trans.*, 2012, **41**, 8643.

69. E. Monflier, H. Bricout, F. Hapiot, S. Tilloy, A. Aghmiz, and A. M. Masdeu-Bultó, *Adv. Synth. Catal.*, 2004, **346**, 425–431.

70. S. Paganelli, O. Piccolo, P. Pontini, R. Tassini, and V. D. Rathod, *Catal. Today*, 2015, **247**, 64–69.

71. T. Lacroix, H. Bricout, S. Tilloy, and E. Monflier, *Eur. J. Org. Chem.*, 1999, 3127–3129.

72. E. Monflier, S. Tilloy, G. Fremy, Y. Barbaux, and A. Mortreux, *Tetrahedron Lett.*, 1995, **36**, 387–388.

73. A. Ponchel and E. Monflier, *Comptes Rendus Chim.*, 2011, **14**, 149–166.

74. F. Hapiot, L. Leclercq, N. Azaroual, S. Fourmentin, S. Tilloy, and E. Monflier, *Curr. Org. Synth.*, 2008, **5**, 162–172.

75. M. Elard, J. Denis, M. Ferreira, H. Bricout, D. Landy, S. Tilloy, and E. Monflier, *Catal. Today*, 2014, **247**, 47–54.

76. B. Sueur, L. Leclercq, M. Sauthier, Y. Castanet, and A. Mortreux, *Chem. Eur. J.*, 2005, **11**, 6228–6236.

77. S. Tilloy, C. Binkowski-Machut, S. Menuel, H. Bricout, and E. Monflier, *Molecules*, 2012, **17**, 13062–72.

78. A. A. Dabbawala, J. N. Parmar, R. V Jasra, H. C. Bajaj, and E. Monflier, *Catal. Commun.*, 2009, **10**, 1808–1812.

79. E. M. M. Del Valle, *Process Biochem.*, 2004, **39**, 1033–1046.

80. L. Leclercq and A. R. Schmitzer, *Organometallics*, 2010, **29**, 3442–3449.

81. H. Bricout, F. Hapiot, A. Ponchel, S. Tilloy, and E. Monflier, *Sustainability*, 2009, **1**, 924–945.

82. S. Tilloy, H. Bricout, and E. Monflier, *Green Chem.*, 2002, **4**, 188–193.

83. F. Hapiot, H. Bricout, S. Tilloy, and E. Monflier, *Eur. J. Inorg. Chem.*, 2012, 1571–1578.

84. E. Monflier, S. Tilloy, Y. Castanet, and A. Mortreux, *Tetrahedron Lett.*, 1998, **39**, 2959–2960.

85. T. Mathivet, C. Méliet, Y. Castanet, A. Mortreux, L. Caron, S. Tilloy, and E. Monflier, *J. Mol. Catal. A Chem.*, 2001, **176**, 105–116.

86. L. Bai, L. Zhang, J. Pan, J. Zhu, Z. Cheng, and X. Zhu, *Macromolecules*, 2013, **46**, 2060–2066.

87. E. Hermanns and J. Hasenjäger, *Top. Organomet. Chem.*, 2008, **23**, 53–66.

88. L. I. Kaoxue, W. Yanhua, J. Jingyang, and J. I. N. Zilin, *Chinese J. Catal.*, 2010, **31**, 1191–1194.

89. Y. Xu, Y. Wang, Y. Zeng, J. Jiang, and Z. Jin, *Catal. Letters*, 2012, **142**, 914–919.

90. C. Zhijun, W. Yanhua, J. Jingyang, and J. I. N. Zilin, *Chinese J. Catal.*, 2011, **32**, 1133–1137.

91. Z. Yan, W. Yanhua, X. U. Yicheng, S. Ying, Z. Jiaqi, J. Jingyang, and J. I. N. Zilin, *Chinese J. Catal.*, 2012, **33**, 402–406.

92. N. Pinault and D. W. Bruce, *Coord. Chem. Rev.*, 2003, **241**, 1–25.

93. D. Wu, J. Zhang, Y. Wang, J. Jiang, and Z. Jin, *Appl. Organomet. Chem.*, 2012, **26**, 718–721.

94. J. Tijani and B. E. Ali, *Appl. Catal. A Gen.*, 2006, **303**, 158–165.

95. D. Müller, E. Esche, T. Pogrzeba, M. Illner, F. K. Leube, R. Schomaecker, and G. Wozny, *Ind. Eng. Chem. Res.*, 2015, DOI: 10.1021/ie5049059.

96. S. L. Desset, S. W. Reader, and D. J. Cole-hamilton, *Green Chem.*, 2009, **11**, 630–637.

97. H. Fu, M. Li, H. Mao, Q. Lin, M. Yuan, X. Li, and H. Chen, *Catal. Commun.*, 2008, **9**, 1539–1544.

98. M. Schwarze, T. Pogrzeba, K. Seifert, T. Hamerla, and R. Schomäcker, *Catal. Today*, 2014, **247**, 55–63.

99. H. H. Yildiz Ünveren, Hesna Hülya Yildiz Ünveren Berlin, 2004.

100. H. Nowothnick, A. Rost, T. Hamerla, R. Schomäcker, C. Müller, and D. Vogt, *Catal. Sci. Technol.*, 2013, **3**, 600.

101. P. Schrader, C. Paasche, and S. Enders, *Chem. Eng. Sci.*, 2014, **115**, 139–147.

102. A. A. Dabbawala, H. C. Bajaj, H. Bricout, and E. Monflier, *Catal. Sci. Technol.*, 2012, **2**, 2273–2278.

103. L. Obrecht, P. C. J. Kamer, and W. Laan, *Catal. Sci. Technol.*, 2013, **3**, 541–551.

104. C. G. Vieira, M. C. De Freitas, K. C. B. De Oliveira, A. D. C. Faria, E. N. Santos, and E. V Gusevskaya, *Catal. Sci. Technol.*, 2015, **5**, 960–966.

105. D. Müller, D. Hoang, V. Alejandro, H. Arellano-garcia, Y. Kasaka, M. Müller, R. Schomäcker, and G. Wozny, *Chem. Eng. Sci.*, 2014, **115**, 127–138.

106. P. J. Low, *Annu. Rep. Prog. Chem., Sect. A,* 2002, **98**, 393–434.

107. P. J. Deuss, R. Denheeten, W. Laan, and P. C. J. Kamer, *Chem. Eur. J.*, 2011, **17**, 4680–4698.

108. M. H. Pørez-Temprano, J. A. Casares, and P. Espinet, *Chem. Eur. J.*, 2012, **18**, 1864–1884.

109. J. Park and S. Hong, *Chem. Soc. Rev.*, 2012, **41**, 6931–6943.

110. G. J. Rowlands, *Tetrahedron*, 2001, **57**, 1865–1882.

111. I. Bratko and M. Gómez, *Dalton Trans.*, 2013, **42**, 10664–81.

112. B. L. Feringa and E. K. van den Beuken, *Tetrahedron*, 1998, **54**, 12985–13011.

113. S. W. S. Choy, M. J. Page, M. Bhadbhade, and B. A. Messerle, *Organometallics*, 2013, **32**, 4726–4729.

114. A. M. Trzeciak, J. J. Ziółkowski, and R. Choukroun, *J. Mol. Catal. A Chem.*, 1996, **110**, 135–139.

115. R. Zhong, Y. Wang, X. Guo, Z. Chen, and X. Hou, *Chem. Eur. J.*, 2011, **17**, 11041–11051.

116. S. Liu, A. Motta, M. Delferro, and T. J. Marks, *J. Am. Chem. Soc.*, 2013, **135**, 8830–8833.

117. D. G. H. Hetterscheid, S. H. Chikkali, B. deBruin, and J. N. H. Reek, *ChemCatChem*, 2013, **5**, 2785–2793.

118. J. A. Mata, F. E. Hahn, and E. Peris, *Chem. Sci.*, 2014, **5**, 1723–1732.

119. J. Launay, *Coord. Chem. Rev.*, 2013, **257**, 1544–1554.

120. M. Madalska, P. Lönnecke, and E. Hey-Hawkins, *J. Mol. Catal. A. Chem.*, 2014, **383-384**, 137–142.

121. R. G. Arrayμs, J. Adrio, and J. C. Carretero, *Angew. Chem. Int. Ed.*, 2006, **45**, 7674–7715.

122. A. M. Trzeciak, P. Štěpnička, E. Mieczyńska, and J. J. Ziółkowski, *J. Organomet. Chem.*, 2005, **690**, 3260–3267.

123. J. C. Hierso, F. Lacassin, R. Broussier, R. Amardeil, and P. Meunier, *J. Organomet. Chem.*, 2004, **689**, 766–769.

124. K. A. Chatziapostolou, K. A. Vallianatou, A. Grigoropoulos, C. P. Raptopoulou, A. Terzis, I. D. Kostas, P. Kyritsis, and G. Pneumatikakis, *J. Organomet. Chem.*, 2007, **692**, 4129–4138.

125. X. Peng, Z. Wang, C. Xia, and K. Ding, *Tetrahedron Lett.*, 2008, **49**, 4862–4864.

126. M. Laly, R. Broussier, and B. Gautheron, *Tetrahedron Lett.*, 2000, **41**, 1183–1185.

127. A. Bertogg and A. Togni, *Organometallics*, 2006, **25**, 622–630.

128. B. D. Evans and A. Osborn, *J. Chem. Soc.*, 1968, **566**, 3133–3142.

129. S. Stockmann, P. Lönnecke, S. Bauer, and E. Hey-Hawkins, *J. Organomet. Chem.*, 2014, **751**, 670–677.

130. M. W. P. Bebbington, S. Bontemps, G. Bouhadir, M. J. Hanton, R. P. Tooze, H. van Rensburg, and D. Bourissou, *New J. Chem.*, 2010, **34**, 1556–1559.

131. O. R. Hughes and D. J. Unruh, *J. Mol. Catal.*, 1981, **12**, 71–83.

132. P. Govender, B. Therrien, and G. S. Smith, *Eur. J. Inorg. Chem.*, 2012, 2853–2862.

133. N. C. Antonels, J. R. Moss, and G. S. Smith, *J. Organomet. Chem.*, 2011, **696**, 2003–2007.

134. P. Govender, N. C. Antonels, J. Mattsson, A. K. Renfrew, P. J. Dyson, J. R. Moss, B. Therrien, and G. S. Smith, *J. Organomet. Chem.*, 2009, **694**, 3470–3476.

135. B. C. E. Makhubela, A. M. Jardine, G. Westman, and G. S. Smith, *Dalton Trans.*, 2012, **41**, 10715–23.

136. S. D. Khanye, J. Gut, P. J. Rosenthal, K. Chibale, and G. S. Smith, *J. Organomet. Chem.*, 2011, **696**, 3296–3300.

137. J. Palomero, J. A. Mata, F. González, and E. Peris, *New J. Chem.*, 2002, **26**, 291–297.

138. D. Astruc and F. Chardac, *Chem. Rev.*, 2001, **101**, 2991–3023.

139. Y. Fonseca, B. Fontal, M. Reyes, T. Suárez, J. C. Diaz, and P. Cancines, *React. Kinet. Mech. Catal.*, 2012, **105**, 307–315.

140. A. Gong, Q. Fan, Y. Chen, H. Liu, C. Chen, and F. Xi, *J. Mol. Catal. A Chem.*, 2000, **159**, 225–232.

141. B. E. Hanson, H. Ding, and C. W. Kohlpaintner, *Catal. Today*, 1998, **42**, 421–429.

142. B. C. E. Makhubela, A. M. Jardine, G. Westman, and G. S. Smith, *Dalton Trans.*, 2012, **41**, 10715–23.

143. D. De Groot, P. G. Emmerink, C. Coucke, J. N. H. Reek, P. C. J. Kamer, and P. W. N. M. Van Leeuwen, *Inorg. Chem. Commun.*, 2000, **3**, 711–713.

144. Y. Y. Huang, H. L. Zhang, G. J. Deng, W. J. Tang, X. Y. Wang, Y. M. He, and Q. H. Fan, *J. Mol. Catal. A Chem.*, 2005, **227**, 91–96.

Chapter 2

Synthesis and Characterisation of water-soluble mononuclear and heterobimetallic complexes

2.1 Introduction

The design and modification of ligands in synthetic chemistry continues to be explored in various avenues, some of which are tailored for catalytic transformations as well as biological potency (cancer, malaria, tuberculosis, etc).[1–7] A ligand can be designed to act as a support for the metal centre as well as to impart unique steric, electronic and solubility properties to the complex. In all cases, the ease of ligand design plays an important role.

Schiff base ligands are very popular because of their good stability and versatility in organometallic chemistry.[8] Schiff base ligands are synthesised in a condensation reaction between an amine and an aldehyde or ketone, producing imines. These have been extensively used in the synthesis of coordination compounds for catalysis and biological applications.[9–18] Good catalytic properties of complexes from Schiff base ligands have been reported in literature.[9,10,19]

Modification with hydrophilic substituents enables solubilisation of ligands and consequently complexes in aqueous media.[9,10,20] Such characteristics are quite beneficial for catalytic reactions which are carried out in water, such as the hydroformylation of olefins in a two phase aqueous-organic media. This enables retention of the water-soluble catalyst precursor in the aqueous layer and facile separation of the product from the catalyst, consequently bringing about huge economical, and ecotoxicological benefits.

Recent efforts in ligand design and modification involve the use of heterobimetallic structures that possess intriguing chemical and biological characteristics. The ability to mimic metalloenzymes (bearing two or more active sites) in the design of organometallic complexes for both catalytic and biological applications is important in the advancement of science.[21] As an extension to our previous work involving water-soluble Rh(I) complexes bearing chelating

N,O-bidentate ligands for catalysis,[9] we were prompted to introduce a second metal into the complexes. The premise behind this approach is that the addition of another metal confers unique and intriguing chemical and catalytic behaviour through cooperative interactions that may exist between the different metal centres.

Widely studied for its redox activity, versatility, and stability as an ancillary ligand, [6,22] ferrocene moieties can be modified through incorporation into Schiff base ligands.[8] When tailored together with known Schiff base ligands, ferrocene can be highly beneficial in acting as an electron reservoir as well as in stabilising the main catalytic centre. Owing to the good activity and selectivity of rhodium based complexes in hydroformylation, a combination of the bidentate-coordinated rhodium centre with the chemically robust ferrocene may prove to be beneficial. Moreover, ferrocene conjugates targeting cancer cells and malaria have been widely reported in literature.[23–31] This shows the versatility, stability and adaptability of ferrocene in various applications.

In this chapter, we discuss the synthesis and characterisation of ferrocenyl mononuclear and ferrocenyl-rhodium heterobimetallic complexes.

2.2 Synthesis and characterisation of 5-sulfonato salicylaldehydes (2.1 and 2.2)

The sulfonated ligands **2.1** and **2.2** (Scheme 2.1) were synthesised following previously described literature procedures.[9] The respective commercially available salicylaldehydes were reacted with aniline to isolate **2.1** and **2.2** *via* a series of aldehyde group protection, sulfonation and acid-catalysed imine hydrolysis reactions.

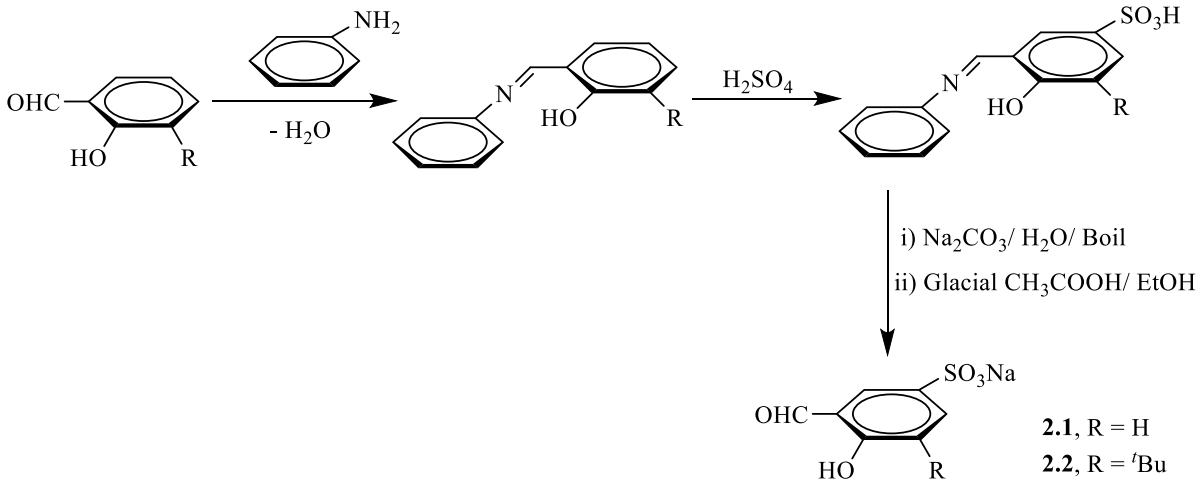

Scheme 2.1 Preparation of monosodium 5-sulfonato salicylaldehydes **2.1** and **2.2**.

In the first step, the aldehyde was reacted with aniline through a Schiff base condensation reaction, affording *N*-phenyl-salicylaldimine. The reaction follows the mechanism in Scheme 2.2.

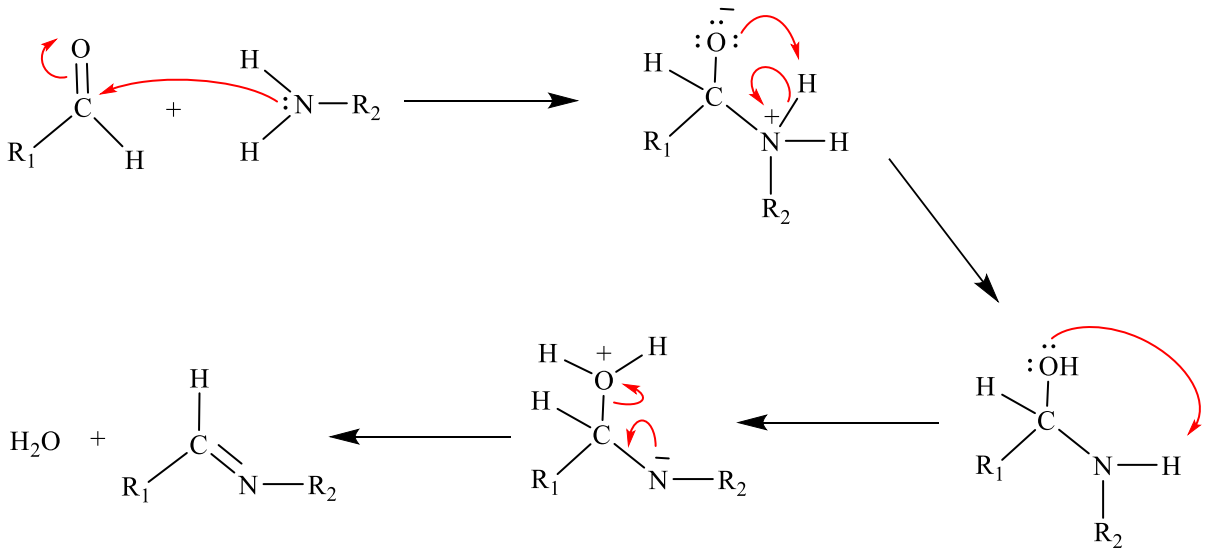

Scheme 2.2 Mechanism of a Schiff base condensation reaction.

The *N*-phenyl-salicylaldimine was isolated as a yellow crystalline solid in good yield in the reaction step leading to **2.1** and as a yellow oil in the reaction step leading to **2.2**. The signals in the ^{1}H NMR spectrum of the crystalline solid correlate with literature,[9] showing a

characteristic signal for the imine proton at δ = 9.98. All the other aromatic protons are accounted for in their expected regions between δ = 8.19 and 7.15.

The first step (protection of the aldehyde) is necessary as the aldehyde group readily gets protonated in the presence of sulfuric acid to form the oxocarbenium ion (Scheme 2.3). The *pi*-bond of the aldehyde donates a pair of electrons as a base to the acidic proton to give the conjugate acid, oxocarbenium ion, along with the conjugate base (the hydrogen sulfate anion).

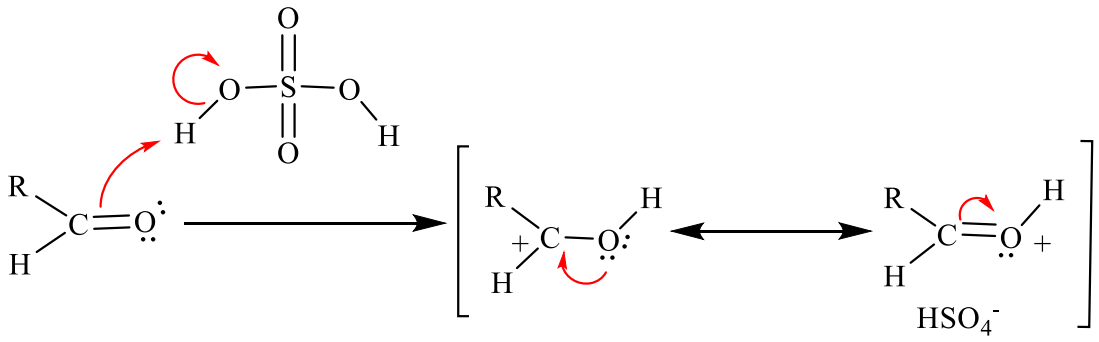

Scheme 2.3 Sulfonation of a deshielded aldehyde group.

In the second step, both the *N*-phenyl-salicylaldimine precursors to the salicylaldehydes **2.1** and **2.2** were reacted with concentrated sulfuric acid to effect sulfonation. The hydroxyl group directs the sulfonate substituent to the *para* position, which is complemented by the imine group, directing the sulfonate substituent to the *meta* position. As a result, sulfonation is favoured at the 5-position of the aromatic ring.

Addition of base to the sulfonated *N*-phenyl-salicylaldimine precursors in step three, followed by acid-catalysed imine hydrolysis affords the sulfonated salicylaldehydes **2.1** and **2.2**. The products (**2.1** and **2.2**) were isolated as crystalline solids in good yield {(beige, 62%) and (light brown, 72.5%)} respectively and have moderate solubility in water {0.08 mg/mL (**2.1**) and 0.072 mg/mL (**2.2**)}. These were characterised using ^{1}H NMR, ^{13}C{^{1}H} NMR, FT-IR spectroscopy, elemental analysis (C, N, H, and S) and mass spectrometry.

The ^{1}H NMR spectra for the sulfonated salicylaldehydes (**2.1** and **2.2**) display signals for the aldehyde proton at δ = 10.0 and δ = 9.93 respectively as well as aromatic peaks in the region of δ = 8.19–7.14. In the ^{13}C{^{1}H} NMR spectra, the carbonyl carbons are observed in their characteristic region at δ = 196.9 (**2.1**) and 198.9 (**2.2**). The infrared (IR) spectroscopic results

further corroborate the presence of the aldehyde functionality in **2.1** and **2.2** with the ν(C=O str.) absorption bands at 1660 cm^{-1} and 1654 cm^{-1} respectively. The ν(O–H str.) absorption bands are observed at 3431 cm^{-1} for compound **2.1** and 3440 cm^{-1} for compound **2.2**.

2.3 Synthesis and characterisation of monosodium 5-sulfonato salicylaldimine ligand (2.3)

The new hydrazone-based monosodium 5-sulfonato salicylaldimine ligand **2.3** was prepared by the Schiff base condensation reaction of hydrazine monohydrate with monosodium 5-sulfonato salicylaldehyde **2.1** in dry ethanol. Ligand **2.3** was isolated in good yield (78%) as a pale yellow solid (Scheme 2.4).

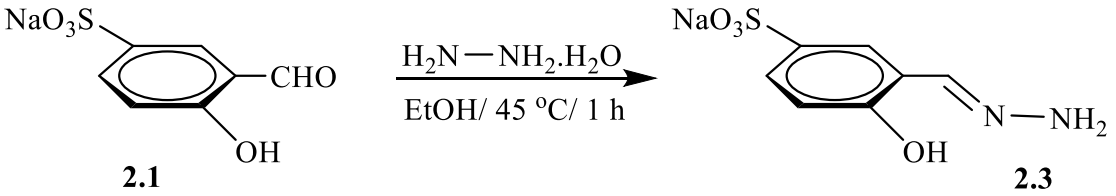

2.1 **2.3**

Scheme 2.4 Synthesis of monosodium 5-sulfonato salicylaldimine **2.3**.

The ligand is soluble in water, dimethylsulfoxide and methanol and has been characterised using elemental analysis (C, H, N and S), FT-IR, ^{1}H NMR and $^{13}C\{^{1}H\}$ NMR spectroscopy as well mass spectrometry. Both the ^{1}H NMR (Figure 2.1) and $^{13}C\{^{1}H\}$ NMR spectra show the presence of the imine proton/carbon at δ = 7.94 (^{1}H) and *ca.* δ = 140 ($^{13}C\{^{1}H\}$) respectively and all the other expected aromatic protons (at δ = 7.48, 7.37 and 6.75) and carbon signals are observed. The proton at δ = 7.48 (H_f) is the most deshielded aromatic proton as it is adjacent to two electron withdrawing groups, *viz*. the imine and the sulfonate groups. This proton is observed as a doublet with coupling constant ^{4}J = 2.0 Hz, indicating long range proton-proton coupling with proton (H_d) at δ = 7.36. The proton at δ = 7.36 (H_d) is seen as a doublet of doublets with coupling constants ^{4}J = 2.0 Hz and ^{3}J = 8.4 Hz due to coupling with proton (H_f, long range coupling) and proton (H_c) respectively. The COSY 2-dimensional NMR spectrum confirms the observed coupling. The proton at δ = 6.75 is the most shielded and occurs upfield relative to proton (H_d) and proton (H_f). The two amine protons of the hydrazone moiety are in the same electronic environment and are thus accounted for as a singlet occurring at δ = 6.88 in the ^{1}H NMR spectrum of **2.3**.

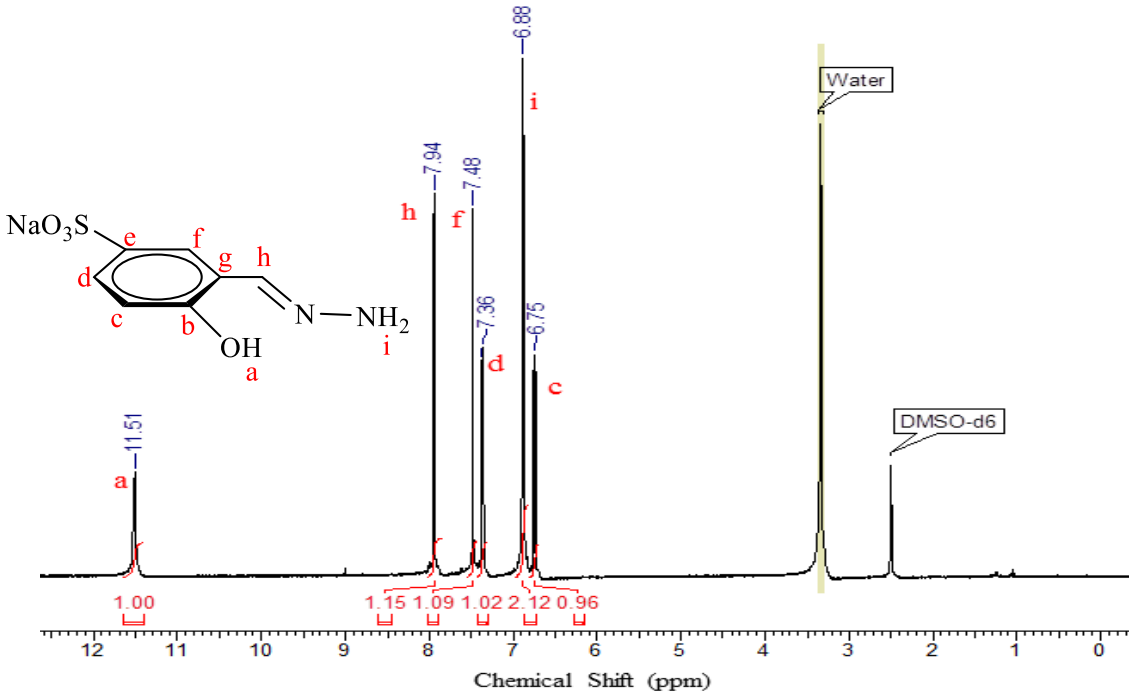

Figure 2.1 ^{1}H NMR (DMSO-d_6) spectrum for ligand **2.3**.

The HSQC 2-dimensional NMR spectrum of ligand **2.3** was used to validate the assignment of the carbons in the $^{13}C\{^{1}H\}$ NMR spectrum of the ligand. The imine carbon is the most deshielded carbon at (δ = 141.9, C_h) in the spectrum. The carbon adjacent to the sulfonate group is observed at (δ = 139.9, C_e) as expected indicating deshielding due to the electron withdrawing effects of the sulfonate group. The HSQC 2-dimensional NMR spectrum also shows carbon (C_g) at δ = 119.0. The HSQC spectrum also permitted the assignment of the aromatic carbons (δ = 126.62 C_d, δ = 125.99 C_f) as well as the carbon (C_b) which is assigned downfield at δ = 157.1.

In the infrared spectrum of the ligand **2.3**, an intense stretching frequency characteristic of the imine is observed at (ν(C=N str.) 1619 cm^{-1}) and the spectrum does not show the aldehyde absorption band (ν(C=O str.) 1660 cm^{-1}) of compound **2.1**. The difference in electronegativity of oxygen (3.5) to that of nitrogen (3.0) leads to a reduced dipole moment, weakening of the double bond character and consequently the observed shift from high frequency for C=O to lower frequency for C=N. Also observed in the spectrum are absorption bands corresponding to ν(N–H str.) at 3409 cm^{-1} and ν(O–H str.) at 3293 cm^{-1}.

The ESI mass spectrum in the negative ion mode corroborates the formation of this ligand by displaying a base peak for $[M]^-$ at *m/z* = 215.01 where M is the anionic ligand. The ligand has good solubility in water, (0.11 mg/mL).

2.4 Synthesis and characterisation of monosodium 5-sulfonatosalicylaldimine-ferrocenylimine complex (2.4)

The mononuclear complex **2.4** was synthesised by the Schiff base condensation reaction of ferrocenecarboxaldehyde with monosodium 5-sulfonato salicylaldimine ligand **2.3** in methanol under reflux. The complex was isolated as a dark red solid in good yield (82%), (Scheme 2.5).

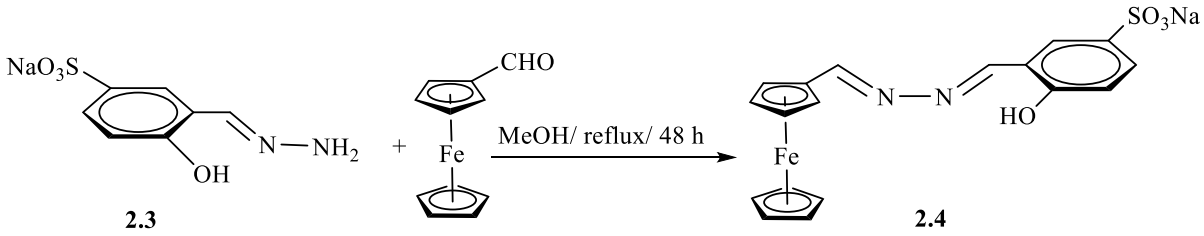

Scheme 2.5 Synthesis of monosodium 5-sulfonatosalicylaldimine-ferrocenylimine complex **2.4**.

The mononuclear complex **2.4** is soluble in water (1.82 mg/mL, r.t.), methanol and dimethylsulfoxide and has been characterised fully using elemental analysis (C, H, N and S), FT-IR, ^{1}H NMR and ^{13}C{^{1}H} NMR spectroscopy as well mass spectrometry.

The ^{1}H NMR spectrum of the mononuclear complex **(**Figure 2.2**)** shows the presence of two imine signals as singlets at (δ = 8.82, H_h) and (δ = 8.64, H_i) respectively. The ferrocenyl group is more electron-donating than the phenyl ring, resulting in less deshielding of the imine proton adjacent to the ferrocenyl moiety (H_i) and occurs upfield relative to proton (H_h). A hydroxyl proton singlet is also observed at δ = 11.51 and three aryl proton signals (at δ = 7.92, δ = 7.60 and δ = 6.90). The unsubstituted cyclopentadienyl protons (H_m) of the ferrocenyl moiety occur in the same electronic environment and are observed as a singlet at δ = 4.27. The monosubstituted cyclopentadienyl protons are accounted for as two broad signals integrating for four protons (at δ = 4.78 and δ = 4.57 respectively). Typically, these protons resonate as a doublet or triplet but these cannot be observed on the given NMR timescale and

these protons average out to one broadened signal over the same chemical shift. The signal observed at δ = 4.78 is assigned to the protons (H_k) as these are deshielded by the adjacent electron withdrawing imine group.

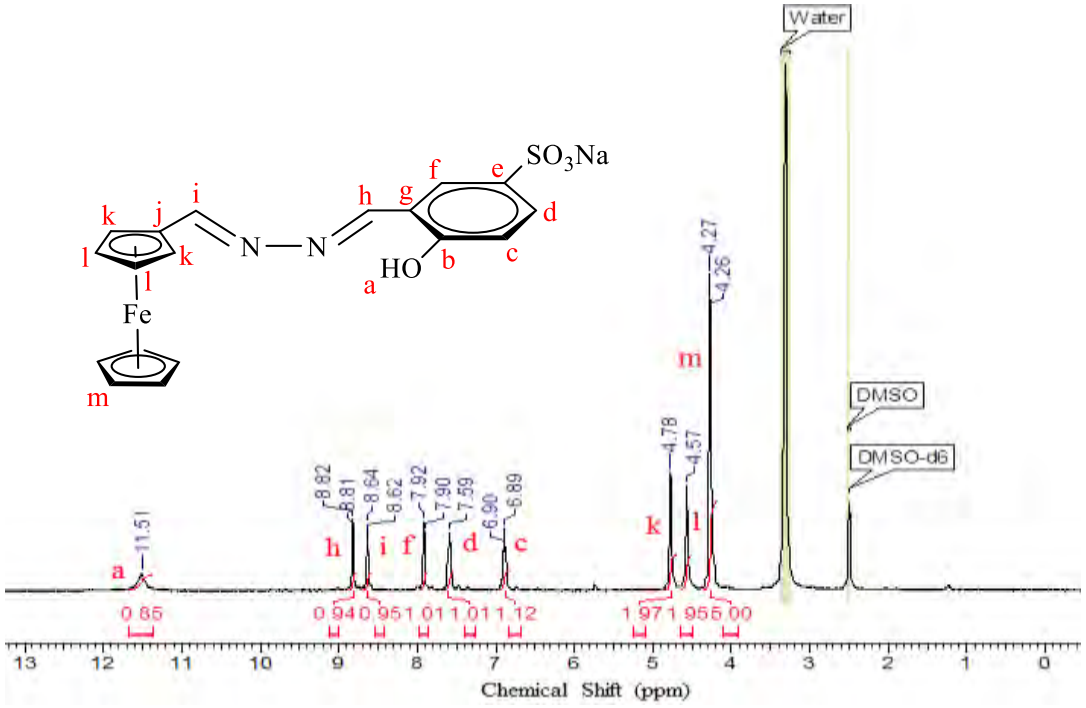

Figure 2.2 ^{1}H NMR (DMSO-d_6) spectrum for ferrocenylimine mononuclear complex **2.4**.

Interpretation and assignment of the carbons of complex **2.4** was done using $^{13}C\{^{1}H\}$ NMR and HSQC 2-dimensional NMR spectroscopy. The spectra show that the imine carbon with the most deshielded proton (H_h) appears upfield (δ = 160.9 C_h) relative to the imine carbon (δ = 164.4 C_i). The carbon (C_j) is assigned at δ = 77.7, whereas the carbon atoms in **2.4** are as observed in the $^{13}C\{^{1}H\}$ NMR spectrum of ligand **2.3**.

The 2-dimensional COSY spectrum (Figure 2.3**)** was used to further corroborate the assignment of the protons in the ^{1}H NMR spectrum of the complex. The spectrum shows coupling of the protons (H_k and H_l) of the substituted cyclopentadienyl ring, which are observed as broad signals in the ^{1}H NMR spectrum. The coupling of the phenyl protons in the 2-dimensional COSY spectrum of **2.4** is similar to that of the ligand **2.3**.

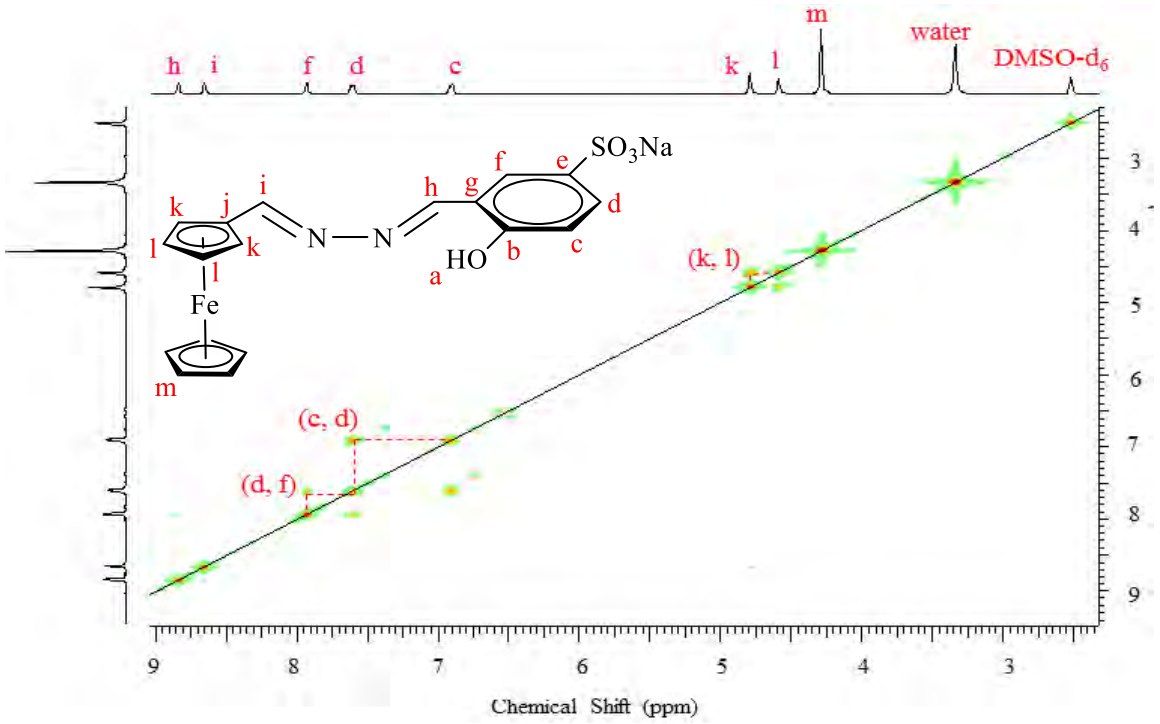

Figure 2.3 ^{1}H-^{1}H COSY 2D-NMR (DMSO-d_6) spectrum of complex **2.4**.

The infrared spectrum of complex **2.4** displays an ν(O–H str.) absorption band at 3440 cm^{-1} as well as the characteristic imine absorption band ν(C=N str.) at 1624 cm^{-1} as an intense band with a shoulder assigned to the second imine (Figure 2.4).

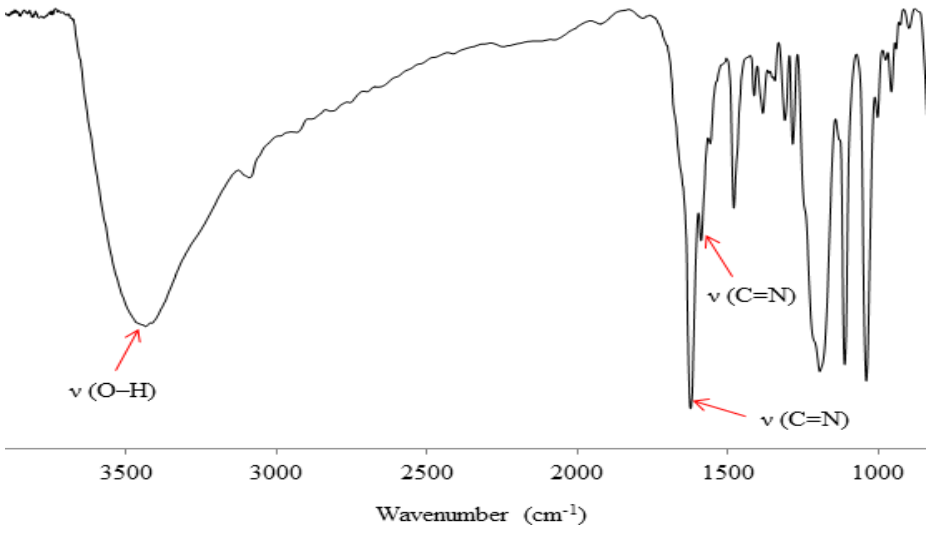

Figure 2.4 FT-IR spectrum of complex **2.4**.

The ESI mass spectrum was recorded in the negative ion mode and shows a base peak for $[M]^{-}$ ion at m/z = 411.01, corresponding to the molecular weight of the anionic complex **2.4**.

2.5 Synthesis and characterisation of the monosodium 5-sulfonatosalicylaldimine-ferrocenylimine rhodium(I) 1,5-cyclooctadiene heterobimetallic complex (2.5)

The new heterobimetallic complex **2.5** was synthesised by reacting the mononuclear complex **2.4** (Scheme 2.6) with the Rh(I) precursor $[Rh(COD)Cl]_2$ (COD = 1,5-cyclooctadiene). Coordination to the rhodium metal occurs in a bidentate chelating manner *via* the imine nitrogen and hydroxyl oxygen of **2.4**.

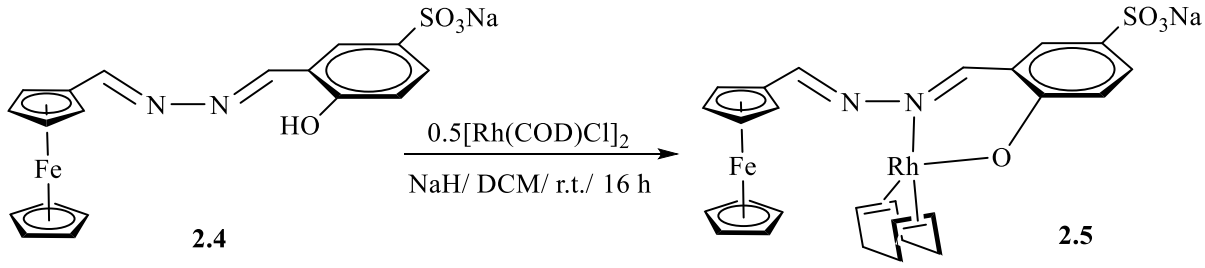

2.4 **2.5**

Scheme 2.6 Synthesis of the heterobimetallic complex **2.5**.

The heterobimetallic complex was isolated as an orange solid in excellent yield (94%) and has better solubility in water (16.7 mg/mL, r.t., **2.5**) than its mononuclear counterpart (1.82 mg/mL, r.t., **2.4**). The complex is also soluble in dimethylsulfoxide and methanol. This new heterobimetallic complex has been characterised fully using elemental analysis (C, H, N and S), FT-IR, ^{1}H NMR and ^{13}C NMR spectroscopy as well mass spectrometry.

The ^{1}H NMR spectrum of complex **2.5** (Figure 2.5) does not show the hydroxyl proton which is observed in the ^{1}H NMR spectrum of **2.4** (δ = 11.51), confirming the deprotonation and subsequent coordination of oxygen to the rhodium metal. An upfield shift of the imine proton signals of **2.4** from (δ = 8.82 and 8.64) to **2.5** at (δ = 8.03 and 7.97) respectively is observed in the ^{1}H NMR spectrum, further confirming coordination to the metal. The shift may be attributed to back-donation of electrons from the rhodium metal to the imine nitrogen, therefore creating increased electron density in the imine functionality and consequently exerting shielding effects on the imine protons. The aryl and the ferrocenyl proton signals of **2.5** are very similar to those previously observed for **2.4**. The vinylic COD protons are observed as overlapping signals in the same region as the protons in the unsubstituted ferrocenyl moiety (δ = 4.33–4.18, H_l + $H_{m,m'}$). Though not observed in this particular

spectrum, in some instances, the olefinic COD protons are observed as separate signals in the proton spectrum, which may be ascribed to the asymmetric environment induced by the chelating *N*,*O*-bidentate ligand.[19] In such cases, the splitting of the signals for these protons may be due to the *trans* effects of the coordinating *N*,*O*-bidentate ligand. The exo- and endo-methylene protons of the COD (δ = 2.42 H_n, δ = 1.9 $H_{n'}$) are observed further upfield as two multiplets.

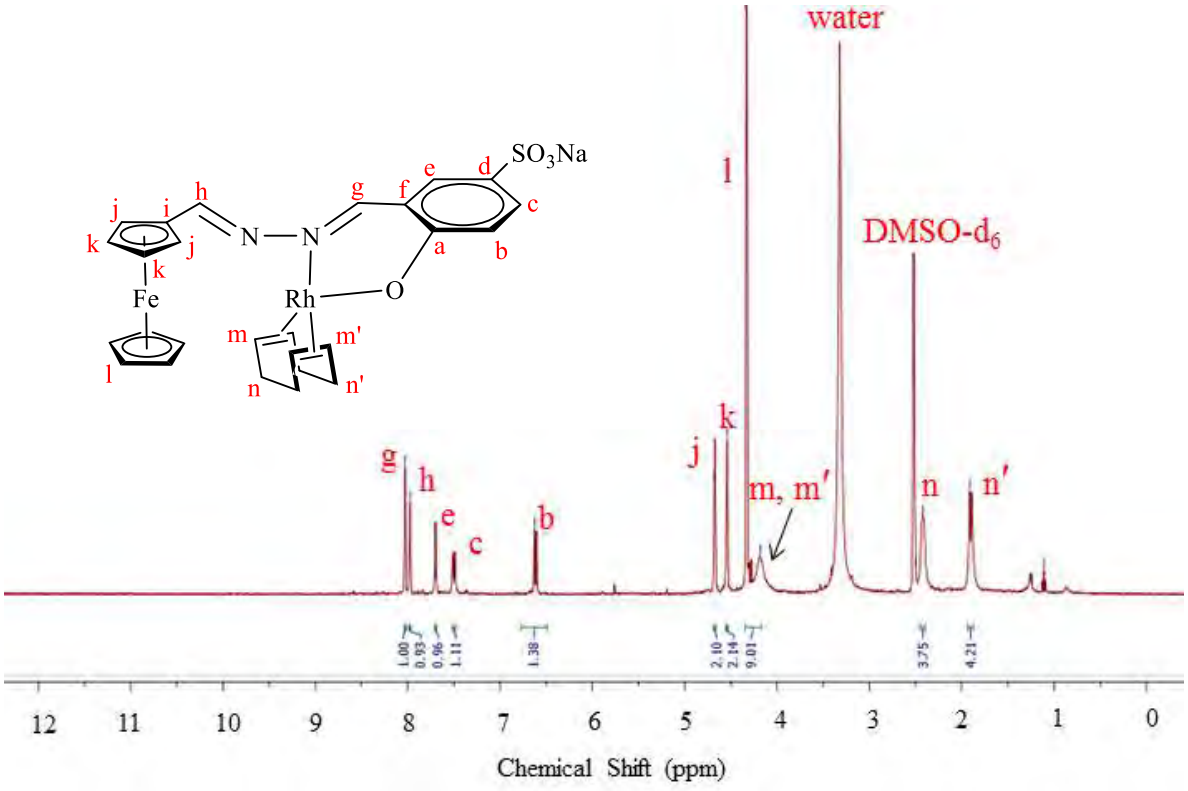

Figure 2.5 ^{1}H NMR (DMSO-d_6) spectrum for the heterobimetallic complex **2.5**.

The $^{13}C\{^1H\}$ NMR spectrum, together with 2D-NMR experiments (HSQC), also support the formation of the heterobimetallic complex **2.5**. The signal for the carbon adjacent to the coordinating oxygen (δ = 165.8 C_a) initially observed in **2.4** at (δ = 158.9 as C_b), is observed to have shifted downfield. This is attributed to the increased deshielding effect exerted by the adjacent oxygen atom as a result of coordination to the rhodium metal centre.

The COSY 2-dimensional NMR spectrum (Figure 2.6) substantiates assignment of the protons in the ^{1}H NMR spectrum of the heterobimetallic complex **2.5**. The COSY spectrum illustrates coupling of protons ($H_{n'}$) with protons (H_n). Also observed is the coupling of the aromatic protons (H_b with H_c, and H_c with H_e) as well as coupling of protons (H_j with H_k) of the monosubstituted ferrocenyl ring, similar to the observation for **2.4**.

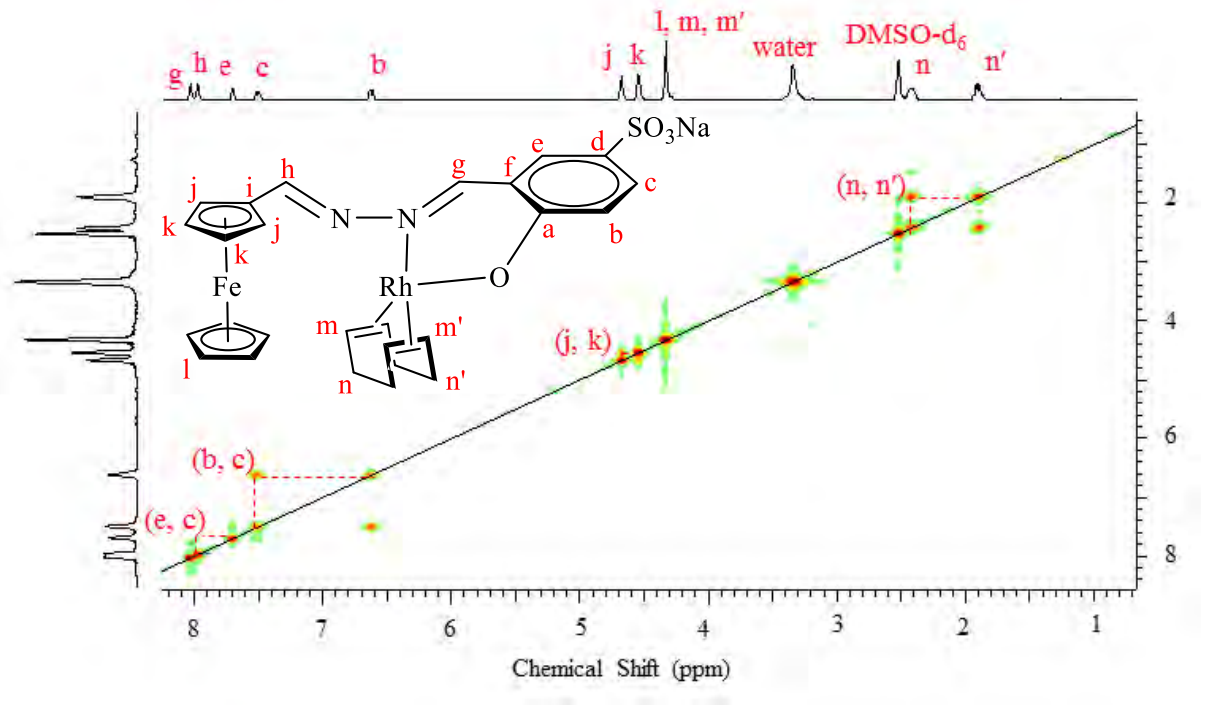

Figure 2.6 ^{1}H-^{1}H COSY 2D-NMR (DMSO-d_6) spectrum of complex **2.5**.

The infrared spectrum of complex **2.5** indicates an intense absorption band at 1600 cm^{-1} assigned to the *ν*(C=N) stretching frequency of the coordinating imine, with a shoulder presumably representing the free non-coordinating imine. The frequency shift of the imine absorption band from complex **2.4** to complex **2.5** (1624 to 1600 cm^{-1}) substantiates coordination of the imine nitrogen to the rhodium metal centre. The shift is due to sigma donation from the nitrogen and subsequent back-donation of electrons from the rhodium metal through synergic effects. As a result, the Rh–N bond strengthens whereas the C=N bond weakens. This decreases the wavenumber of the C=N bond in the infrared as observed in the infrared spectrum of complex **2.5** from **2.4**. Such imine shifts have also been reported for similar compounds in the literature.[9,10]

The ESI mass spectrum was recorded in the negative ion mode and shows a base peak for $[M– Rh(COD)]^{-}$ ion at *m/z* = 411.01, corresponding to the molecular weight of the anionic complex **2.5**. The fragmentation of the heterobimetallic complex **2.5** in ESI mass spectroscopy is unique, perhaps due to the ferrocenyl moiety as such is not observed in similar water-soluble Rh(I) mononuclear complexes.[9]

2.6 Synthesis and characterisation of 3-^{t}butyl-5-sulfonato salicylaldimine-ferrocenylimine complex (2.6)

Unlike **2.4**, the 3-^{t}butyl-5-sulfonato salicylaldimine-ferrocenylimine mononuclear complex **2.6** was successfully prepared through a one-pot synthesis by the Schiff base condensation reaction of monosodium 3-^{t}butyl-5-sulfonatosalicylaldehyde with hydrazine monohydrate and ferrocenecarboxaldehyde (Scheme 2.7).

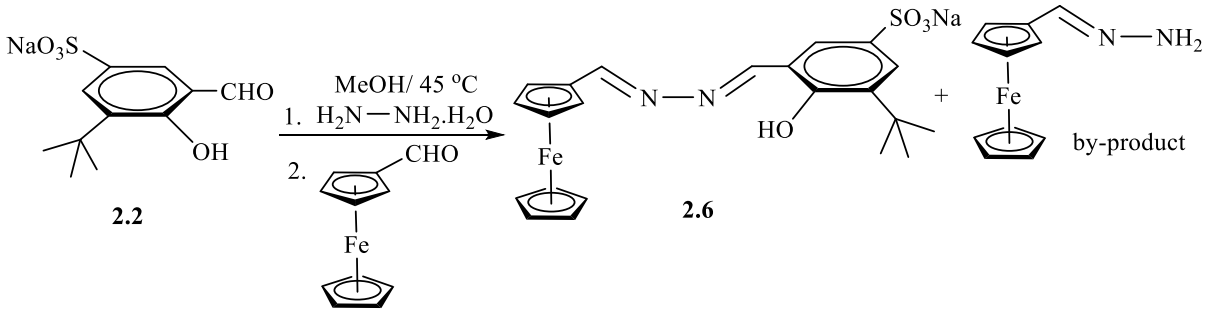

Scheme 2.7 Synthesis 3-^{t}butyl-5-sulfonato salicylaldimine-ferrocenylimine complex **2.6**.

Complex **2.6** was isolated as a dark brown solid in good yield (82%), with the ferrocenecarbaldehyde hydrazone as a by-product. The mononuclear complex **2.6** has good solubility in water (4 mg/mL, r.t.). This new complex was characterised using FT-IR, ^{1}H NMR and ^{13}C{^{1}H} NMR as well as 2-dimensional NMR (COSY and HSQC) spectroscopy.

Similar to **2.4**, the ^{1}H NMR spectrum of **2.6 (**Figure 2.7**)** confirms formation of the complex, showing the presence of two imine proton peaks as singlets at δ = 8.82 and δ = 8.68 respectively. All the other aromatic protons appear in similar chemical shifts to **2.4**. Further upfield at δ = 1.42 is a singlet integrating for the nine tertiary butyl protons (H_d).

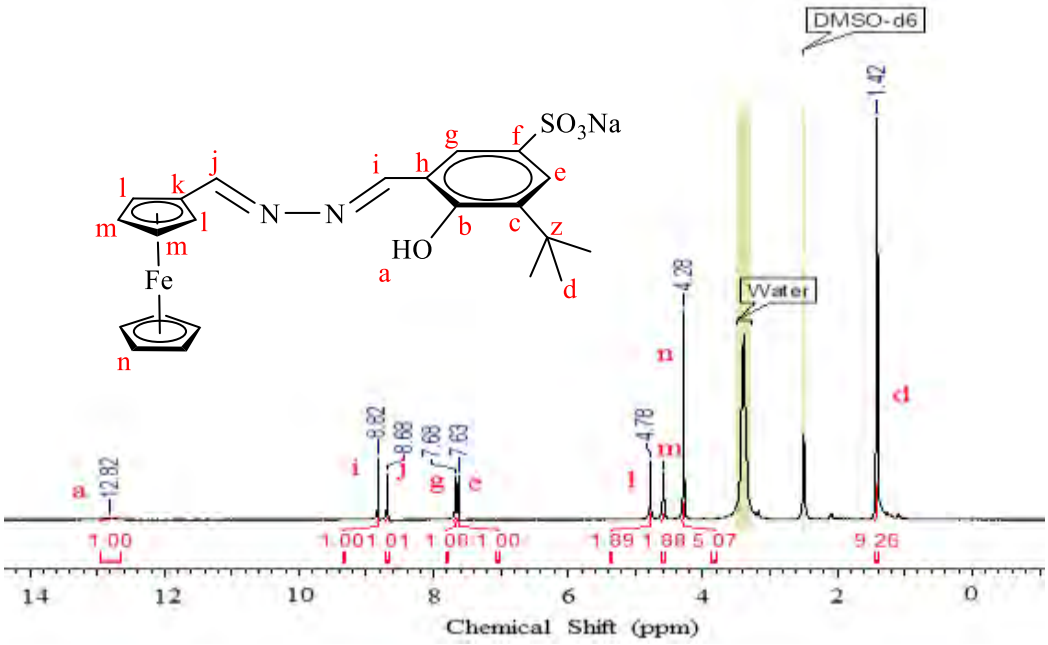

Figure 2.7 ^{1}H NMR (DMSO-d_6) spectrum for the mononuclear ferrocenyl complex **2.6**.

The $^{13}C\{^{1}H\}$ NMR as well as the 2-dimensional NMR experiments (HSQC and COSY) also corroborate formation of the complex. All the carbon atoms, and proton-proton coupling are assigned accordingly in the spectra.

The infrared spectrum of the complex **2.6** displays an ν(O–H str.) absorption band at 3390 cm^{-1} as well as the characteristic imine absorption band ν(C=N str.) at 1615 cm^{-1} as an intense broad band with a shoulder at 1590 cm^{-1} assigned to the second imine.

The negative ion mode ESI mass spectrum is consistent with the structure of **2.6**, displaying a base peak for $[M]^-$ ion at m/z = 467.07 corresponding to the molecular weight of the anion of **2.6**.

The by-product was also characterised using various techniques. The ^{1}H NMR spectrum of the by-product shows a singlet assigned to the imine proton at δ = 8.48. The four protons of the substituted cyclopentadienyl ring are accounted for as two broadened signals at (δ = 4.71 and 4.76) each integrating for two protons. A singlet integrating for five protons at δ = 4.24 is assigned to the protons of the unsubstituted ferrocenyl ring.

The $^{13}C\{^{1}H\}$ NMR spectrum shows the imine carbon signal at δ = 161.2, and a signal for the *ipso*- carbon at δ = 78.1. All the other carbon atoms are accounted for in the $^{13}C\{^{1}H\}$ NMR

spectrum of the by-product at (δ = 70.9, 69.3 and 68.7). The infrared spectrum of the ferrocenecarbaldehyde hydrazone shows absorption bands ν(C=N str.) at 1627 cm^{-1} and ν(N–H str.) at 3095 cm^{-1}.

2.7 Synthesis and characterisation of monosodium 3-^{t}butyl-5-sulfonato salicylaldimine-ferrocenylimine rhodium(I)1,5-cyclooctadiene heterobimetallic complex (2.7)

The new heterobimetallic complex **2.7** was synthesised by reacting the mononuclear complex **2.6** with the Rh(I) precursor $[Rh(COD)Cl]_2$ according to (Scheme 2.8). This complex was obtained as a brown solid in excellent yield (97%) and was characterised using FT-IR, ^{1}H NMR and ^{13}C NMR spectroscopy. The complex is sparingly soluble in water at room temperature. The poor solubility may be due to the greater hydrophobic nature of the tertiary-butyl substituent.

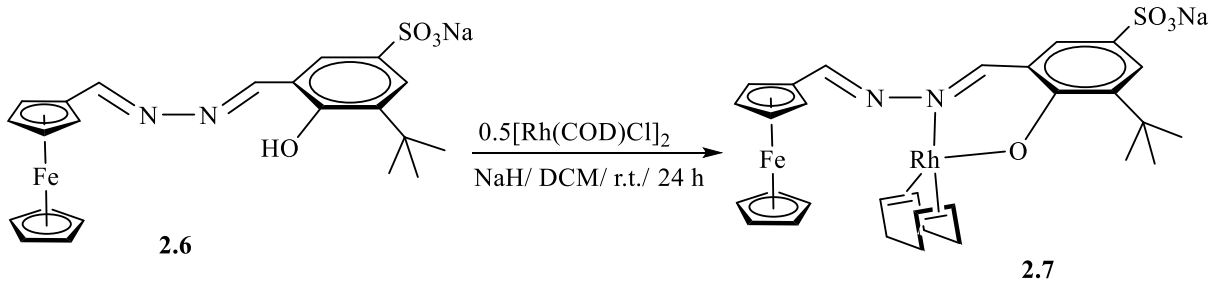

Scheme 2.8 Synthesis of the heterobimetallic complex **2.7**.

Deprotonation and subsequent coordination to the rhodium metal is confirmed by the ^{1}H NMR spectrum, which does not display a signal corresponding to the hydroxyl proton (Figure 2.8).

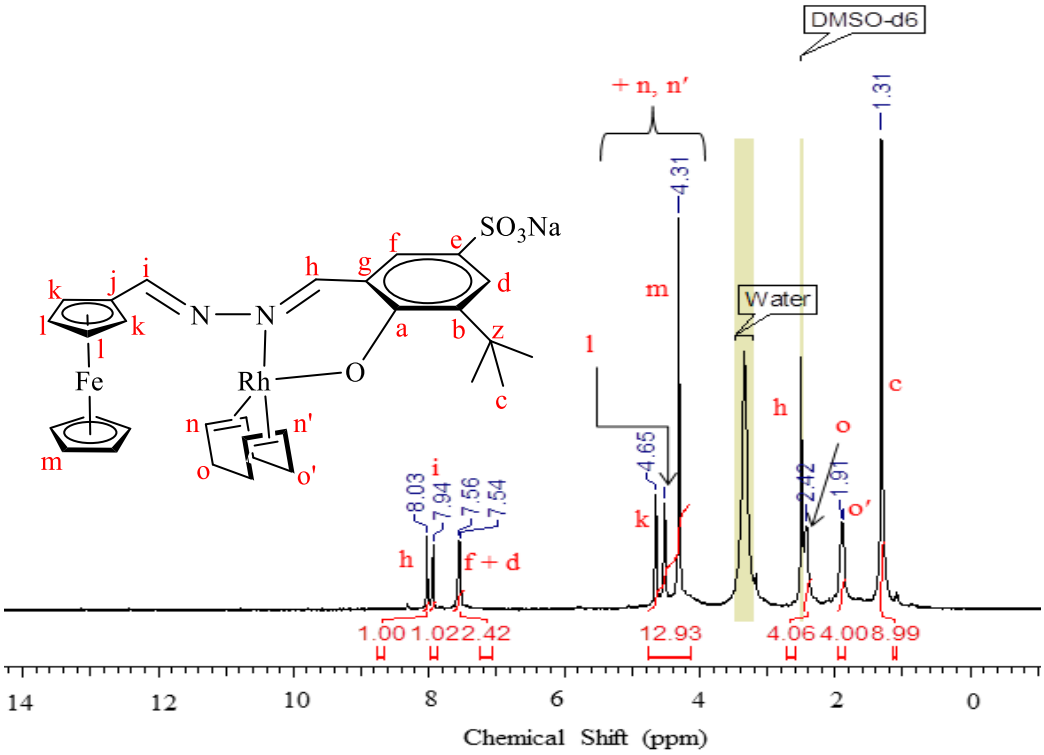

Figure 2.8 ^{1}H NMR (DMSO-d_6) spectrum for the heterobimetallic complex **2.7**.

In a similar manner to **2.5**, the vinylic COD protons of **2.7** are observed as overlapping signals in the same region as the protons of the ferrocenyl moieties (δ = 4.65–4.31). The exo- and endo-methylene protons of the COD maintain their multiplicity upfield (δ = 2.42 H_o, δ = 1.91 $H_{o'}$). The tertiary-butyl protons are accounted for as a singlet in their characteristic region (δ = 1.31) integrating for nine protons.

The $^{13}C\{^{1}H\}$ NMR together with the HSQC 2-dimensional NMR spectra of **2.7** show a similar trend as observed with **2.6**. The carbon (δ = 115.7 C_b) occurs upfield relative to (C_a, C_e and C_g) due to shielding through inductive effects by the tertiary-butyl substituent. All the other carbon atoms are accounted for in the $^{13}C\{^{1}H\}$ NMR spectra of **2.7**.

The infrared spectrum of the complex **2.7** displays a characteristic imine absorption band ν(C=N str.) at 1592 cm^{-1} as an intense broad band with a shoulder assigned to the second imine.

The ESI mass spectrum was recorded in the negative ion mode and shows a base peak for $[M– Rh(COD)]^{-}$ ion at *m/z* = 467.07, corresponding to the molecular weight of the anionic complex **2.7**. The fragmentation pattern is similar to that of **2.5**, both heterobimetallic complexes showing base peaks similar to their mononuclear counterparts.

2.8 Synthesis and characterisation of formylated monosodium 5-sulfonatosalicylaldimine-ferrocenylimine mononuclear complex (2.8)

In the past, we have synthesised water-soluble Rh(I) metallodendrimers (prepared *in situ*) bearing multiple active sites.[9] The basis is that a multinuclear compound would possess improved properties over that of a mononuclear complex through the numerous active sites on the periphery. In line with extending our previous work, we sought to synthesise G1-metallodendrimers of the water-soluble ferrocenyl-Rh(I) heterobimetallic complexes. The work entails the synthesis of the mononuclear complex **2.8**, by the Schiff base condensation reaction of 1,1′-ferrocenedicarboxaldehyde with monosodium 5-sulfonato salicylaldimine **2.3** (Scheme 2.9). The complex was isolated by precipitation in diethyl ether as a dark red solid in good yield (86%). The mononuclear complex **2.8** has good solubility in water (11 mg/mL, r.t.).

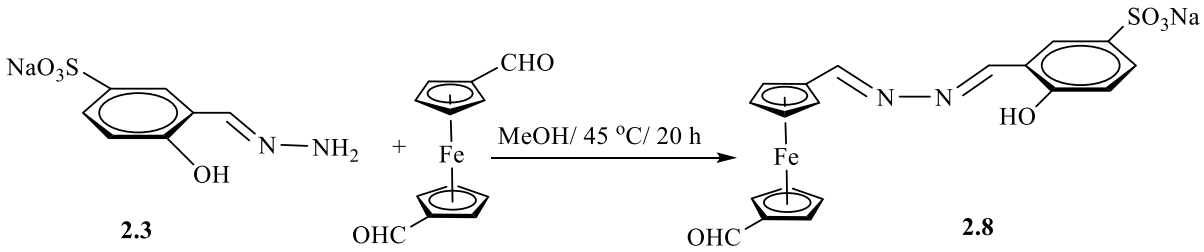

Scheme 2.9 Synthesis of the mononuclear complex **2.8**.

The 1,1′-ferrocenedicarboxaldehyde was successfully functionalised on one aldehyde end in a Schiff base condensation reaction through a controlled dropwise addition of a methanolic solution of **2.3**. The ^{1}H NMR spectrum (Figure 2.9) supports formation of **2.8** by showing a singlet at δ = 9.88, assigned to the aldehyde proton. All the phenyl protons are observed in their characteristic region (δ = 7.94 H_f, δ = 7.59 H_d, δ = 6.91 H_c respectively). Interesting to note, (from the insert on the spectrum) are the ferrocenyl protons H_n which appear as a broad signal overlapping with protons H_k at δ = 4.89 and integrating for four protons. This overlap may be due to the slight magnetic in-equivalence of the two ferrocenyl moieties brought about by the differing functionality (C=N and C=O) of each moiety. The protons H_l and H_m are observed as two broad signals at *ca*. δ = 4.70 for reasons similar to **2.4** and **2.6** of the monosubstituted moiety.

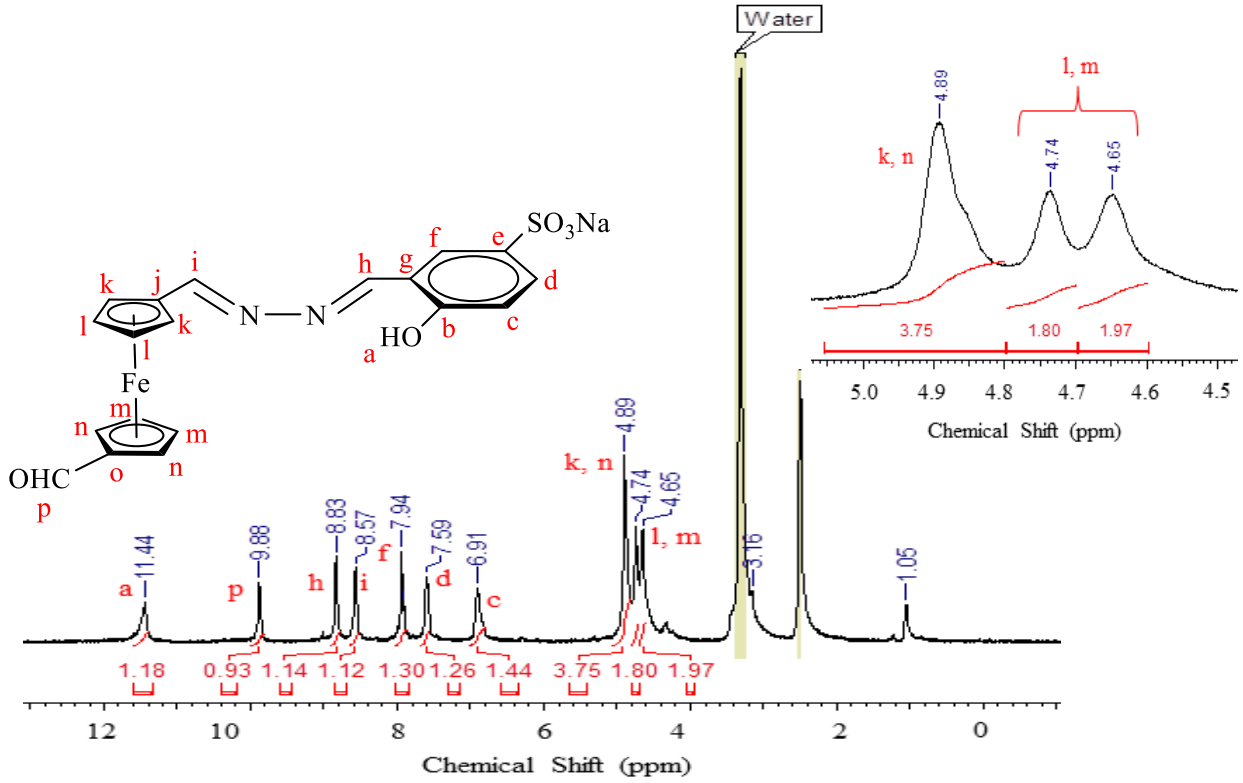

Figure 2.9 ^{1}H NMR (DMSO-d_6) spectrum for the mononuclear complex **2.8**.

The $^{13}C\{^{1}H\}$ NMR as well as the 2-dimensional NMR experiments (HSQC and COSY) also substantiate formation of the complex. All the carbon atoms, and proton-proton coupling is assigned accordingly in the spectra.

The infrared spectrum of complex **2.8** displays an ν(O–H str.) absorption band at 3417 cm^{-1} as well as the characteristic imine absorption band ν(C=N str.) at 1619 cm^{-1} as an intense broad band with a shoulder assigned to the second imine. The aldehyde absorption band ν(C=O str.) of **2.8** is observed at 1657 cm^{-1}.

The negative ion mode ESI mass spectrum is consistent with the structure of **2.8**, displaying a base peak for $[M]^-$ ion at m/z = 439.01 corresponding to the molecular weight of the anion of **2.8**.

2.9 Synthesis and characterisation of formylated monosodium 5-sulfonatosalicylaldimine-ferrocenylimine rhodium(I) 1,5-cyclooctadiene heterobimetallic complex (2.9)

The new heterobimetallic complex **2.9** was synthesised by reacting the mononuclear complex **2.8** with the Rh(I) precursor $[Rh(COD)Cl]_2$ according to (Scheme 2.10). This complex was obtained as a brown solid in excellent yield (93%) and was characterised fully using FT-IR, ^{1}H NMR and ^{13}C NMR spectroscopy.

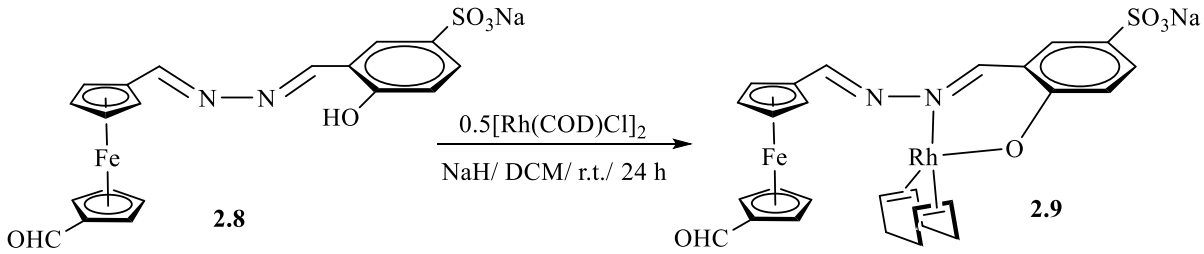

Scheme 2.10 Synthesis of the heterobimetallic complex **2.9**.

The ^{1}H NMR spectrum accounts for all protons in the structure of **2.9** (Figure 2.10), and does not show the hydroxyl proton of **2.8**.

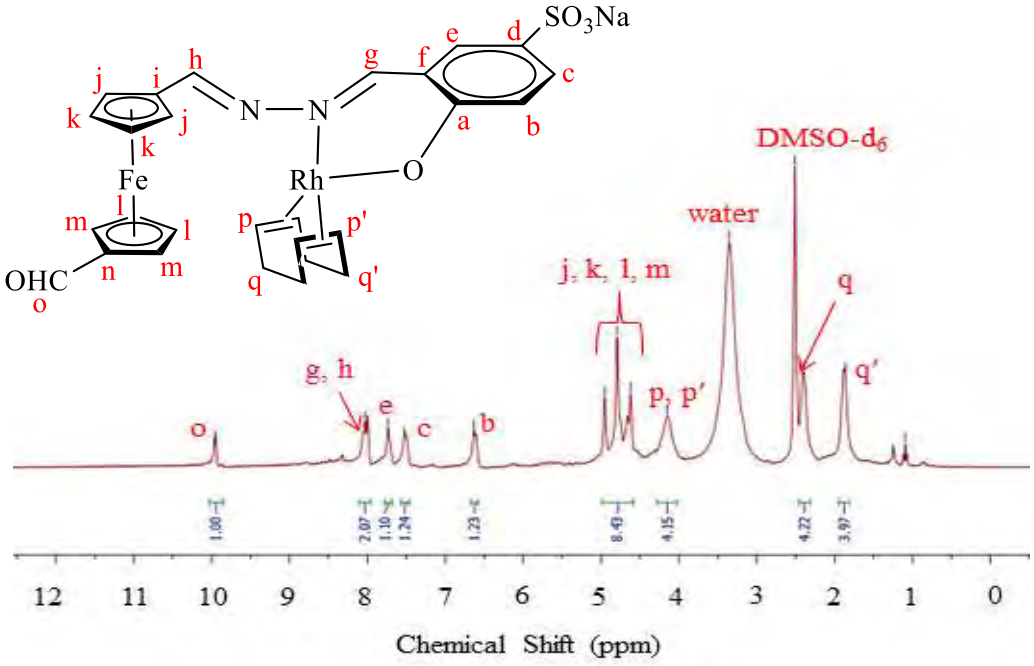

Figure 2.10 ^{1}H NMR (DMSO-d_6) spectrum for the heterobimetallic complex **2.9**.

The $^{13}C\{^{1}H\}$ NMR as well as the 2-dimensional NMR experiments (HSQC and COSY) were also employed to corroborate formation of the complex. The spectra permitted assignment of all carbon atoms, and identification of proton-proton coupling accordingly.

The infrared spectrum of complex **2.9** displays a characteristic imine absorption band *ν*(C=N str.) at a lower wavenumber to that of **2.8**, occurring at 1600 cm^{-1} as an intense broad band with a shoulder assigned to the second imine. The aldehyde functionality of **2.9** is observed at a similar absorption band *ν*(C=O str.) to that of **2.8 (**1657 cm^{-1}).

The ESI mass spectrum was recorded in the negative ion mode and shows a base peak for $[M– Rh(COD)]^{-}$ ion at *m/z* = 439.00, corresponding to the molecular weight of the anionic complex **2.8**. The fragmentation pattern is similar to that of **2.5 and 2.7**, with all heterobimetallic complexes showing base peaks similar to their mononuclear counterparts.

2.9.1 Attempts to anchor complexes (2.8) and (2.9) onto a dendrimer

Dendrimers have also attracted attention in catalytic applications as homogeneous and/or heterogeneous complexes. This owes to the multinuclear nature of dendritic structures, bearing multiple active sites which often lead to improved catalytic activity. Such properties have formed the basis to anchor the ferrocenyl-Rh(I) complexes onto a low-generation dendrimer.

Our initial attempts were to conjugate the complexes **2.8** and **2.9** onto the DAB-Generation 1 dendrimer scaffold (Scheme 2.11). The condensation reaction of either **2.8** or **2.9** with the G1-dendrimer was carried out under various reaction conditions. This also involved changing the solvent system as well as varying the reaction time and temperature. Addition of a catalytic amount of acid is known to promote a Schiff base reaction.[18] However, in this system of compounds, addition of a catalytic amount of sulfuric acid/ acetic acid could not drive the reaction towards formation of the products **2.10** or **2.11**. Despite the several efforts carried out to conjugate the complexes, the intended products could not be attained. This could be attributed to poor reactivity of the remaining aldehyde upon functionalisation of the disubstituted ferrocene in **2.8** and **2.9**. A number of examples of ferrocene derivatives grafted onto a dendrimer are reported in the literature,[32–37] but very few are known with disubstituted functionality on ferrocene.[38–40]

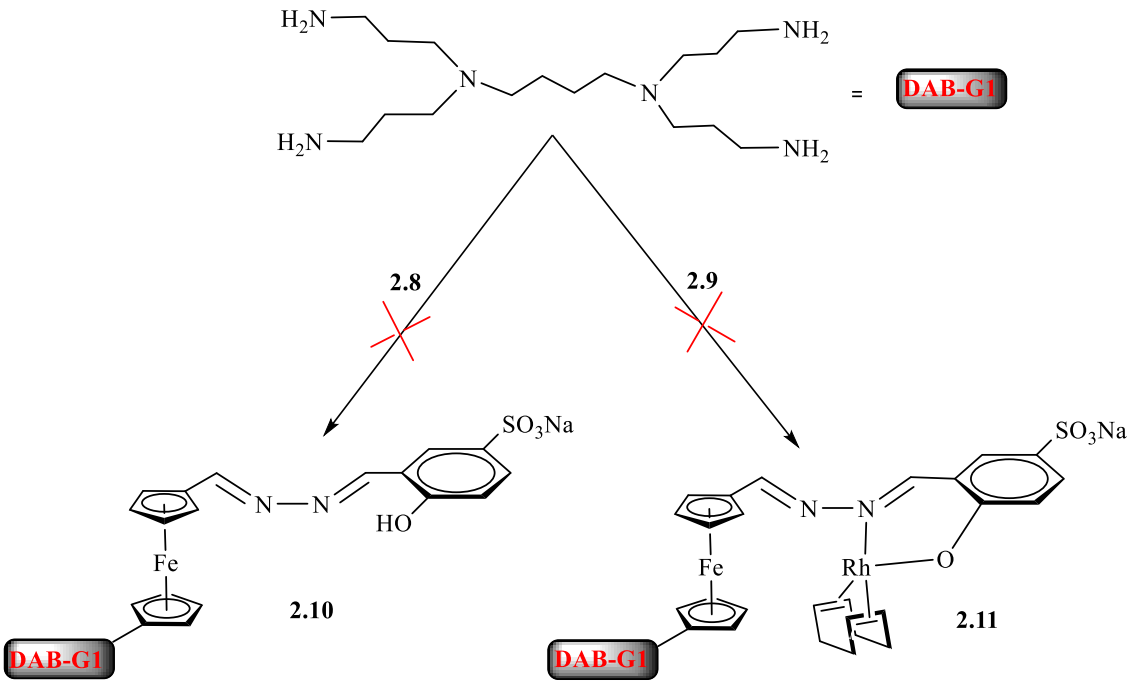

Scheme 2.11 Anchoring complexes **2.8** and **2.9** onto DAB-G1 dendrimer.

In this work, the non-reactivity of the aldehyde functionality of **2.8** or **2.9** towards the Schiff base condensation reaction was also observed with reactions using propylamine. Similar behaviour of the compounds in solution was observed to that of the reactions with the DAB-G1 dendrimer. This could lead to a conclusion that the remaining aldehyde functionality of **2.8** or **2.9** may not be as reactive to afford a stable compound.

2.10 Summary

A series of ferrocene-based mononuclear complexes bearing *N,O*-chelating donor atoms were prepared and successfully used in the synthesis of water-soluble Rh(I)-ferrocenyl heterobimetallic complexes. These mononuclear and heterobimetallic complexes were characterised using various spectroscopic and analytical techniques which include; ^{1}H NMR and ^{13}C{^{1}H} NMR spectroscopy, FT-IR spectroscopy, elemental analysis as well as mass spectrometry. The complexes will be employed as catalyst precursors in the aqueous biphasic hydroformylation of 1-octene and the results from these evaluations are discussed in the following chapter.

2.11 References

1. J. Halpern, *Pure Appl. Chem.*, 2001, **73**, 209–220.

2. N. Farrell, *Met. Complexes as Drugs Chemother. Agents*, 1989, **11**, 809–840.

3. E. Hermanns and J. Hasenjäger, *Top. Organomet. Chem.*, 2008, **23**, 53–66.

4. S. Köcher, B. Walfort, G. P. M. van Klink, G. van Koten, and H. Lang, *J. Organomet. Chem.*, 2006, **691**, 3955–3961.

5. K. C. B. Oliveira, S. N. Carvalho, M. F. Duarte, E. V. Gusevskaya, E. N. dos Santos, J. El Karroumi, M. Gouygou, and M. Urrutigoïty, *Appl. Catal. A Gen.*, 2015, **497**, 10–16.

6. R. A. Krüger and T. Baumgartner, *Dalton Trans.*, 2010, **39**, 5759–67.

7. L. Leclercq and A. R. Schmitzer, *Organometallics*, 2010, **29**, 3442–3449.

8. V. Kovač, A. Višnjevac, V. Rapić, and B. Kojić-Prodić, *J. Mol. Struct.*, 2004, **687**, 107–110.

9. E. B. Hager, B. C. E. Makhubela, and G. S. Smith, *Dalton Trans.*, 2012, **41**, 13927–35.

10. L. C. Matsinha, S. F. Mapolie, and G. S. Smith, *Dalton Trans.*, 2015, **44**, 1240–1248.

11. B. C. E. Makhubela, A. M. Jardine, G. Westman, and G. S. Smith, *Dalton Trans.*, 2012, **41**, 10715–23.

12. V. A. Daier, C. M. Palopoli, C. Hureau, A. De Candia, and S. R. Signorella, *Arkivoc*, 2011, **2011**, 327–342.

13. S. Mandal, D. K. Poria, D. K. Seth, P. S. Ray, and P. Gupta, *Polyhedron*, 2014, **73**, 12–21.

14. D. Astruc and F. Chardac, *Chem. Rev.*, 2001, **101**, 2991–3023.

15. R. Zhong, Y. Wang, X. Guo, Z. Chen, and X. Hou, *Chem. Eur. J.*, 2011, **17**, 11041–11051.

16. N. C. Antonels, J. R. Moss, and G. S. Smith, *J. Organomet. Chem.*, 2011, **696**, 2003–2007.

17. R. Chinchilla and C. Nájera, *Chem. Soc. Rev.*, 2011, **40**, 5084–5121.

18. K. Nakao, G. Choi, Y. Konishi, H. Tsurugi, and K. Mashima, *Eur. J. Inorg. Chem.*, 2012, **17**, 1469–1476.

19. C. Janiak, A.-C. Chamayou, A. K. M. R. Uddin, M. Uddin, S. K. Hagen, and M. Enamullah, *Dalton Trans.*, 2009, **19**, 3698–3709.

20. K. H. Shaughnessy, *Chem. Rev.*, 2009, **109**, 643–710.

21. S. Liu, A. Motta, M. Delferro, and T. J. Marks, *J. Am. Chem. Soc.*, 2013, **135**, 8830–8833.

22. R. G. Arrayμs, J. Adrio, and J. C. Carretero, *Angew. Chem. Int. Ed.*, 2006, **45**, 7674–7715.

23. C. Ornelas, *New J. Chem.*, 2011, **35**, 1973–1985.

24. P. C. Bruijnincx and P. J. Sadler, *Curr. Opin. Chem. Biol.*, 2008, **12**, 197–206.

25. A. M. Pizarro, A. Habtemariam, and P. J. Sadler, *Top. Organomet. Chem.*, 2010, **32**, 21–56.

26. S. Rafique, M. Idrees, A. Nasim, H. Akbar, and A. Athar, *Mol. Biol.*, 2010, **5**, 38–45.

27. C. Y. Acevedo-Morantes, E. Meléndez, S. P. Singh, and J. E. Ramírez-Vick, *J. Cancer Sci. Ther.*, 2012, **4**, 271–275.

28. D. Plazìuk, J. Zakrzewski, M. Salmain, A. Błauzì, B. Rychlik, P. Strzelczyk, A. Bujacz, and G. Bujacz, *Organometallics*, 2013, **32**, 5774–5783.

29. N. Lease, V. Vasilevski, M. Carreira, A. De Almeida, M. Sanau, P. Hirva, and A. Casini, *J. Med. Chem.*, 2013, **56**, 5806–5818.

30. S. D. Khanye, J. Gut, P. J. Rosenthal, K. Chibale, and G. S. Smith, *J. Organomet. Chem.*, 2011, **696**, 3296–3300.

31. W. Nkoana, D. Nyoni, P. Chellan, T. Stringer, D. Taylor, P. J. Smith, A. T. Hutton, and G. S. Smith, *J. Organomet. Chem.*, 2014, **752**, 67–75.

32. J. Palomero, J. A. Mata, F. González, and E. Peris, *New J. Chem.*, 2002, **26**, 291–297.

33. P. Govender, B. Therrien, and G. S. Smith, *Eur. J. Inorg. Chem.*, 2012, 2853–2862.

34. M. I. R. Valderrama, R. A. V. García, T. Klimova, E. Klimova, L. Ortiz-Frade, and M. M. García, *Inorg. Chim. Acta*, 2008, **361**, 1597–1605.

35. S. Sengupta, S. Sengupta, S. K. Sadhukhan, and S. K. Sadhukhan, *Organometallics*, 2001, **20**, 1889–1891.

36. E. G. Morales-Espinoza, K. E. Sanchez-Montes, E. Klimova, T. Klimova, I. V. Lijanova, J. L. Maldonado, G. Ramos-Ortíz, S. Hernández-Ortega, and M. Martínez-García, *Molecules*, 2010, **15**, 2564–2575.

37. S. Nlate, J. Ruiz, D. Astruc, and J.-C. Blais, *Chem. Commun.*, 2000, 417–418.

38. C. O. Turrin, J. Chiffre, D. De Montauzon, J. C. Daran, A. M. Caminade, E. Manoury, G. Balavoine, and J. P. Majoral, *Macromolecules*, 2000, **33**, 7328–7336.

39. E. R. De Jong, E. Manoury, J. C. Daran, C. O. Turrin, J. Chiffre, A. Sournia-Saquet, W. Knoll, J. P. Majoral, and A. M. Caminade, *J. Organomet. Chem.*, 2012, **718**, 22–30.

40. D. L. Stone, D. K. Smith, and P. T. McGrail, *J. Am. Chem. Soc.*, 2002, **124**, 856–864.

Chapter 3

Catalytic evaluation of water-soluble mononuclear and heterobimetallic complexes in aqueous biphasic hydroformylation of 1-octene

3.1 Introduction

The use of homogeneous catalysts which often display greater activity and selectivity than related homogeneous ones is often confounded by complications involving catalyst recovery and recycling. Employing homogeneous catalysts under aqueous biphasic conditions, as in the hydroformylation reaction (transition metal-catalysed reaction of olefins with hydrogen and carbon monoxide to afford aldehydes, Scheme 3.1) is one of many strategies that have been developed.[1–8] The aqueous biphasic system is ideal as it utilises water, which is an eco- and user-friendly, relatively cheap, abundant and non-flammable solvent, in line with green chemistry principles.[2,9–14] Moreover, water is immiscible with most organic solvents, alleviating some of the challenges associated with homogeneous catalysis, such as long chain aldehyde product recovery. [15–22] Such efforts aim to overcome the difficulties associated with the recovery of expensive and ever-diminishing transition metal resources. The technique strikes a "characteristic" balance between heterogeneous and homogeneous processes for the hydroformylation reaction.

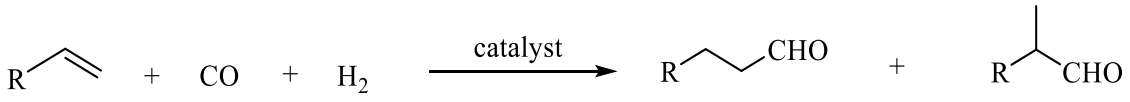

R= alkyl, aromatic group

Scheme 3.1 Hydroformylation of olefins.

The aldehydes generated from the atom-economical hydroformylation reaction are typically processed into valuable consumer products in the cosmetics, bulk and fine chemicals industries.[23–25] Apart from the aldehydes, the hydroformylation reaction can be characterised with side reactions through isomerisation of the olefin as well as hydrogenation of the

aldehydes to give alcohols. Selectivity (chemo- and regio-selectivity) of a catalyst is one of the main factors that are considered in catalyst development and evaluation. A typical industrial hydroformylation catalyst would possess excellent chemoselectivity towards aldehydes as well as excellent regioselectivity towards either linear or branched aldehydes (depending on the intended downstream product).[12,23,26–28]

Current industrial hydroformylation catalysts are based on cobalt [$Co_2(CO)_8$] and rhodium [$HRh(CO)(PPh_3)_3$] metal catalysts. Rhodium-based metal complexes are generally preferred over other transition metals (Co, Ru, Ir, etc.) as hydroformylation catalysts due to the high activity and selectivity of the rhodium complexes under milder reaction conditions.[15,29–31] However, due to the greater expense of rhodium, novel strategies are required to ensure element sustainability. Immobilising the catalyst in water for aqueous-organic biphasic media is one such strategy aimed at element recovery and reuse.

Catalyst design continues to intrigue scientists worldwide. Recent efforts in the field of catalysis involve the use of bimetallic catalyst precursors in various olefin transformation reactions.[32–39] This stems from often improved activities and reaction rates conferred by metalloenzymes bearing two or more active metal centres.[38,40–42]

A typical example may involve one metal acting as the main catalytic centre whereas the other metal serves as an electron reservoir, stabilising the electron density around the catalytic centre. Ferrocene, a redox-active sandwich complex, has been included in several heterobimetallic complexes in combination with other transition metals, bridged by various ligand structures. In this context, the inclusion of ferrocene moieties modified with phosphorus donor sites is very common.[35,36,39,43] The application of such complexes in the aqueous-organic biphasic hydroformylation of higher olefins, from an efficient catalyst design and green chemistry perspective, is also intriguing. As an extension of our previous work in catalysis,[44] we were prompted to evaluate the effect of heterobimetallic complexes in the hydroformylation process.

3.2 Results and Discussion

3.2.1 Aqueous biphasic hydroformylation using complexes (2.4) and (2.5)

Initial catalytic studies to obtain the optimum conditions for the hydroformylation of 1-octene in aqueous biphasic media were performed with the mononuclear complex **2.4** and the heterobimetallic complex **2.5** (Figure 3.1).

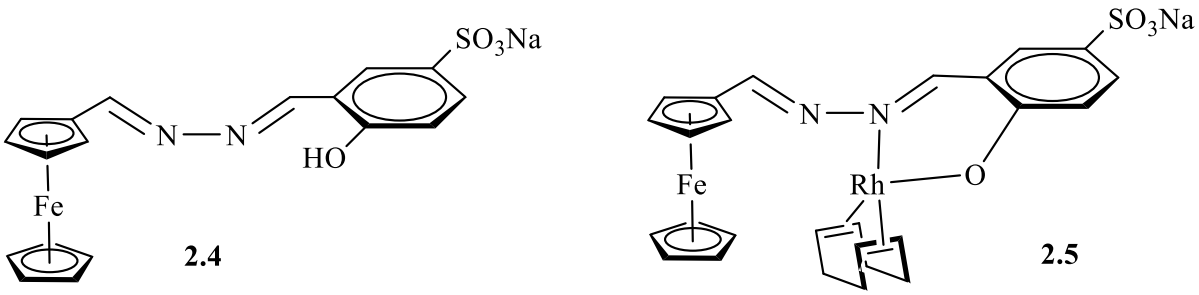

Figure 3.1 Catalyst precursors used for optimisation studies.

The conditions of the study (Scheme **3.2**) were based on the previously reported conditions for the hydroformylation of 1-octene using analogous Rh(I) catalyst precursors containing *N,O*-bidentate ligands.[44] The reactions were first performed at a fixed temperature and time of 75 °C and 8 hours respectively, with varying pressures (Table 3.1).

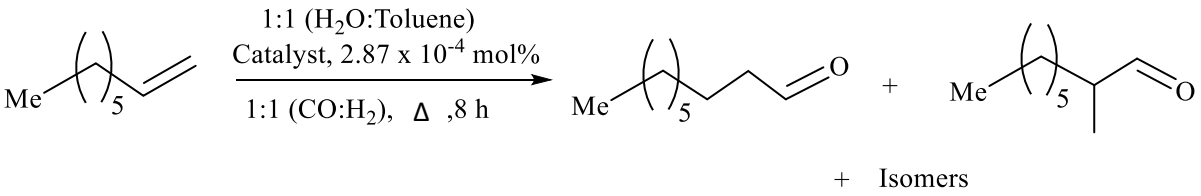

Scheme 3.2 Hydroformylation of 1-octene in aqueous biphasic media using **2.4** and **2.5**

The Effect of Pressure

The pressure was varied at a fixed temperature (Table 3.1) to determine the effect of the syngas pressure on chemoselectivity and regioselectivity in hydroformylation of 1-octene as well as to establish optimum pressure conditions. The mononuclear complex **2.4** shows no activity at the conditions of this study. To our knowledge, there has been no reported data on the use of ferrocenyl mononuclear complexes as sole catalysts in the hydroformylation of

olefins. This investigation of **2.4** is necessary to aid in ascertaining the contribution of the ferrocenyl moiety to the overall hydroformylation reaction.

Table 3.1 Hydroformylation of 1-octene using complexes **2.4** and **2.5** as catalyst precursors at 75 °C.[a]

Pressure (bar)	Complex	Conv. (%)	Aldehydes (%)			*Iso*-octenes (%)	*n/iso*	TOF (h^{-1})
			Total aldehydes	Nonanal	Branched			
20	**2.4**	-	-	-	-	-	-	-
20	**2.5**	44.66	22.15	99.60	0.39	77.85	255.38	30.91
30	**2.4**	-	-	-	-	-	-	-
30	**2.5**	25.71	31.77	99.44	0.56	68.23	177.57	25.53
40	**2.4**	-	-	-	-	-	-	-
40	**2.5**	60.03	77.62	74.28	25.71	22.38	2.89	145.61
50	**2.4**	-	-	-	-	-	-	-
50	**2.5**	25.78	50.20	32.43	67.57	49.80	0.48	40.44

[a]Reactions carried out with ($CO:H_2$) (1:1) at 75 ºC, 8 h in distilled water (5 mL) and toluene (5 mL) with 7.175 mmol of 1-octene and 2.87×10^{-3} mmol Rh catalyst. GC conversions obtained using *n*-decane as an internal standard in relation to authentic standard *iso*-octenes and aldehydes. [b]TOF = (mol product/ mol cat.) h^{-1} and is based on total aldehydes produced. Standard deviation ± 3.3 (**2.5**).

The best hydroformylation activity for **2.5** is observed at 40 bar. At this pressure, the catalyst also displays the best conversion of 1-octene to products, as well as good chemoselectivity for aldehydes (about 78%). Under these conditions (40 bar, 95 °C, 8 hours), the heterobimetallic catalyst displays similar regioselectivity to the water-soluble mononuclear catalyst reported by Hager and co-workers.[44] Very poor conversion of 1-octene and chemoselectivity is observed at lower pressure (20 bar and 30 bar) but the catalyst shows excellent regioselectivity to linear aldehydes. Isomerisation of 1-octene is highest at 20 bar with 78% of the products being internal octenes.

The Effect of Temperature

With the optimum pressure set at 40 bar, hydroformylation studies of complexes **2.4** and **2.5** were carried out at varying temperatures (55, 75, 95 ºC) (Table 3.2). The heterobimetallic complex **2.5** shows excellent activity (99.9%) at a high temperature of 95 ºC.

Table 3.2 Hydroformylation of 1-octene using complexes **2.4** and **2.5** as catalyst precursors at 40 bar.[a]

Temp. (°C)	Complex	Conv. (%)	Aldehydes (%)			*Iso*-octenes (%)	*n/iso*	TOF (h^{-1})
			Total aldehydes	Nonanal	Branched			
55	**2.4**	-	-	-	-	-	-	-
55	**2.5**	69.60	68.06	83.31	16.19	31.94	5.15	148.02
75	**2.4**	-	-	-	-	-	-	-
75	**2.5**	60.03	77.62	74.28	25.71	22.38	2.89	145.61
95	**2.4**	-	-	-	-	-	-	-
95	**2.5**	99.90	99.90	39.00	61.00	-	0.64	313.00

[a]Reactions carried out with ($CO:H_2$) (1:1) at 40 bar, 8 h in distilled water (5 mL) and toluene (5 mL) with 7.175 mmol of 1-octene and 2.87×10^{-3} mmol Rh catalyst. GC conversions obtained using *n*-decane as an internal standard in relation to authentic standard *iso*-octenes and aldehydes. [b]TOF = (mol product/ mol cat.) h^{-1} and is based on total aldehydes produced. Standard deviation ± 1. 9 (**2.5**).

Excellent chemoselectivity for aldehydes is also observed at 95 ºC. The regioselectivity to linear aldehydes is poor, as indicated by the dominance of branched aldehydes (61%) over linear aldehydes (39%), which is also reflected by the low *n*:*iso* ratio (0.64). However, the mononuclear complex reported by Hager and co-workers [44] favours the formation of linear aldehydes to branched aldehydes at similar reaction conditions. The higher percentage of branched aldehydes with **2.5** could be a result of possible hydroformylation of the isomerisation products to branched aldehydes with the introduction of a second metal at high temperatures. At 75 °C, the complex displays a good linear aldehyde production of 74%, as well as a moderate 1-octene conversion of 60%. The best regioselectivity to linear aldehydes is obtained at 55 °C with 83% nonanal produced. However, the conversion at 55 °C (70%) is lower than at 95 °C (99.9%). Overall, the complex favours branched aldehydes at the conditions that give the best conversion, that is, at 40 bar and 95 °C. These conditions were chosen for further reactions using catalyst precursors **2.4** – **2.7**.

3.2.2 Aqueous biphasic hydroformylation using complexes (2.5) and (2.7)

Similar to complex **2.4**, the mononuclear complex **2.6** does not show any activity in the hydroformylation of 1-octene. At the conditions of 40 bar and 95 °C, the catalyst precursor **2.5** displays excellent conversion (99.9%) of 1-octene as well as outstanding

chemoselectivity (99.9%) towards aldehydes (Table 3.3, Entry 1). The catalyst exclusively forms aldehydes at these conditions. Catalyst precursor **2.7** (Figure 3.2) also shows excellent conversion (95%) and good chemoselectivity for aldehydes (77%) (Table 3.3, Entry 2).

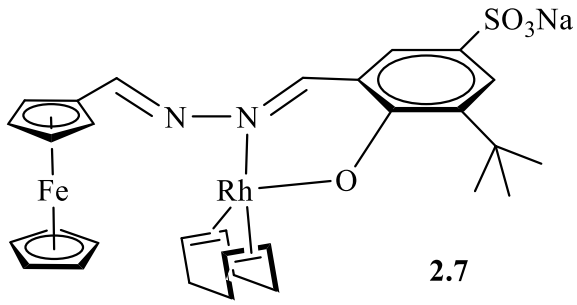

2.7

Figure 3.2 Catalyst precursor **2.7**

Isomerisation of 1-octene is also observed with this catalyst precursor under the optimum conditions. Furthermore, the presence of the electron-donating tertiary-butyl substituent in catalyst precursor **2.7** seems to lower the chemoselectivity, yet improves the regioselectivity towards linear aldehydes. The improved regioselectivity for linear aldehydes in catalyst **2.7** is expected due to the steric effects from the bulkier tertiary-butyl substituent. Also influencing the regioselectivity is the migratory insertion of the olefin into the Rh-H of the complex favouring anti-Markovnikov route, giving rise to a straight-chain alkyl ligand which leads to linear aldehydes (nonanal) as the final product.[45,46] This is similar to the data observed for related tertiary-butyl substituted catalysts bearing *N,O*-bidentate ligands reported by Hager and Matsinha.[44,47] Good catalytic activity is observed for both catalyst precursors (**2.5**, 313 h^{-1}) and (**2.7**, 229 h^{-1}).

Table 3.3 Hydroformylation of 1-octene with catalyst precursors **2.5** and **2.7** at 8 h.[a]

Entry	Complex	Conv. (%)	Aldehydes (%)			*Iso*-octenes (%)	*n/iso*	TOF (h^{-1})
			Total aldehydes	Nonanal	Branched			
1	**2.5**	99.9	99.9	39	61	-	0.64	313
2	**2.7**	95	76.5	55	45	23.5	1.2	229

[a]Reactions carried out with ($CO:H_2$) (1:1) at 40 bar, 95 °C in distilled water (5 mL) and toluene (5 mL) with 7.175 mmol of 1-octene and 2.87 × 10^{-3} mmol Rh catalyst. GC conversions obtained using *n*-decane as an internal standard in relation to authentic standard *iso*-octenes and aldehydes. [b]TOF = (mol product/mol cat.) h^{-1} and is based on total aldehydes produced. Standard deviation ± 0.01 (**2.5**), ± 3.6 (**2.7**).

Both complexes are good hydroformylation catalysts, as evidenced by the good yields for aldehydes as well as low isomerisation products and the absence of hydrogenation products (alcohols).

3.2.3 Recyclability studies

Reusability of a catalyst is key to an effective and sustainable design and application strategy. This has a bearing on the economics of an industrial scale setup.[48] The studies were carried out by simply decanting off the organic layer after the first catalytic reaction, followed by addition of a fresh sample of 1-octene and *n*-decane (internal standard) dissolved in toluene, onto the aqueous layer. This was repeated for each successive catalytic reaction using the same aqueous phase.

The catalyst precursor **2.5** could be recycled for at least 5 cycles with a gradual loss in activity and 1-octene conversion (Figure. 3.3). Catalyst precursor **2.7** could be recycled 4 times with a slight decrease in conversion before any loss in catalytic activity was observed. The observed decrease in conversion of 1-octene for both catalyst precursors could be due to a decrease in activity of the catalysts. This could also be ascribed to partial agglomeration of *in situ* formed nanoparticles (from the catalyst) observed in the aqueous layer. This was attested to through mercury poisoning tests; wherein a drop of mercury was added to a fresh catalytic reaction so as to suppress the particles in each cycle and renders them unavailable for catalysis. The results of this experiment are presented in section 3.2.5 of this report. Moreover, loss of the catalyst due to leaching from the aqueous layer, shown by the discolouration of the aqueous layer with each recycling could also possibly result in the observed steady decrease in 1-octene conversions. Inductively coupled plasma optical emission spectrometry (ICP-OES) was used to analyse the aqueous layer for possible loss of metal catalyst with each successive run.

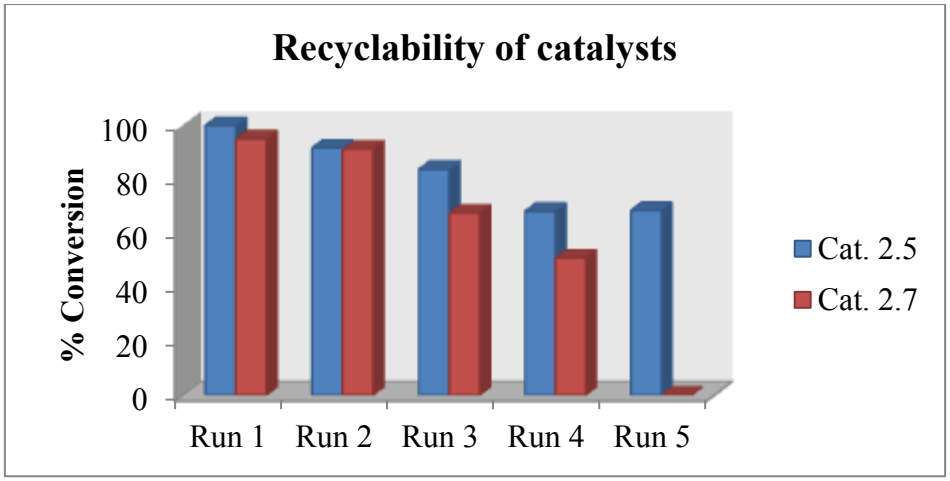

Figure 3.3 Conversion of the catalysts in recyclability studies, performed at 95 °C, 40 bar in a 90 mL stainless steel pipe reactor. Solvent (1:1, toluene:water), substrate (1-octene, 7.175 mmol), internal standard (*n*-decane, 1.435 mmol), metal catalyst (Rh, 2.87 × 10^{-3} mmol), syngas (1:1, CO:H_2), reaction time (8 h). Standard deviation ± 3.2% (**2.5**), ± 1.3% (**2.7**).

*Chemoselectivity of complex (**2.5**)*

The catalyst precursor **2.5** shows excellent chemoselectivity for aldehydes in the first cycle/ run of the experiments (Figure 3.3). When the catalyst-containing aqueous layer is recycled in the second run, about 40% isomerisation products are formed. Isomerisation of 1-octene is induced in the second cycle and becomes more pronounced with each successive cycle. At the fifth cycle, the predominant products are *iso*-octenes.

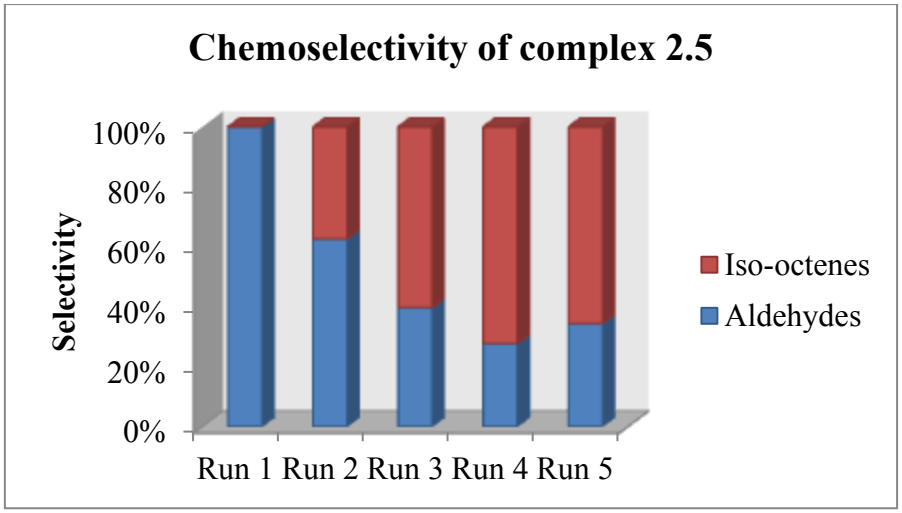

Figure 3.4 Chemoselectivity of the catalyst precursor **2.5** in recyclability studies, performed at 95 °C and 40 bar in a 90 mL stainless steel pipe reactor. Solvent (1:1, toluene:water), substrate (1-octene, 7.175 mmol), internal standard (*n*-decane, 1.435 mmol), metal catalyst (Rh, 2.87 × 10^{-3} mmol), syngas (1:1, $CO:H_2$), reaction time (8 h). Standard deviation ± 3.2%.

The significant increase of the *iso*-octenes with each successive recycle is indicative of loss of catalyst activity during hydroformylation, possibly as a result of the change in the actual active species. High pressure NMR studies could shed more light on the behaviour of the catalyst under hydroformylation conditions.

*Chemoselectivity of complex (**2.7**)*

The catalyst precursor **2.7** shows good chemoselectivity for aldehydes (77%) in the first cycle of the experiments (Figure 3.5). Isomerisation is induced in the first cycle and increases with each successive cycle, similar to the observation with **2.5**.

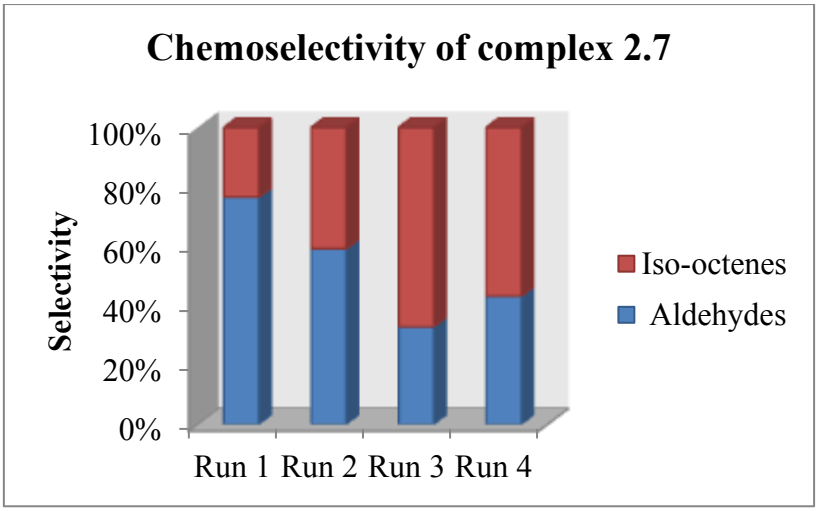

Figure 3.5 Chemoselectivity of the catalyst precursor **2.7** in recyclability studies, performed at 95 °C and 40 bar in a 90 mL stainless steel pipe reactor. Solvent (1:1, toluene:water), substrate (1-octene, 7.175 mmol), internal standard (*n*-decane, 1.435 mmol), metal catalyst (Rh, 2.87×10^{-3} mmol), syngas (1:1, $CO:H_2$), reaction time (8 h). Standard deviation ± 1.3%.

*Regioselectivity of complex (**2.5**)*

In the first cycle of the experiments, complex **2.5** gives 60% branched aldehydes, as shown in Figure 3.6. The higher percentage of the branched aldehydes in the first cycle may be attributed to the flexibility of the ligand, promoting isomerisation of 1-octene well before hydroformylation could occur.

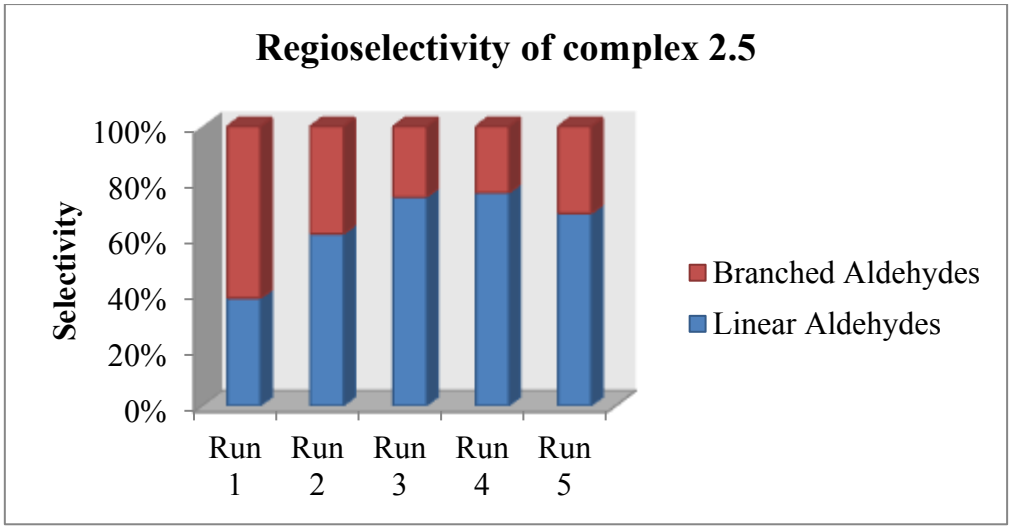

Figure 3.6 Regioselectivity of the catalyst precursor **2.5** in recyclability studies, performed at 95 °C and 40 bar in a 90 mL stainless steel pipe reactor. Solvent (1:1, toluene:water), substrate (1-octene, 7.175 mmol), internal standard (*n*-decane, 1.435 mmol), metal catalyst (Rh, 2.87×10^{-3} mmol), syngas (1:1, $CO:H_2$), reaction time (8 h). Standard deviation ± 3.2%.

*Regioselectivity of complex (**2.7**)*

The complex **2.7** shows better regioselectivity for linear aldehydes with 55% nonanal in the first cycle of the experiments (Figure 3.7). This would be expected as the bulkier groups on the catalysts would favour linear products in the hydroformylation reactions.

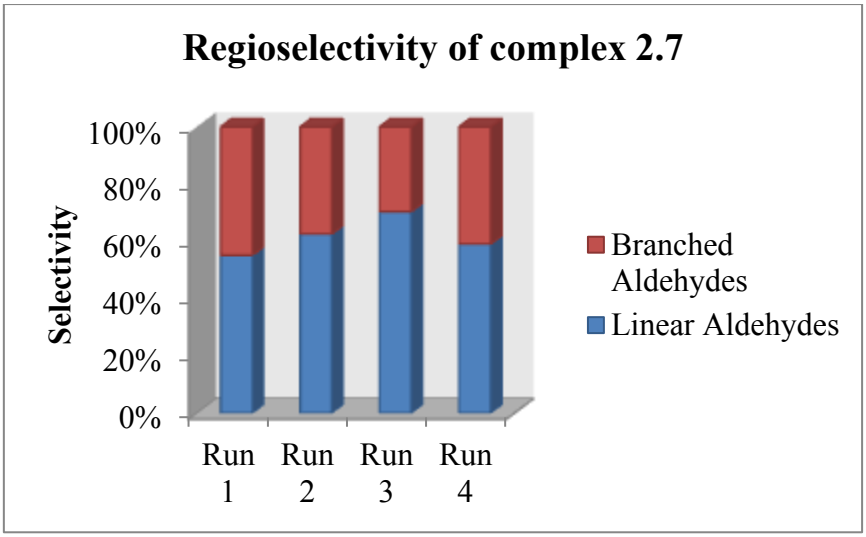

Figure 3.7 Regioselectivity of the catalyst precursor **2.7** in recyclability studies, performed at 95 °C and 40 bar in a 90 mL stainless steel pipe reactor. Solvent (1:1, toluene:water), substrate (1-octene, 7.175 mmol), internal standard (*n*-decane, 1.435 mmol), metal catalyst (Rh, 2.87 × 10^{-3} mmol), syngas (1:1, CO:H_2), reaction time (8 h). Standard deviation ± 1.3%.

The effects of ligand flexibility are not observed with catalyst precursor **2.7**, as the tertiary-butyl substituent imparts the bulkiness required to favour linear products. An average linear to branched aldehyde ratio of 60:40 is realised for both catalyst precursors. The observed regioselectivity for both catalysts is consistent with literature for related substituted *N,O*-bidentate ligands.[44,47] Phosphine modified ligands in heterobimetallic complexes of ferrocene and rhodium have been reported to show improved catalytic activity compared to their mononuclear counterparts in the hydroformylation of olefins.[43,49] The heterobimetallic catalyst precursors bearing *N,O*-bidentate ligands in this study showed comparable activity to their monometallic counterparts reported in previous studies.

3.2.4 Metal Leaching studies

The aqueous layer of each complex (**2.5** and **2.7**) was analysed for rhodium metal using inductively coupled plasma optical emission spectrometry (ICP-OES). The catalysts show poor conversions after the fifth and fourth cycle for compounds **2.5** and **2.7** respectively, with almost a 90% loss of metal observed. This could be due to the solubility of the metal complexes in 1-octene under the hydroformylation conditions of elevated temperature and

pressure. This substantiates the observed decrease in catalytic activity and 1-octene conversion during recyclability studies, particularly after the fifth recycle. Discolouration of the catalyst-containing aqueous layer was also observed, suggesting solubility of the catalyst in the organic layer under hydroformylation conditions (Figure 3.8).

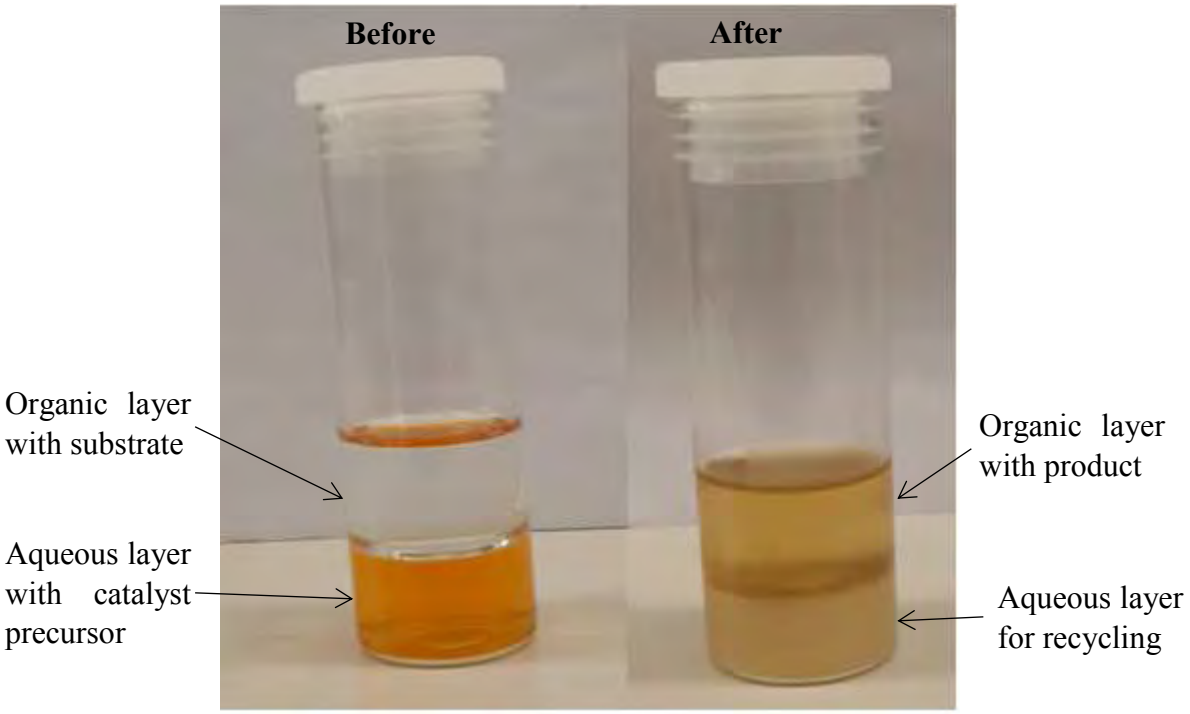

Figure 3.8 Biphasic catalytic system of complex **2.5**.

The accumulating black nano-particles in the aqueous layer with each cycle could be responsible for the observed catalytic behaviour (since isomerisation starts to rise). These together with the little amount of metal catalyst left in the aqueous phase could be responsible for the conversion of 1-octene to aldehydes and *iso*-octenes. This is in agreement to the observation by Matsinha and co-workers working with similar catalyst precursors, in which they attributed the increase in the *iso*-octenes with each successive cycle to the rhodium nano-particles.[47] Mercury poisoning tests were then carried out to confirm the presence of the rhodium nano-particles.

3.2.5 Mercury poisoning studies

The formation of nano-particles results in activity and conversion that is due to a combination of both homogeneous and heterogeneous systems. Addition of mercury suppresses the metal particles by amalgamation, making them unavailable for catalysis. A drop of mercury was added into the reactor after loading the catalyst, solvents (water and toluene) and internal standard. The reactions were run for 8 hours and recycled in a similar manner as in the absence of mercury (Table 3.4).

Table 3.4 Mercury poisoning experiments using complex **2.5**.[a]

Cycle	Conv. (%)	Aldehydes (%)			*Iso*-octenes (%)	*n/iso*	TOF (h^{-1})
		Total aldehydes	Nonanal	Branched			
no mercury							
1	99.90	99.90	39.00	61.00	-	0.64	313.00
2	92.00	63.00	62.00	38.00	37.00	1.63	178.00
3	84.00	40.00	75.00	25.00	60.00	3.00	102.00
4	68.00	68.00	76.00	24.00	72.00	3.20	59.00
5	69.00	34.00	69.00	31.00	66.00	2.20	71.00
with mercury							
1	63.00	48.00	72.00	28.00	52.00	2.57	93.00
2	67.00	32.00	73.00	27.00	68.00	2.70	67.00
3	49.00	40.00	70.00	30.00	60.00	2.33	69.00
4	-	-	-	-	-	-	-
5	-	-	-	-	-	-	-

[a]Reactions carried out with ($CO:H_2$) (1:1) at 40 bar, 95 °C, 8 h in distilled water (5 mL) and toluene (5 mL) with 7.175 mmol of 1-octene, 2.87×10^{-3} mmol Rh catalyst and a drop of mercury. GC conversions obtained using *n*-decane as an internal standard in relation to authentic standard *iso*-octenes and aldehydes. [b]TOF = (mol product/mol cat.) h^{-1} and is based on total aldehydes produced. Standard deviation ± 3.2% (no mercury) and ± 0.78% (with mercury).

In the presence of mercury, the catalyst could only be recycled 3 times. The catalyst shows a decrease in 1-octene conversion and activity to the third cycle. In the first cycle conversion can be said to be entirely due to homogeneous catalysis. From the second to the third cycle conversion drops considerably and at this stage both homogeneous and heterogeneous catalysis are responsible for the conversions observed. The species formed during each

successive cycle also favours formation of internal olefins. Such behaviour has been observed in the past.[44,47]

3.3 Summary

The ferrocenyl monometallic complexes and the ferrocenyl-Rh(I) heterobimetallic complexes were evaluated as aqueous biphasic hydroformylation catalyst precursors. The monometallic complexes **2.4** and **2.6** were not active in the hydroformylation of 1-octene. The heterobimetallic complexes **2.5** and **2.7** showed good activity and selectivity in the hydroformylation experiments. The conversion and selectivity of the heterobimetallic complexes is comparable to the results obtained by Hager and co-workers with the water-soluble mononuclear Rh(I) complex. The effects of incorporating ferrocene as a second metal were not pronounced, possibly due to the distance between the two metals which did not enable cooperativity. Moreover, the imine bond could be labile allowing the ferrocenyl moiety to be oriented in a fashion that would not confer effective cooperativity with the rhodium metal centre. The high metal losses as well as the accumulation of nano-particles on recycling have a significant bearing on the observed loss in catalyst activity, chemoselectivity and 1-octene conversion. In the past, formation and accumulation of these colloidal particles (during recycling) has been associated with an increase in the rate of isomerisation, and such observations are also reported in this work. A closer look at this behaviour may lead to a strategic approach in designing catalysts for isomerisation, which can eventually enable efficient hydroformylation of internal olefins from naphtha.

3.4 References

1. B. Cornils, W. A. Herrmann, I. T. Horvath, W. Leitner, S. Mecking, H. Olivier-Bourbigou, and D. Vogt, in *Multiphase Homogeneous Catalysis*, Wiley-VCH Verlag GmbH & Co. KGaA, Weinheim, 2nd edn., 2005, pp. 3–21.

2. A. E. C. Collis and I. T. Horváth, *Catal. Sci. Technol.*, 2011, **1**, 912–919.

3. D. J. Cole-Hamilton, *Catalysis*, 2003, **299**, 1702–1707.

4. E. A. Karakhanov and A. L. Maksimov, *Russ. J. Gen. Chem.*, 2009, **79**, 1370–1383.

5. C. De Rumpa, S. Sumanta, A. Ghosh, K. Mukherjee, S. Bhattacharyya, Sekhar, and B. Saha, *Res. Chem. Intermed.*, 2013, **39**, 3463–3474.

6. Â. C. B. Neves, M. J. F. Calvete, M. V. D. Pinho, and M. M. Pereira, *Eur. J. Org. Chem.*, 2012, 6309–6320.

7. B. Subramaniam, *Ind. Eng. Chem. Res.*, 2010, **49**, 10218–10229.

8. B. P. J. Dyson, D. J. Ellis, and T. Welton, *Platin. Met. Rev.*, 1998, **42**, 135–140.

9. D. Adams, P. Dyson, and S. Taverner, in *Chemistry in Alternative Reaction Media*, John Wiley & Sons Ltd, Chichester, 2nd edn., 2004, pp. 37–39.

10. B. Cornils and W. A. Herrmann, in *Aqueous-Phase Organometallic Catalysis*, Wiley-VCH Verlag GmbH & Co. KGaA, 2nd edn., 2004, pp. 7–8.

11. W. Keim, *Green Chem.*, 2003, **5**, 105–111.

12. B. Cornils, *Top. Curr. Chem.*, 1999, **206**, 133–149.

13. M. Lombardo and C. Trombini, in *RSC Green Chemistry Series: Eco-Friendly Synthesis of Fine Chemicals*, Royal Society of Chemistry, 1st edn., 2009, pp. 1–79.

14. R. A. Sheldon, *Green Chem.*, 2005, **7**, 267.

15. R. Franke, D. Selent, and A. Bo, *Chem. Rev.*, 2012, **112**, 5675–5732.

16. B. Cornils, W. A. Herrmann, and M. Rasch, *Angew. Chem. Int. Ed.*, 1994, **33**, 2144–2163.

17. S. K. Sharma and R. V. Jasra, *Catal. Today*, 2015, **247**, 70–81.

18. A. Rost, M. Müller, T. Hamerla, Y. Kasaka, G. Wozny, and R. Schomäcker, *Chem. Eng. Process. Process Intensif.*, 2013, **67**, 130–135.

19. N. Pinault and D. W. Bruce, *Coord. Chem. Rev.*, 2003, **241**, 1–25.

20. S. M. Mercer, T. Robert, D. V. Dixon, and P. G. Jessop, *Catal. Sci. Technol.*, 2012, **2**, 1315–1318.

21. P. Pollet, R. J. Hart, C. A. Eckert, and C. L. Liotta, *Acc. Chem. Res.*, 2010, **43**, 1237–1245.

22. L. Obrecht, P. C. J. Kamer, and W. Laan, *Catal. Sci. Technol.*, 2013, **3**, 541–551.

23. B. Cornils, *Org. Process Res. Dev.*, 1998, **1**, 121–127.

24. B. Cornils, *J. Mol. Catal. A Chem.*, 1999, **143**, 1–10.

25. G. T. Whiteker and C. J. Colbey, *Top. Organomet. Chem.*, 2012, **42**, 35–46.

26. B. Cornils and E. G. Kuntz, *J. Organomet. Chem.*, 1995, **502**, 177–186.

27. B. Cornils and W. A. Herrmann, *J. Catal.*, 2003, **216**, 23–31.

28. H. U. Blaser, A. Indolese, and A. Schnyder, *Curr. Sci.*, 2000, **78**, 1336–1344.

29. B. Cornils and W. A. Herrmann, in *Applied Homogeneous Catalysis with Organometallic Compounds*, Wiley-VCH Verlag GmbH & Co. KGaA, Weinheim, 2nd edn., 2002, pp. 601–625.

30. G. D. Frey and O. Roelen, *J. Organomet. Chem.*, 2014, **754**, 5–7.

31. B. R. James, P. W. N. M. Van Leeuwen, S. D. Ittel, A. Nakamura, R. L. Richards, and A. Yamamoto, in *Rhodium Catalyzed Hydroformylation*, Kluwer Academic Publishers, New York, 1st edn., 2002, pp. 6–277.

32. A. M. Trzeciak, J. J. Ziółkowski, and R. Choukroun, *J. Mol. Catal. A Chem.*, 1996, **110**, 135–139.

33. J. Park and S. Hong, *Chem. Soc. Rev.*, 2012, **41**, 6931–6943.

34. A. M. Trzeciak, P. Štěpnička, E. Mieczyńska, and J. J. Ziółkowski, *J. Organomet. Chem.*, 2005, **690**, 3260–3267.

35. M. Madalska, P. Lönnecke, and E. Hey-Hawkins, *J. Mol. Catal. A. Chem.*, 2014, **383-384**, 137–142.

36. R. G. Arrayμs, J. Adrio, and J. C. Carretero, *Angew. Chem. Int. Ed.*, 2006, **45**, 7674–7715.

37. M. H. Pørez-Temprano, J. A. Casares, and P. Espinet, *Chem. Eur. J.*, 2012, **18**, 1864–1884.

38. D. G. H. Hetterscheid, S. H. Chikkali, B. deBruin, and J. N. H. Reek, *ChemCatChem*, 2013, **5**, 2785–2793.

39. J. A. Mata, F. E. Hahn, and E. Peris, *Chem. Sci.*, 2014, **5**, 1723–1732.

40. K. Nakao, G. Choi, Y. Konishi, H. Tsurugi, and K. Mashima, *Eur. J. Inorg. Chem.*, 2012, **17**, 1469–1476.

41. P. J. Low, *Annu. Rep. Prog. Chem., Sect. A,* 2002, **98**, 393–434.

42. J. I. van der Vlugt, *Eur. J. Inorg. Chem.*, 2012, **2012**, 363–375.

43. M. W. P. Bebbington, S. Bontemps, G. Bouhadir, M. J. Hanton, R. P. Tooze, H. van Rensburg, and D. Bourissou, *New J. Chem.*, 2010, **34**, 1556–1559.

44. E. B. Hager, B. C. E. Makhubela, and G. S. Smith, *Dalton Trans.*, 2012, **41**, 13927–35.

45. L. A. van der Veen, P. C. J. Kamer, and P. W. N. M. van Leeuwen, *Organometallics*, 1999, **18**, 4765–4777.

46. C. P. Casey, G. T. Whiteker, M. G. Melville, L. M. Petrovich, J. A. Gavney, and D. R. Powell, *J. Am. Chem. Soc.*, 1992, **114**, 5535–5543.

47. L. C. Matsinha, S. F. Mapolie, and G. S. Smith, *Dalton Trans.*, 2015, **44**, 1240–1248.

48. I. Vural Gürsel, T. Noel, Q. Wang, and V. Hessel, *Green Chem.*, 2015, **17**, 2012–2026.

49. S. Stockmann, P. Lönnecke, S. Bauer, and E. Hey-Hawkins, *J. Organomet. Chem.*, 2014, **751**, 670–677.

Chapter 4

Experimental

4.1 General experimental

All reactions were carried out in air unless otherwise stated. All solvents were reagent grade and used as received from Sigma-Aldrich, unless otherwise stated. $RhCl_3.3H_2O$ was purchased from Heraeus South Africa. Ethanol and dichloromethane were dried in the presence of molecular sieves. All other chemicals were purchased from Sigma Aldrich and used as received. Nuclear Magnetic Resonance (NMR) spectra were recorded on either a Bruker Ultrashield 400 Plus (^{1}H: 400.22 MHz; ^{13}C: 100.65 MHz) or a Bruker 300 MHz (^{1}H: 300.08 MHz; ^{13}C: 75.46 MHz) spectrometer. Chemical shifts were reported in parts per million (ppm) relative to the internal standard tetramethylsilane (δ 0.00). FT-IR spectra were recorded as KBr pellets using a Perkin Elmer 100 Spectrum One spectrometer or using Attenuated Total Reflectance Infrared spectroscopy (ATR-IR).

Melting points were determined using a Büchi melting point apparatus B-540. Mass spectrometry was carried out on a Waters Synapt G2 electron spray ionisation mass spectrometer in the positive or negative-ion mode. Elemental analyses were carried out using a Fission EA 110 CHNS Analyser.

4.2 Synthesis of the water-soluble ligands

4.2.1 Preparation of monosodium 5-sulfonatosalicylaldehyde (2.1)[1]

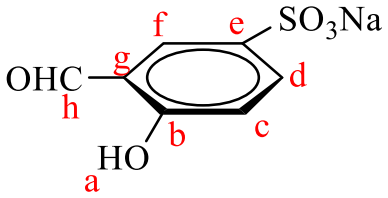

Salicylaldehyde (4.63 g, 37.9 mmol) and aniline (3.53 g, 37.9 mmol) were stirred in methanol (50 cm^3) overnight at room temperature. The solvent was reduced to a minimum (approximately 10 cm^3) and a yellow crystalline product was observed. The round bottomed flask containing the product was then immersed in an ice bath for further crystallisation of the product. The resultant yellow crystalline product (*N*-phenyl-salicylaldimine) was filtered using a Büchner funnel and washed with cold methanol, and dried in vacuum. *N*-phenyl-salicylaldimine (3.41 g, 17.7 mmol) was then added to concentrated sulfuric acid (10 cm^3) slowly with stirring. The yellow reaction mixture was heated at 100–105 °C for 2.5 hours. The hot solution was poured carefully into a beaker containing approximately 100 cm^3 of ice water. A yellow product precipitated immediately and this suspension was redissolved to give a bright orange solution. The solution was filtered by gravity and the filtrate left to stand at room temperature to allow crystallisation. The product (*N*-phenyl-5-sulfonatosalicylaldimine) was filtered and washed with small portions of cold water and dried. *N*-Phenyl-5-sulfonatosalicylaldimine (1.49 g, 5.37 mmol) and sodium carbonate (0.600 g, 5.62 mmol) were brought to boil in an open flask containing distilled water (10 cm^3) for 2 hours with periodic replenishment of water when necessary. The resultant solution was cooled and glacial acetic acid (6 cm^3) was then added. The same amount of ethanol was added and the solution cooled in an ice-bath for several hours. A beige precipitate was formed. The product (monosodium 5-sulfonatosalicylaldehydes, **2.1**) was filtered using a Büchner funnel and washed with cold ethanol, and dried under vacuum. Yield: (0.740 g, 62%). M.P.: 331–336 °C (Literature value: 331–334 °C). **^{1}H NMR** (D_2O, δ ppm): 10.03 (s, 1 H, H_h), 8.19 (d, ^4J = 2.0 Hz, 1 H, H_f), 8.00 (dd, ^3J = 8.6 Hz, ^4J = 2.4 Hz, 1 H, H_d), 7.15 (d, ^3J = 8.8 Hz, 1 H, H_c). **^{13}C{^{1}H} NMR** (D_2O, δ ppm): 196.9 ($\mathbf{C}_{aldehyde}$), 161.9 ($\mathbf{C}_{Ar}$), 134.9 ($\mathbf{C}_{Ar}$), 134.0 ($\mathbf{C}_{Ar}$), 131.0, 120.5, 118.1 ($\mathbf{C}H_{Ar}$). **FT-IR** (ν_{max}/cm^{-1}): 3478s (O–H str.), 1660s (C=O str.). **Elemental analysis** (%) Calcd. For $C_7H_5NaO_5S.H_2O$: C, 34.72; H, 2.91; S, 13.24. Found: C, 34.59; H,

2.86; S, 12.82. **ESI-MS (*m/z*)** = 200.99 ($[M]^-$ where M is the anion). $S_{25\ °C}$ = 125 mg/mL in water.

4.2.2 Preparation of monosodium 3-^{t}butyl-5-sulfonatosalicylaldehyde (2.2)[1]

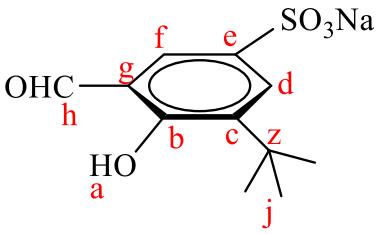

3-*tert*-Butyl-2-hydroxybenzaldehyde (0.890 g, 4.98 mmol) and aniline (0.464 g, 4.98 mmol) were stirred in ethanol (20 cm^3). Anhydrous magnesium sulfate was added to the solution and the reaction mixture stirred overnight. The reaction mixture was then filtered under gravity and the solvent removed to afford the product (*N*-phenyl-3-^{t}butyl-salicylaldimine) as a yellow oil. The round-bottomed flask with *N*-phenyl-3-^{t}butyl-5-sulfonatosalicylaldimine was submerged in an ice bath and 6 cm^3 of concentrated sulfuric acid were added slowly with stirring. A very dark orange solution was observed and this was heated at 105–110 °C for 2.5 hours. The solution was allowed to cool in an ice bath. Ice was added into the solution to induce crystallisation. A yellow-white precipitate (*N*-phenyl-3-^{t}butyl-5-sulfonatosalicylaldimine) was observed; this was filtered using a Büchner funnel and washed with ice cold water and dried under vacuum. *N*-phenyl-3-^{t}butyl-5-sulfonatosalicylaldimine (0.352 g, 1.06 mmol) was then dissolved in hot distilled water (100 cm^3) and Na_2CO_3 (0.112 g, 1.06 mmol) was added slowly to the solution over several minutes. The solution was left to boil in an open flask for three hours, with periodic replenishment of water when necessary. The solution was then removed from the heat followed by addition of acetic acid (3 cm^3) and ethanol (3 cm^3). The solution was allowed to cool for several hours and no precipitate was observed. The solvent was then removed to afford a solid. Ethanol was then added to the solid (monosodium 3-^{t}butyl-5-sulfonatosalicylaldehyde, **2.2**) to remove traces of acetic acid and washed well in a Büchner funnel. Yield: (0.215 g, 72.5%). M.P.: 164–167 °C (Literature value: 158–161 °C). **^{1}H NMR** (D_2O, δ ppm): 9.93 (s, 1 H, H_h), 8.03 (d, ^4J = 2.0 Hz, 1 H, H_f), 8.01 (d, ^4J = 2.0 Hz, 1 H, H_d), 1.44 (s, 9 H, H_j). **^{13}C{^{1}H} NMR** (D_2O, δ ppm): 198.9 ($\mathbf{C}_{aldehyde}$), 162.4 ($\mathbf{C}_{Ar}$), 139.4 ($\mathbf{C}_{Ar}$), 133.9 ($\mathbf{C}_{Ar}$), 131.1, 130.1, 119.8 ($\mathbf{CH}_{Ar}$), 34.5 ($\mathbf{C}^t_{Butyl}$), 28.5 ($\mathbf{CH}^t_{Butyl}$). (**FT-IR** (ν_{max}/cm^{-1}, KBr): 3440s (O–H str.), 1654s (C=O str.).

Elemental analysis (%) Calcd. $C_{11}H_{13}NaO_5S.4H_2O$: C, 37.50; H, 6.01; S, 9.10. Found: C, 37.60; H, 5.68; S, 8.66. **ESI-MS (*m/z*)** = 239.11 ($[M]^-$ where M is the anion). $S_{25\,°C}$ = 26 mg/mL in water.

4.2.3 Preparation of monosodium-5-sulfonatosalicylaldimine (2.3)

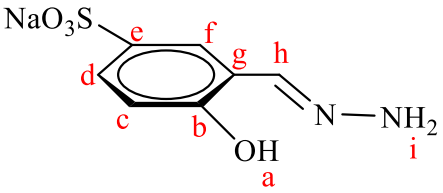

Hydrazine hydrate (0.805 g, 16.1 mmol) was added to a stirring solution of monosodium-5-sulfonato salicylaldehyde (1.80 g, 8.04 mmol) in ethanol (30 cm^3) and the reaction mixture refluxed for 1 hour. The resultant hot suspension was filtered using a Büchner funnel and the solid collected was washed with hot ethanol to afford the product **2.3** as a pale yellow solid. Yield: (1.50 g, 78%). M.P.: decomposes without melting, onset occurs at 394 °C. **^{1}H NMR** (DMSO-d_6, δ ppm): 11.51 (s, 1 H, H_a), 7.94 (s, 1 H, H_h), 7.48 (d, ^4J = 2.0 Hz, 1 H, H_f), 7.37 (dd, ^3J = 2.0 Hz, ^4J = 8.4 Hz, 1 H, H_d), 6.88 (s, 2 H, N**H**$_2$), 6.75 (d, ^3J = 8.4 Hz, 1 H, H_c). **^{13}C{^{1}H} NMR** (DMSO-d_6, δ ppm): 157.1 (**C**$_{Ar}$), 141.9 (**C**$_{imine}$), 139.9 (**C**$_{Ar}$), 126.9 (**C**H$_{Ar}$), 126.0 (**C**H$_{Ar}$), 119.0 (**C**$_{Ar}$), 115.2 (**C**H$_{Ar}$). **FT-IR** (ν_{max}/cm^{-1}, KBr): 3409 (N–H str.), 3297 (O–H str.), 1619 (C=N str.). **Elemental analysis** (%) Calcd. For $C_7H_7N_2NaO_4S$: C, 35.30; H, 2.96; N, 11.76. Found: C, 35.23; H, 2.70; N, 11.69. **ESI-MS (*m/z*)** = 215.01 ($[M]^-$ where M is the anion). $S_{25\,°C}$ = 0.11 mg/mL in water.

4.3 Synthesis of the water-soluble mononuclear and heterobimetallic complexes

4.3.1 Preparation of monosodium 5-sulfonatosalicylaldimine-ferrocenylimine (2.4)

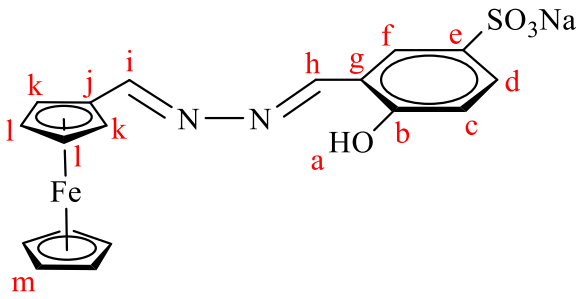

Monosodium-5-sulfonatosalicylaldimine (0.101 g, 0.426 mmol) was added to a stirring solution of ferrocenecarboxaldehyde (9.10×10^{-2} g, 0.426 mmol) in methanol (20 cm^3) and the reaction mixture refluxed for 48 hours. The dark red solution was cooled to room temperature and filtered under gravity. The solvent was reduced to approximately 5 cm^3 and dichloromethane (30 cm^3) was added to reveal a precipitate which was collected by filtering using a Büchner funnel to afford **2.4** as a dark red solid product. Yield: (0.151 g, 82%). M.P.: decomposes without melting, onset occurs at 174 °C. **^{1}H NMR** (DMSO-d_6, δ ppm): 11.51 (s, 1 H, H_a), 8.82 (s, 1 H, H_h), 8.64 (s, 1 H, H_i), 7.91 (d, ^4J = 1.4 Hz, 1 H, H_f), 7.59 (dd, ^3J = 8.4 Hz, ^4J = 1.6 Hz, 1 H, H_d), 6.89 (d, ^3J = 8.4 Hz, 1 H, H_c), 4.78 (br s, 2 H, H_{Fc}), 4.57 (br s, 2 H, H_{Fc}), 4.27 (s, 5 H, H_{Fc}). **^{13}C{^{1}H} NMR** (DMSO-d_6, δ ppm): 164.4 (**C**$_{imine}$), 160.9 (**C**$_{imine}$), 158.9 (**C**$_{Ar}$), 140.6 (**C**$_{Ar}$), 130.5 (**C**H$_{Ar}$), 128.7 (**C**H$_{Ar}$), 117.7 (**C**$_{Ar}$), 115.9 (**C**H$_{Ar}$), 77.7 (**C**$_{Fc}$), 71.8 (**C**H$_{Fc}$), 69.8 (**C**H$_{Fc}$), 69.4 (**C**H$_{Fc}$). **FT-IR** (ν_{max}/cm^{-1}, KBr): 1624 (C=N str.), 1589 (C=N str.). **Elemental analysis** (%) Calcd. For $C_{18}H_{15}FeN_2NaO_4S.4H_2O$: C, 42.70; H, 4.58; N, 5.53. Found: C, 42.89; H, 4.44; N, 5.70. **ESI-MS (*m/z*)** = 411.01 ($[M]^-$ where M is the anion). $S_{25\,°C}$ = 1.87 mg/mL in water.

4.3.2 Preparation of monosodium 5-sulfonatosalicylaldimine ferrocenylimine rhodium(I) 1,5-cyclooctadiene heterobimetallic complex (2.5)

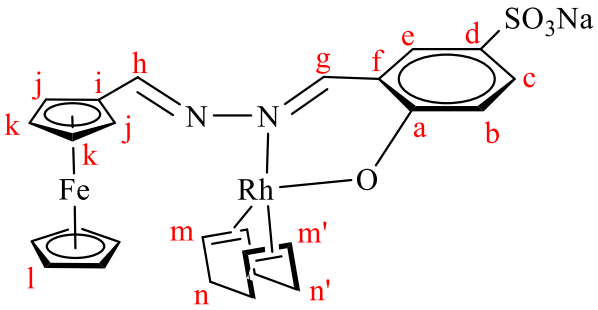

Monosodium 5-sulfonatosalicylaldimine-ferrocenylimine (0.100 g, 0.231 mmol) and sodium hydride (6.00×10^{-3} g, 0.231 mmol) were stirred together in dichloromethane (20 cm^3) for 90 minutes. $[Rh(COD)Cl]_2$ (5.70×10^{-2} g, 0.116 mmol) was added and the reaction mixture was stirred for 16 hours. Methanol (10 cm^3) was added to quench the NaH and the solution was filtered by gravity. The solvent was reduced to approximately 5 cm^3 and diethyl ether (20 cm^3) was added to reveal **2.5** as a yellow solid product which was collected using a Hirsh funnel, washed with diethyl ether, and dried under vacuum. Yield: (0.140 g, 94.2%). M.P.: decomposes without melting, onset occurs at 263 °C. **^{1}H NMR** (DMSO-d_6, δ ppm): 8.03 (s, 1 H, H_g), 7.97 (s, 1 H, H_h), 7.70 (d, ^4J = 2.2 Hz, 1 H, H_e), 7.50 (dd, ^3J = 8.8 Hz, ^4J = 2.1 Hz, 1 H, H_c), 6.61 (d, ^3J = 8.7 Hz, 1 H, H_b), 4.57 (br s, 1 H, H_j), 4.54 (br s, 1 H, H_k), 4.33 (m, 9 H, H_l + CH_{COD}), 2.42 (m, 4 H, CH_{2COD}), 1.90 (m, 4 H, CH_{2COD}). **^{13}C{^{1}H} NMR** (DMSO-d_6, δ ppm): 165.8 (C_{Ar}), 158.7 (C_{imine}), 153.4 (C_{imine}), 135.2 (C_{Ar}), 132.6 (CH_{Ar}), 132.2 (CH_{Ar}), 120.2 (CH_{Ar}), 115.9 (C_{Ar}), 77.4 (C_{Fc}), 71.4 (CH_{Fc}), 69.8 (CH_{Fc} + CH_{2COD}), 69.0 (CH_{Fc}), 30.3 (CH_{COD}). **FT-IR** (ν_{max}/cm^{-1}, KBr): 1600 (C=N str.). **Elemental analysis** (%) Calcd. For $C_{26}H_{26}FeN_2NaO_4RhS.4DCM$: C, 36.62; H, 3.48; N, 2.85. Found: C, 36.99; H, 3.90; N, 2.67. **ESI-MS (*m/z*)** = 411.01 ($[M - Rh(COD)]^-$ where M is the anion). $S_{25\ °C}$ = 16.7 mg/mL in water.

4.3.3 Preparation of 3-^{t}butyl-5-sulfonato salicylaldimine-ferrocenylimine complex (2.6)

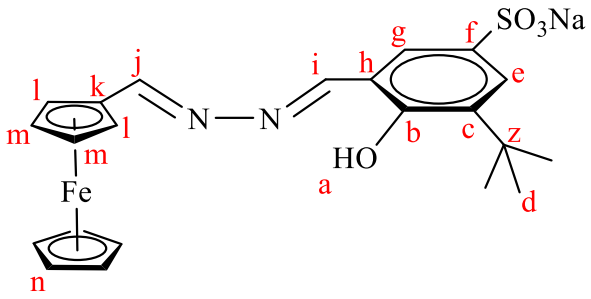

Hydrazine hydrate (0.187 g, 3.73 mmol) was added dropwise to a stirring solution of 3-^{t}butyl-5-sulfonatosalicylaldehyde (1.05 g, 3.73 mmol) in methanol (20 cm^3) and the reaction heated for 6 hours at 45 ºC. Ferrocenecarboxaldehyde (0.799 g, 3.731 mmol) was then added and the reaction mixture heated at 45 ºC for 24 hours. The dark brown solution was filtered by gravity to remove an orange precipitate of ferrocenylcarbaldehyde hydrazone. The volume of the filtrate was then reduced to approximately 5 cm^3 and diethyl ether (20 cm^3) was added to form a brown solid (**2.6**) which was collected using a Büchner funnel and dried under vacuum. Yield: (1.50 g, 82%). M.P.: decomposes without melting, onset occurs at 248 °C. **^{1}H NMR** (DMSO-d_6, δ ppm): 12.82 (s, 1 H, H_a), 8.82 (s, 1 H, H_i), 8.68 (s, 1 H, H_j), 7.68 (d, ^4J = 2.25 Hz, 1 H, H_g), 7.63 (d, ^4J = 2.25 Hz, 1 H, H_e), 4.78 (br s, 2 H, H_l), 4.58 (br s, 2 H, H_m), 4.28 (s, 5 H, H_n), 1.42 (s, 9 H, H_d). **^{13}C{^{1}H} NMR** (DMSO-d_6, δ ppm): 164.1 (C_{imine}), 162.7 (C_{imine}), 157.9 (C_{Ar}), 138.9 (C_{Ar}), 135.2 (C_{Ar}), 127.7 (CH_{Ar}), 126.8 (CH_{Ar}), 116.3 (C_{Ar}), 76.74 (C_{Fc}), 71.17 (CH_{Fc}), 69.07 (CH_{Fc}), 68.67 (CH_{Fc}), 34.22 (C^t_{Butyl}), 28.88 (CH^t_{Butyl}). **FT-IR** (ν_{max}/cm^{-1}, KBr): 3390 (O–H str.), 1615 (C=N str.), 1590 (C=N str.). **Elemental analysis** (%) Calcd. For $C_{22}H_{23}FeN_2NaO_4S.6.5H_2O$: C, 43.50; H, 5.97; N, 4.61. Found: C, 43.62; H, 5.12; N, 4.39. **ESI-MS (*m/z*)** = 467.07 ($[M]^-$ where M is the anion). $S_{25\ ^oC}$ = 4 mg/mL in water.

Ferrocenylcarbaldehyde hydrazone (by-product of 2.6):

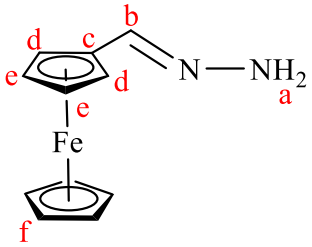

Yield (0.072 g) M.P.: decomposes without melting, onset occurs at 264 °C. **^{1}H NMR** ($CDCl_3$, δ ppm): 8.48 (s, 1 H, H_b), 4.71 (s, 2 H, H_d), 4.46 (s, 2 H, H_e), 4.24 (s, 5 H, H_f), 1.61 (s, 2 H, NH_2). **^{13}C{^{1}H} NMR** ($CDCl_3$, δ ppm): 161.2 (C_{imine}), 78.1 (C_{Fc}), 70.9 (CH_{Fc}), 69.3 (CH_{Fc}), 68.7 (CH_{Fc}). **FT-IR** (ν_{max}/cm^{-1}, KBr): 3095 (N–H str.), 1627 (C=N str.).

4.3.4 Preparation of monosodium 3-^{t}butyl-5-sulfonato salicylaldimine-ferrocenylimine rhodium(I)1,5-cyclooctadiene heterobimetallic complex (2.7)

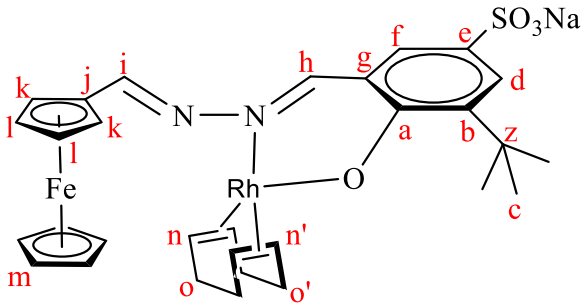

3-^{t}Butyl-5-sulfonato salicylaldimine-ferrocenylimine (0.102 g, 0.207 mmol) and sodium hydride (5.00×10^{-3} g, 0.211 mmol) were stirred together in dichloromethane (20 cm^3) at room temperature for 90 minutes. $[Rh(COD)Cl]_2$ (5.11×10^{-2} g, 0.104 mmol) was added and the reaction mixture stirred for 24 hours. Methanol (10 cm^3) was added to quench the NaH and the solution was filtered by gravity. The solvent was then reduced to approximately 5 cm^3 and diethyl ether (20 cm^3) was added to reveal a precipitate (**2.7**) which was collected by filtration using a Hirsh funnel and washed with diethyl ether. The brown solid product was then dried under vacuum. Yield: (0.140 g, 97%). M.P.: decomposes without melting, onset occurs at 335 °C. **^{1}H NMR** (DMSO-d_6, δ ppm): 8.03 (s, 1 H, H_h), 7.94 (s, 1 H, H_i), 7.56 (s, 1 H, H_f), 7.54 (s, 1 H, H_d), 4.65 (br s, 2 H, H_k), 4.52 (br s, 2 H, H_l), 4.31 (m, 9 H, H_m + CH_{COD}),

2.42 (m, 4 H, C**H**$_{2COD}$), 1.90 (m, 4 H, C**H**$_{2COD}$), 1.31 (s, 9 H, H$_d$). **^{13}C{^{1}H} NMR** (DMSO-d$_6$, δ ppm): 164.0 (**C**$_{Ar}$), 158.3 (**C**$_{imine}$), 153.5 (**C**$_{imine}$), 137.8 (**C**$_{Ar}$), 133.6 (**CH**$_{Ar}$), 130.5 (**CH**$_{Ar}$), 128.1 (**C**$_{Ar}$), 115.7 (**C**$_{Ar}$), 76.95 (**C**$_{Fc}$), 70.86 (**CH**$_{Fc}$), 69.26 (**CH**$_{Fc}$ + **CH**$_{2COD}$), 68.44 (**CH**$_{Fc}$), 34.65 (**C**$^t_{Butyl}$), 29.49 (**CH**$_{COD}$ + **CH**$^t_{Butyl}$). **FT-IR** (ν_{max}/cm^{-1}, KBr): 1592 (C=N str.). **Elemental analysis** (%) Calcd. For $C_{30}H_{34}FeN_2NaO_4RhS.4DCM$: C, 39.26; H, 4.07; N, 2.69. Found: C, 39.08; H, 4.64; N, 2.65. ESI-MS (*m/z*) = 467.07 ([M – Rh(COD)]$^-$ where M is the anion). $S_{25\,°C}$ = 0.8 mg/mL in water.

4.4 Synthesis of mononuclear and heterobimetallic precursors to DAB-G1 dendrimer

4.4.1 Preparation of formylated monosodium 5-sulfonatosalicyladmine-ferrocenylimine mononuclear complex (2.8)

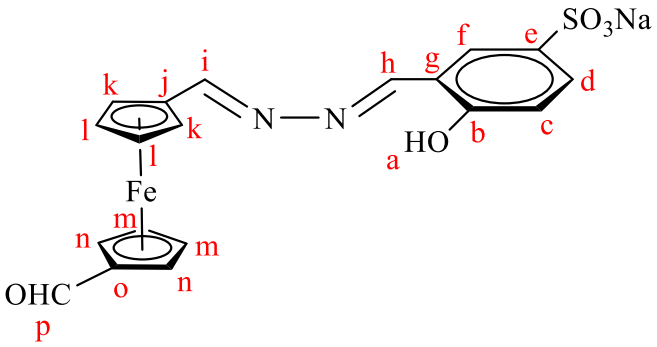

Monosodium 5-sulfonatosalicylaldimine (0.102 g, 0.426 mmol) was dissolved in methanol (10 cm^3) and the solution was added slowly dropwise to a stirring solution of 1,1′-ferrocenedicarboxaldehyde (0.104 g, 0.428 mmol) in methanol (15 cm^3). The reaction was heated for 20 hours at 45 ºC and the solvent was reduced to a minimal (5 cm^3). Diethyl ether was then added to precipitate out **2.8** as a dark red solid which was then collected using a Hirsh funnel and washed thoroughly with diethyl ether, and dried under vacuum. Yield: (0.190 g, 86%). M.P.: decomposes without melting, onset occurs at 215 °C. **^{1}H NMR** (DMSO-d$_6$, δ ppm): 11.44 (s, 1 H, H$_a$), 9.88 (s, 1 H, H$_p$), 8.83 (s, 1 H, H$_h$), 8.57 (s, 1 H, H$_i$), 7.94 (d, ^4J = Hz, 1 H, H$_f$), 7.59 (dd, ^3J = Hz, ^4J = Hz, 1 H, H$_d$), 6.91 (d, ^3J = Hz, 1 H, H$_c$), 4.89 (br s, 4 H, H$_{n,\,k}$), 4.74 (br s, 2 H, H$_l$), 4.65 (br s, 2 H, H$_m$). **^{13}C{^{1}H} NMR** (DMSO-d$_6$, δ ppm): 193.4 (**C**$_{aldehyde}$), 162.3 (**CH**$_{imine}$), 160.8 (**C**$_{imine}$), 158.5 (**C**$_{Ar}$), 140.0 (**C**$_{Ar}$), 130.1

($\mathbf{C}H_{Ar}$), 128.1 ($\mathbf{C}H_{Ar}$), 117.1 ($\mathbf{C}_{Ar}$), 115.4 ($\mathbf{C}H_{Ar}$), 80.13 ($\mathbf{C}_{Fc}$), 78.40 ($\mathbf{C}_{Fc}$), 74.09 ($\mathbf{C}H_{Fc}$), 72.34 ($\mathbf{C}H_{Fc}$), 70.53 ($\mathbf{C}H_{Fc}$), 69.95 ($\mathbf{C}H_{Fc}$). **FT-IR** (ν_{max}/cm^{-1}, KBr): 3417 (O–H str.), 1657 (C=O str.), 1619 (C=N str.). **Elemental analysis** (%) Calcd. For $C_{19}H_{15}FeN_2NaO_5S.5H_2O$: C, 41.32; H, 4.56; N, 5.07. Found: C, 41.70; H, 4.18; N, 5.53. **ESI-MS (*m/z*)** = 439.01 ($[M]^-$ where M is the anion). $S_{25\,°C}$ = 11 mg/mL in water.

4.4.2 Preparation of formylated monosodium 5-sulfonatosalicyladmine-ferrocenylimine rhodium(I) 1,5-cyclooctadiene heterobimetallic complex (2.9)

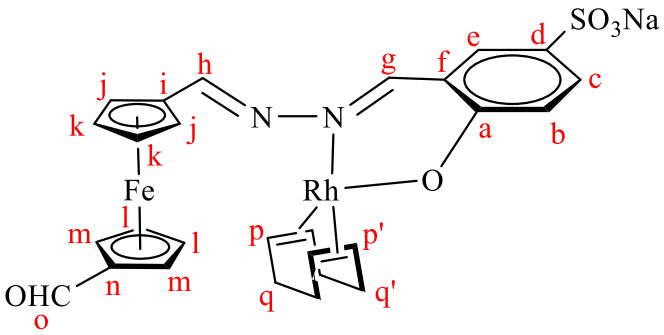

The mononuclear complex **2.7** (0.164 g, 0.354 mmol) was stirred together with sodium hydride (9.00×10^{-3} g, 0.364 mmol) in dichloromethane (20 cm^3) for 90 minutes at room temperature to afford deprotonation of the ferrocenyl compound. $[Rh(COD)Cl]_2$ (8.74×10^{-2} g, 0.177 mmol) was added and the reaction mixture was stirred for 24 hours. Methanol (10 cm^3) was added to quench the NaH and the solution was filtered by gravity. The solvent was then reduced to a minimum (5 cm^3) and diethyl ether (20 cm^3) was added resulting in a brown precipitate (**2.9**) which was collected using a Hirsh funnel, washed with diethyl ether and dried under vacuum. Yield: (0.222 g, 93%). M.P.: decomposes without melting, onset occurs at 291.3 °C. **^{1}H NMR** (DMSO-d_6, δ ppm): 9.97 (s, 1 H, H_o), 8.03 (br s, 2 H, $H_{h,g}$), 7.74 (br s, 1 H, H_e), 7.53 (br s, 1 H, H_c), 6.63 (br s, 1 H, H_b), 4.95-4.62 (m, 8 H, H_{j-m}), 4.14 (m, 4 H, $\mathbf{C}H_{COD}$), 2.40 (m, 4 H, $\mathbf{C}H_{2COD}$), 1.86 (m, 4 H, $\mathbf{C}H_{2COD}$). **^{13}C{^{1}H} NMR** (DMSO-d_6, δ ppm): 193.7 ($\mathbf{C}_{aldehyde}$), 165.9 ($\mathbf{C}_{Ar}$), 157.3 ($\mathbf{C}H_{imine}$), 152.9 ($\mathbf{C}H_{imine}$), 134.5 ($\mathbf{C}_{Ar}$), 132.7 ($\mathbf{C}H_{Ar}$), 131.5 ($\mathbf{C}H_{Ar}$), 120.4 ($\mathbf{C}H_{Ar}$), 115.5 ($\mathbf{C}_{Fc}$), 113.1 ($\mathbf{C}_{Ar}$), 74.8 ($\mathbf{C}_{Fc}$), 72.9 ($\mathbf{C}_{Fc}$), 71.3 ($\mathbf{C}_{Fc}$), 70.3 ($\mathbf{C}_{Fc}$), 30.0 ($\mathbf{C}H_{COD}$). **FT-IR** (ν_{max}/cm^{-1}, KBr): 1657 (C=O str.), 1599 (C=N str.). **Elemental analysis** (%) Calcd. For $C_{19}H_{15}FeN_2NaO_5S.8DCM$: C, 31.10; H, 3.13; N, 2.07.

Found: C, 31.17; H, 3.98; N, 2.29. **ESI-MS (*m/z*)** = 439.00 ([M – Rh(COD)]$^-$ where M is the anion). $S_{25\,°C}$ = 8 mg/mL in water.

4.5 General hydroformylation procedure

Conditions for the catalytic reactions were based on the previously reported conditions of the hydroformylation of 1-octene using analogous Rh(I) catalyst precursors containing *N,O*-bidentate ligands.[1] The water-soluble catalyst precursors were dissolved in distilled water (5 cm^3) at a catalyst loading of 2.87 × 10^{-3} mmol and metal to substrate ratio (Rh : 1-octene) of 2500 : 1. This was charged into 90 mL stainless steel pipe reactors, followed by 1-octene (805 mg, 7.175 mmol) and the internal standard *n*-decane (204 mg, 1.435 mmol) in toluene (5 cm^3). The reactors were flushed three times with N_2 (g) followed with syngas (CO : H_2, 1:1 ratio), then pressurised and heated to the desired syngas pressure and temperature respectively. A Perkin Elmer Clarus 580 GC instrument equipped with a flame ionisation detector and a 30 metre capillary column was used for analysing and quantifying the catalytic products. Authentic *iso*-octenes and aldehydes, alcohols and *n*-octane were used to confirm the products. For the leaching studies, inductively coupled plasma optical emission spectroscopy experiments were conducted on an ICP-OES Varian 730-ES spectrophotometer.

4.6 References

1. E. B. Hager, B. C. E. Makhubela, and G. S. Smith, *Dalton Trans.*, 2012, **41**, 13927–35.

Chapter 5

Overall Summary and Future Outlook

5.1 Overall Summary

A series of water-soluble *N,O*-chelating Schiff base ligands were synthesised (**2.3** and in one-pot for **2.6**). These were reacted with ferrocenecarboxaldehyde through Schiff base condensation reactions, leading to water-soluble ferrocenylimine mononuclear complexes (**2.4** and **2.6**). The monometallic complexes were reacted with a dimeric rhodium precursor $[Rh(COD)Cl]_2$ to produce a series of new ferrocenylimine-Rh(I) heterobimetallic complexes (**2.5** and **2.7**). Both the monometallic and heterobimetallic complexes were found to have good solubility in water. The ligand (**2.3**) and the complexes (**2.4**–**2.7**) were characterised fully using various spectroscopic and analytical techniques. Mononuclear and heterobimetallic precursors (**2.8** and **2.9** respectively) to DAB-G1 metallodendrimers were also prepared and characterised fully. All complexes are stable in air at room temperature. The water-soluble monometallic and heterobimetallic complexes were evaluated as catalyst precursors in the aqueous biphasic hydroformylation of 1-octene.

The ferrocenyl monometallic complexes were not active in the hydroformylation experiments of 1-octene. The heterobimetallic complexes posted good catalytic activity for 1-octene, giving aldehydes (both linear and branched) and isomerisation products (*cis* and *trans* 2- and 3-octene). It is worth noting that a comparison of the conversion, reaction rate and selectivity of the heterobimetallic complexes with that of rhodium(I)-mononuclear complex (reported by Hager and co-workers) shows comparable results. The effect of the ferrocene moiety to the overall reaction rates was not pronounced. This could be ascribed to lack of electronic metal-metal communication between the two metals in the heterobimetallic systems. Where there is interaction of the metals, formation of a weak interaction between iron and rhodium would allow electron donation from iron to rhodium, thereby increasing the electron density around the catalytic rhodium metal centre. This might offer improved catalytic properties for the heterobimetallic complexes.

Catalyst recyclability was achieved by using aqueous-organic biphasic medium. The catalyst was recovered for reuse through decantation of the product-containing organic layer. The catalyst-containing aqueous layer could be recycled up to 4 times, and metal loss from the aqueous layer was determined using ICP-OES. Formation of isomerisation products increased with each cycle, indicating a change in the active catalytic species.

5.2 Future outlook

The use of heterobimetallic complexes in catalysis is slowly increasing as researchers seek to design suitable catalysts for industrial applications. This work contributes to the novel approaches which can be used as a platform for designing heterobimetallic pre-catalysts that possess good catalytic activity and selectivity. Similar complexes can be designed with a rigid (*pi*- conjugated) linker between the two metals to allow direct communication of the metals without the possibility of changes in catalyst conformation. These could offer improved catalytic rates and selectivity at low catalyst loading. Varying the electronic properties of the complexes through electron-withdrawing and electron-donating substituent groups may be another avenue to explore in designing the heterobimetallic complexes. These have in the past been reported to be influential in the rates and selectivity of a catalyst. New heterobimetallic complexes of rhodium and a different metallocene, for example, the dicyclopentadienyl derivatives of ruthenium and osmium (which are somewhat similar in chemical reactivity and stability to ferrocene) can be of interest for future evaluation as hydroformylation pre-catalysts.